Long-term effects of prenatal hypoxia on cardiomyocyte function

A thesis submitted to The University of Manchester for the degree of Doctor of Philosophy in the Faculty of Biology, Medicine and Health

2019

Kim T. Hellgren

School of Medical Sciences, Division of Cardiovascular Sciences

Table of contents

Word count: 24,979

List of figures

List of tables

List of equations

List of abbreviations

AmR	Amplex Red
BCDA	Bathocuproine disulfonic acid disodium salt
BDM	2,3-Butanedione 2-monoxime
BPM	Beats per minute (heart rate)
BSA	Bovine serum albumin
BW	Body weight
$Ca^{2+}{}_m$	Mitochondrial Ca^{2+}
cDNA	Complementary DNA
CI	Complex I
CII	Complex II
CIII	Complex III
CIV	Complex IV
CoA	Coenzyme A
CS	Citrate synthase
CV	Complex V
Cyt-c	Cytochrome c
Da	Daltons – Unit of weight
DCPIP	Diamino-2-methylpropane
dD	Left ventricular diastolic diameter
DETAPAC	Diethylenetriaminepentaacetic acid
dIVS	Diastolic intra ventricular septum diameter
dPW	Diastolic posterior wall thickness
E-C	Excitation contraction
EF	Ejection fraction
ELISA	Enzyme-linked immunosorbent assay
EM	Electron microscopy
ET pathway	Electron transfer pathway
ET-max	Maximum uncoupled electron transfer-pathway capacity
FAs	Fatty acids
FCCP	Carbonyl cyanide-*4*-(trifluoromethoxy)phenylhydrazone
FI	Food intake
G	Glutamate
GD	Gestation day
H	Hypoxic
HRP	Horseradish peroxidase
I/R	Ischaemia and reperfusion
ISO	Isoprenaline

IUGR	Intrauterine growth restriction
K_m	Binding affinity
KP_i	Potassium phosphate buffer
L/E	Leak control ratio
LDS	Lithium dodecyl sulphate
LV	Left ventricular
LVDP	Left ventricular diastolic pressure
LVEDP	Left ventricular end-diastolic pressure
M	Malate
MCU	Mitochondrial Ca^{2+} uniporter
mPTP	Mitochondrial permeability transition pore
N	Normoxic
NBT	Nitroblue tetrazolium
NCX	Na^{+}- Ca^{2+} exchanger
NT	Normal Tyrode's
OXPHOS	Oxidative phosphorylation
P	Pyruvate
P/E	Phosphorylation system control ratio
PBS	Phosphate buffered saline
P_i	Inorganic phosphate
PKCε	Protein kinase C epsilon
PMCA	Plasma membrane Ca^{2+}-ATPase
Q-cycle	Ubiquinol/ubiquinone cycle
RCR	Respiratory acceptor control ratio
RIPA	Radio-Immuno Precipitation Assay
ROS	Reactive oxygen species
ROX	non-mitochondrial oxygen consumption
RyR	Ryanodine receptor
SA	Sinoatrial
sD	Left ventricular systolic diameter
SERCA	Sarco/endoplasmic reticulum Ca^{2+} ATPase
sIVS	Systolic ventricular septum diameter
SOD	Superoxide dismutase
SUIT	Substrate-inhibitor titration
sPW	Systolic posterior wall thickness
SR	Sarcoplasmic reticulum
TBS-T	Tris-buffered saline plus tween
TEM	Transmission electron microscope
TMPD	N,N,N',N'-tetramethyl-p-phenylenediamine
V_{max}	Maximal enzymatic activity rate
WI	Water intake

Abstract

It is well known that lifestyle and genetics play a role in the development of cardiovascular diseases. Comparatively less is known about the impact of the intrauterine environment on the adult cardiovascular system. Studies show a clear link between prenatal insults and the development of different diseases. Insults such as maternal nutrition, stress and low oxygen (hypoxia) can lead to the developmental programming of heart structure and function, causing long-lasting effects on the cardiovascular system. This study aimed to develop a mouse model prenatal hypoxia and determine the effects on the adult cardiac phenotype. In particular, the study focussed on the effects of prenatal hypoxia on structure and function, as well as cardiomyocyte intracellular Ca^{2+} handling.

Pregnant mice were subjected to 14% oxygen between gestational days 6-18. This level of hypoxia did not affect the dams' body weight, food or water intake. Newborn offspring showed no signs of intrauterine growth restriction. Prenatal hypoxia had no effect on adult offspring whole heart function or response to ischaemia and reperfusion. Mitochondrial content was unaffected by prenatal hypoxia, but both adult males and females from hypoxic pregnancies showed decreased cristae density, compared to their normoxic counterparts. Males from hypoxic pregnancies exhibited no differences in mitochondrial enzyme activity or mitochondrial oxygen consumption. However, prenatal hypoxia led to increased ROS production in most of the male mitochondrial respiratory states. In females, complex I and II activity were decreased while complex IV activity was increased in offspring from hypoxic pregnancies. In addition, mitochondrial respiration was increased and ROS production was decreased in most respiratory states. Prenatal hypoxia also had effects on intracellular Ca^{2+} handling; increased Ca^{2+} clearance capabilities were observed in adult females and increased SERCA 2a protein abundance in males from hypoxic pregnancies. In summary, we showed prenatal hypoxia had different effects in adult male and female offspring with regards to Ca^{2+} handling and mitochondrial function.

Declaration

No portion of the work referred to in the thesis has been submitted in support of an application for another degree or qualification of this or any other university or other institute of learning.

Kim Hellgren

Division of Cardiovascular Sciences

School of Medical Sciences

Copyright statement

i. The author of this thesis (including any appendices and/or schedules to this thesis) owns certain copyright or related rights in it (the "Copyright") and s/he has given The University of Manchester certain rights to use such Copyright, including for administrative purposes.

ii. Copies of this thesis, either in full or in extracts and whether in hard or electronic copy, may be made **only** in accordance with the Copyright, Designs and Patents Act 1988 (as amended) and regulations issued under it or, where appropriate, in accordance with licensing agreements which the University has from time to time. This page must form part of any such copies made.

iii. The ownership of certain Copyright, patents, designs, trade marks and other intellectual property (the "Intellectual Property") and any reproductions of copyright works in the thesis, for example graphs and tables ("Reproductions"), which may be described in this thesis, may not be owned by the author and may be owned by third parties. Such Intellectual Property and Reproductions cannot and must not be made available for use without the prior written permission of the owner(s) of the relevant Intellectual Property and/or Reproductions.

iv. Further information on the conditions under which disclosure, publication and commercialisation of this thesis, the Copyright and any Intellectual Property and/or Reproductions described in it may take place is available in the University IP Policy (see http://documents.manchester.ac.uk/DocuInfo.aspx?DocID=24420), in any relevant Thesis restriction declarations deposited in the University Library, The University Library's regulations (see http://www.library.manchester.ac.uk/about/regulations/) and in The University's policy on presentation of Theses.

Acknowledgements

First I would like to thank the medical research council for funding this work.

I would like to thank my official supervisors Gina and Andy for their inspiration and guidance. For all the hours spent listening to my crazy ideas and for letting me pursue at least some of them. I would also like to extend my gratitude to those who were not officially a part of the supervisory team but offered me their time and knowledge none the less, thank you, Holly, David and Kat. I would also like to thank my advisor Allison for all the advice she has given me.

This time has been a trial on so many levels but it has also been wonderful, much due to my beloved friends and colleagues. Thank you, Charlotte, Sarah, Nathan, Lauren, Jess, George, Charlene, Callum, Lorenz, Dave, Emma, Becky, Charlie, Caitlyn, Amy, Lori, Miriam, Claire, Lottie, Dan, Ilan, Martins, James and Mike. Thank you all for all the wonderful moments, the Grafton, the ale trail, beer festivals, themed parties, for all the Christmas and Monday curries, all the conferences, regions day, for all your help in the lab and for all the words you've taught me. I well got English now!

I'd also like to thank all the non-academic friends that I have made during this period, Edd, Stephen, Andy, Matt, Tibbers, Patrick and everyone at Jiu Fa Quan. Thank you for all the training, walks, surf, mountain biking and all the times we just went for a pint.

Massive thanks to my oldest friends back home and my family who have all supported me through this whole process. Especially thanks to my mom who taught me that I can do whatever I set my mind to.

As always, I have saved the best for last. Thank you, my wonderful Jessica, my bride to be. I couldn't have done this without you, you've been such a big part of this adventure and I can't wait to start our next one together. I love you.

1 Introduction

1.1 Cardiovascular diseases – an ever-growing health issue

In today's ageing society, cardiovascular diseases are one of our greatest threats which weigh heavily on healthcare systems across the world [1]. Previously, the focus has been on understanding the impact of lifestyle and genetics, and the combination of the two [2]. Indeed, it is almost considered common knowledge that lifestyle plays a great role in the risk of developing cardiovascular disease. Everything you eat and everything you do will tip the balance towards health or disease. For example, obesity, smoking and alcohol use could all greatly increase the risk of cardiovascular diseases, while exercise and a healthy diet can help keep the risks down [3, 4]. However, lately, there has been increased interest in early life conditions as the impact of the prenatal environment on the risk for developing cardiovascular disease has become more apparent. Already in 1977, a correlation was found between atherosclerotic heart disease and infant mortality in Norway [5]. There was a higher risk of atherosclerotic heart disease if born in a year with high infant mortality. The author suggested that heart disease could be a consequence of poor living conditions during childhood and adolescence, and subsequent prosperity, since the variations seen could not be explained by present-day living standards. Similar observations were subsequently made in Finland [6] and the USA [7].

1.2 Prenatal environment

The British epidemiologist, David Barker, discovered correlations between the prenatal environment and cardiovascular diseases around 1990. He observed that cardiovascular diseases were more prevalent in certain parts of England and Wales. He was also able to correlate the prevalence of heart disease with low birth weight and further down the line with nutritional stress during pregnancy. He then formed a hypothesis, now aptly called the 'Barker hypothesis', that the early life environment can play an important role in the development of hypertension, ischaemic heart disease and non-insulin-dependent diabetes [8]. Barker suggested that the environment during development could lead to "programming" of

behaviour, physiology and morphology in utero and that this phenomenon could lead to altered functionality and the development of disease in adulthood.

1.2.1 Prenatal insults

Studies have shown effects from a range of prenatal stressors. There have been very good reviews published for stressors such as nutrition [9], hormonal stress [10] and oxygen [11] utilizing epidemiological and animal studies. The stressor, timing, duration and severity, of the insult, are all factors affecting the outcome. There are also examples of combined stressors in utero, and separating the effects of one from the other can be difficult. For instance, low oxygen (hypoxia) has been shown to decrease appetite and could, therefore, lead to an additional nutritional insult [12-14]. The current work will focus on hypoxia and the cardiovascular system, for broader information, the author recommends the excellent work by Fowden et al. [14] or Padmanabhan et al. [15].

1.3 Prenatal hypoxia

The effects of hypoxia on the foetal phenotype are fairly well documented. There is however far less information available on any changes to the adult phenotype. At present, some changes have been recorded in adult offspring including; increased sensitivity to ischaemia and reperfusion (I/R) injuries [16-18], decreased expression of protein kinase C epsilon (PKCe), ventricular diastolic dysfunction, sympathetic dominance and increased resting contractility [19, 20]. So far, most studies have focused on the phenotype at the whole-animal and isolated organ level, while the cellular mechanisms underlying the phenotype remain largely unknown. Currently, there are great knowledge gaps regarding the effect of prenatal hypoxia on cardiomyocyte function, including; contractility, Ca^{2+} handling and cell metabolism [18, 20-23]. More details about the known effects of prenatal hypoxia on cardiac phenotype will be discussed in section 1.5.

1.3.1 Causes

Prenatal hypoxia can be caused by a range of different environmental and medical circumstances and is, worldwide, the most common pregnancy-related

complication [24]. Medically, preeclampsia, placental insufficiency, cord compression and anaemia reduces the oxygen availability for the foetus and causes prenatal hypoxia. However, environmental factors also play a role. Maternal smoking may affect arterial oxygen levels, and high altitude pregnancies have been shown to affect foetal oxygen availability. It is worth noting that 140 million people live at an altitude higher than 2500 metres above sea level and may, therefore, be affected by these challenges [25]. When the insult is left untreated it leads to permanent changes in protein expression and lifelong alterations to the cardiac phenotype. These alterations may also be inherited and affect future offspring over generations. When a prenatal event, such as hypoxia, permanently alters a phenotype in this matter it is referred to as "developmental programming" [14, 21].

1.3.2 Models and approaches

A range of models and approaches have been used in an effort to study the impact of hypoxia on a foetus during pregnancy. From David Barkers epidemiological studies to model animals, such as sheep, guinea pigs, rats, chicken and mice; all of which have merit. Barker was able to show us that there is an effect of prenatal stress in humans and that this may impact health across the world [26]. Using sheep as an experimental model gets us close to the human cardiac physiology but still allows for better control of environmental influences, both prenatally and in adulthood [27]. While sheep have similar-sized hearts and similar heart rate, they also have a fairly long lifespan and are difficult to keep in an experimental setting, making it an expensive model to study. A lot of studies regarding prenatal hypoxia, therefore, involve rodents [17, 28-31]. Rodents have a short life span, making them ideal models for longitudinal developmental studies. The full genome has been sequenced in both mice and, at least 80% of human genes have a perfect match in mice [32]. Mice are commonly used for cardiovascular studies, and while there are obvious differences between rodents and humans, a combination of genetic knowledge, short gestation time and fast generation time make the mouse a viable candidate for prenatal hypoxia studies. I also mentioned chickens as a model for prenatal hypoxia. Although chickens are not mammals and the physiological similarities to humans are less compared to rodents, they have allowed researchers

to study the effect of prenatal hypoxia on an offspring without maternal influence [33].

Despite all the differences in these models, they have all shown adverse effects of prenatal hypoxia on the adult phenotype of a range of different systems, including the cardiovascular system. To allow a deeper look at the effects of prenatal hypoxia on the cardiovascular system, we first need to revisit the normal function of the heart.

1.4 Cardiac function

Arguably the most important muscle in the human body is the heart; its four chambers acting in an orchestrated unison, circulating blood through the human body delivering oxygen and nutrients to the different organs and tissues. The human heart beats approximately 100,000 times each day, pumping 23,000 litres of blood through the body. Blood, low in oxygen, comes from the body to the right side of the heart and, aided by the right atria, fills the right ventricle. The heart contracts and blood is pumped out to the lungs where it can be re-oxygenated. From the lungs, the oxygenated blood enters the left side of the heart, via the pulmonary veins, and the left ventricle is filled with the aid of the left atria. The heart contracts again, and the oxygenated blood is pumped through the aorta, out through the body. Each heartbeat is responsible for sending deoxygenated blood to the lungs as well as oxygenated blood to the body. During rest, each ventricle in the adult human heart sends on average five litres of blood per minute through the body which, during periods of increased activity, can reach up to 30 litres per minute. Due to the nature of the two ventricles, the regulation of the contractions of the heart needs to be precise to assure the same volume is pumped from each ventricle and to meet increasing or decreasing demand from changes in activity [34, 35].

1.4.1 Cellular function, E-C coupling and contraction

Contraction of the heart's four chambers is instigated by electrical stimulations (action potentials) leading to mechanical contraction of the myocyte. The action

potential is initiated by the sinoatrial (SA) node which is a cluster of myocytes with leaking ion channels, called 'funny' channels, allowing for spontaneous periodical depolarisation. This is the heart's own pacemaker and it is subject to control from the autonomic nervous system and voltage hyperpolarisations. Once enough ions leak in through the 'funny' channels a threshold is reached leading to depolarization and an action potential. This action potential leads to an electric pulse that travels through the electrical conduction system, to the right atrium and then through the rest of the heart, culminating in a myocardial contraction pumping blood through the body [36, 37].

The resting cardiomyocyte holds a membrane potential of around -90 to -80mV meaning that the inside of the cell is negatively charged with respect to the outside. This is mediated by ion pumps on the cell membrane. To trigger contraction, an action potential arrives at a heart cell (cardiomyocyte) and depolarises the cell by the inflow of Na^+. This depolarisation allows for the opening of the L-type Ca^{2+} channel, which allows a small amount of Ca^{2+} to enter the cell. This, in turn, triggers the ryanodine receptors (RyRs), situated on the sarcoplasmic reticulum (an intracellular Ca^{2+} store; SR), to open and release a greater quantity of Ca^{2+} into the cytosol. At this point, the high concentration of Ca^{2+} allows Ca^{2+} to bind to the myofilaments which generate a contraction of the cell. This describes the events leading up to the systolic period. The diastolic period (relaxation) is controlled by the removal of Ca^{2+} from the cytosol. The majority of the Ca^{2+} is removed by reuptake into the SR by the sarco/endoplasmic reticulum ATPase (SERCA), located on the SR membrane, and the Na^+-Ca^{2+} exchanger (NCX), located on the cell membrane. In addition to this, the plasma membrane Ca^{2+} ATPase (PMCA) and the mitochondrial Ca^{2+} uniporter (MCU) are responsible for the removal of small amounts of Ca^{2+} [38-40]. See figure 1-1 for a visual scheme of E-C coupling.

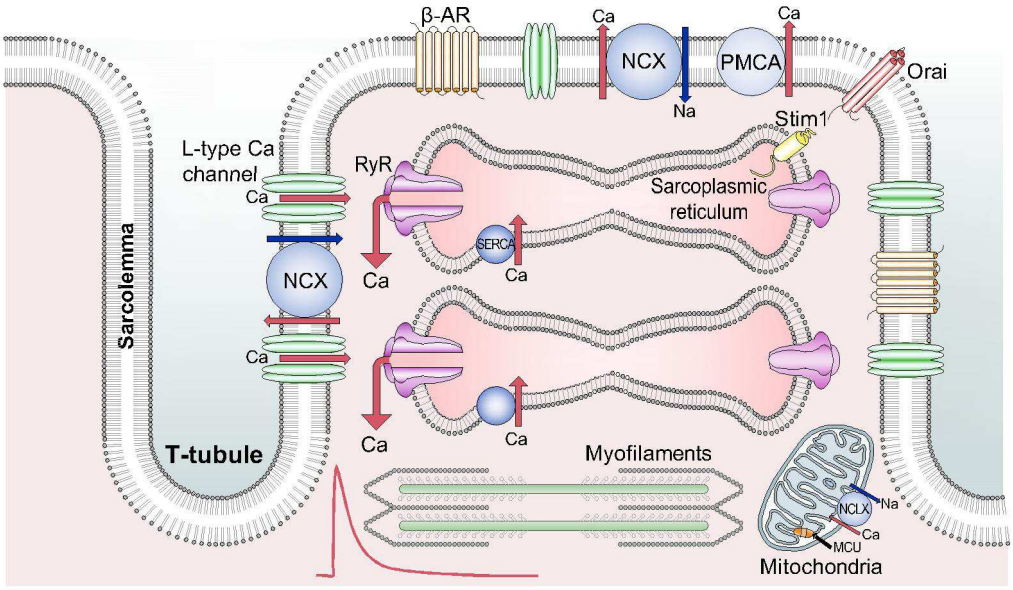

Figure 1-1 Illustration of E-C coupling. Image from Eisner et al. of Ca^{2+} excitation-contraction coupling [41].

1.4.2 Metabolism

As the heart is constantly active it is one of the most energy-demanding organs in the body. In the heart, the major cellular energy currency is adenosine triphosphate, more commonly known by its abbreviation ATP, formed by the addition of inorganic phosphate (P_i) to adenosine diphosphate (ADP). The production of ATP comes mainly from the catabolism of fatty acids (FAs) or glucose through three consecutive processes, namely glycolysis, the Krebs cycle and oxidative phosphorylation OXPHOS; [42]. In the healthy adult heart, there is a preference for FAs oxidation which supplies about 70% of ATP. However, studies have shown that this preference is shifted towards glucose in diseased and ischaemia stressed myocardium, in both animal models and humans [43-45].

1.4.3 Glycolysis

The lysing of glucose is called glycolysis. This is a process that occurs in the cytosol of a cell and it is one of the three major aerobic energy-producing steps. Glycolysis both utilizes and produces ATP, but more importantly, it breaks down the six-carbon molecule, glucose, into two pyruvate molecules with three carbons each, that can, later on, be utilized in the Krebs cycle to produce substrates for mitochondria. Briefly, glucose is phosphorylated, reconfigured and divided in a series of steps. Initially the process uses a total of two ATPs for each glucose molecule, but eventually also produces four ATPs for each glucose molecule ending up with a net production of two ATPs. In this process, there is also a reduction of two NAD^+ to NADH. The produced pyruvate then goes through pyruvate oxidation (not strictly a part of glycolysis nor the Krebs cycle) and becomes Acetyl CoA, a two-carbon molecule, which can enter the Krebs cycle (discussed in detail in 1.4.3 and 1.4.5). As a bi-product, pyruvate oxidation also reduces one NAD^+ to NADH [46].

1.4.4 Fatty acid oxidation

As previously mentioned, the healthy adult heart relies more on FA oxidation than on glycolysis. With the help of ATP, the FAs are activated in the cytosol, in the presence of CoA-SH and acyl-CoA synthetase and bound to carnitine. The molecules then go through pores in the outer mitochondrial membrane and are transported past the inner membrane, by acylcarnitine transferase, into the mitochondrial matrix where oxidation occurs. The carnitine is split off the acyl-CoA and the acyl-CoA enters a cycle of oxidation. Briefly, Acyl-CoA dehydrogenase starts a dehydrogenation, which is dependent on FAD, where a double bond is formed between the second and third carbon freeing up two electrons and generating $FADH_2$. Water is then added by enoyl-CoA hydratase forming 3-hydroxy acyl-CoA. This molecule is then dehydrogenated by 3-hydroxy acyl-CoA dehydrogenase, which is associated with NAD+, which converts the hydroxyl group, located on the third carbon, to a keto group with a 3-ketoacyl-CoA group as a result. The bond between the second and third carbon can now be cleaved by thiolase, releasing acetyl-CoA and acyl-CoA. The acyl-CoA is now two carbons shorter than it was initially and will

again enter the cycle to be cleaved further. The newly formed NADH and $FADH_2$ are used as substrates for the nearby complex I and II, respectively (discussed further in section 1.4.5.1) [47].

1.4.5 Krebs cycle

Also known as the citric acid cycle and the tricarboxylic acid cycle, the Krebs cycle was discovered by Hans Krebs in 1937 for which he was awarded a Nobel Prize in 1953. The Krebs cycle is indirectly responsible for up to two-thirds of oxygen consumption and total energy generation in the body. The cycle itself does not consume any energy directly; it will however only operate during aerobic conditions [48]. As we remember from previous sections, one of the resulting products from fatty acid oxidation is acetyl-CoA which can be directly used by the Krebs cycle. The resulting product from glycolysis is pyruvate which enters the mitochondria, and in the matrix, is decarboxylated and bound to CoA enzyme, forming an acetyl-CoA. In the process, a CO_2 molecule is lost and one NAD^+ is reduced to NADH. Thereby, the product from glycolysis is now also ready to enter the Krebs cycle. The Krebs cycle is detailed in figure 1-2 and the details will not be discussed at any depths in this text. Worth noting however are the three NADH producing steps and the $FADH_2$ producing step as these are both electron donors for complex I and complex II, respectively [49].

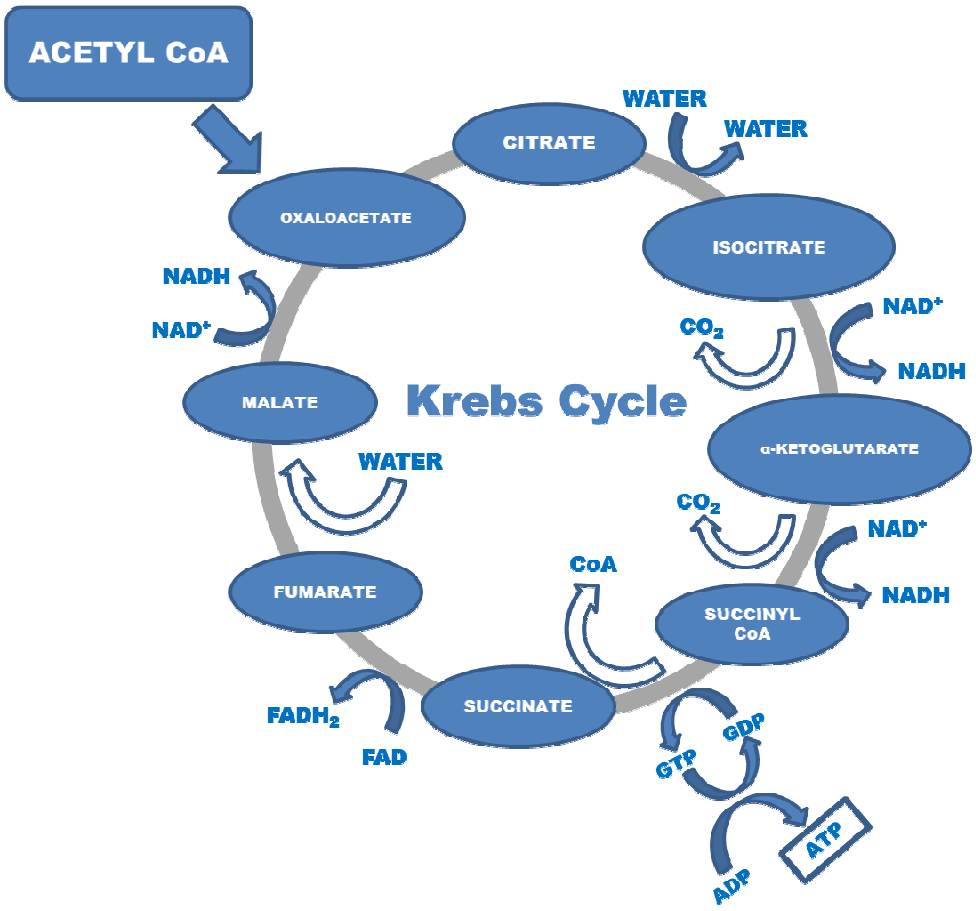

Figure 1-2 Graphical scheme of the Krebs cycle. The different steps of the Krebs cycle are detailed in this diagram. The steps are as follows, starting from the acetyl-CoA in the top moving clockwise: 1) Condensation, acetyl-CoA and oxaloacetate are converted to citrate catalyzed by citrate synthase. 2) Isomerization of citrate, citrate is converted to isocitrate, with cis-aconitate as an intermediate both steps involve aconitase. 3) Generation of CO_2 by an NAD+ Linked Enzyme, isocitrate is dehydrogenated to oxalosuccinate which is decarboxylated to alpha-ketoglutarate. This produces one NADH. 4) Second oxidative decarboxylation step, alpha-ketoglutarate is converted to succinyl-CoA by alpha-ketoglutarate dehydrogenase. This produces another NADH 5) Substrate-level phosphorylation, Succinyl-CoA is converted by succinic thiokinase to succinate. This reaction produces one ATP. 6) Flavin-dependent dehydrogenation, succinate dehydrogenase converts succinate to fumaric acid. This step produces one $FADH_2$. 7) Hydration of a carbon-carbon double bond, fumarase catalyses a carbon double bond to form malate. 8) Oxaloacetate regeneration, dehydrogenation of malate, by malate dehydrogenase, produces oxaloacetate that can react with acetyl-CoA in step one and restart the cycle. In this step, one $NADH_2$ is produced.

1.4.6 Mitochondrial physiology

1.4.6.1 Electron transfer pathway

The electron transfer pathway (ET-pathway; figure 1-3) is a collective name for the processes that create the proton motive force that is necessary for ATP production. It is made up of five protein complexes aptly named Complex I-V. Complex I obtains an electron donated from NADH which it transfers into the Q-junction where it is picked up by the ubiquinol/ubiquinone cycle (Q-cycle). From there, the electron is transported to complex III, picked up by cytochrome c (cyt-c) and further transported to complex IV where water acts as a final electron receptor through the reduction of oxygen. With each step through the pathway, the electron moves from a higher to a lower energy state, releasing energy to facilitate proton pumping into the intermembrane space. There is also complex II, which receives an electron from $FADH_2$ that is then transported along the same pathway as the electrons coming through complex I from NADH. However, unlike complexes I, III and IV, complex II does not pump a proton into the intermembrane space. The built-up energy, due to proton motive force, is then used by complex V, where the protons go with the gradient (as opposed of being pumped against), to create ATP from ADP and inorganic phosphate (P_i). [50].

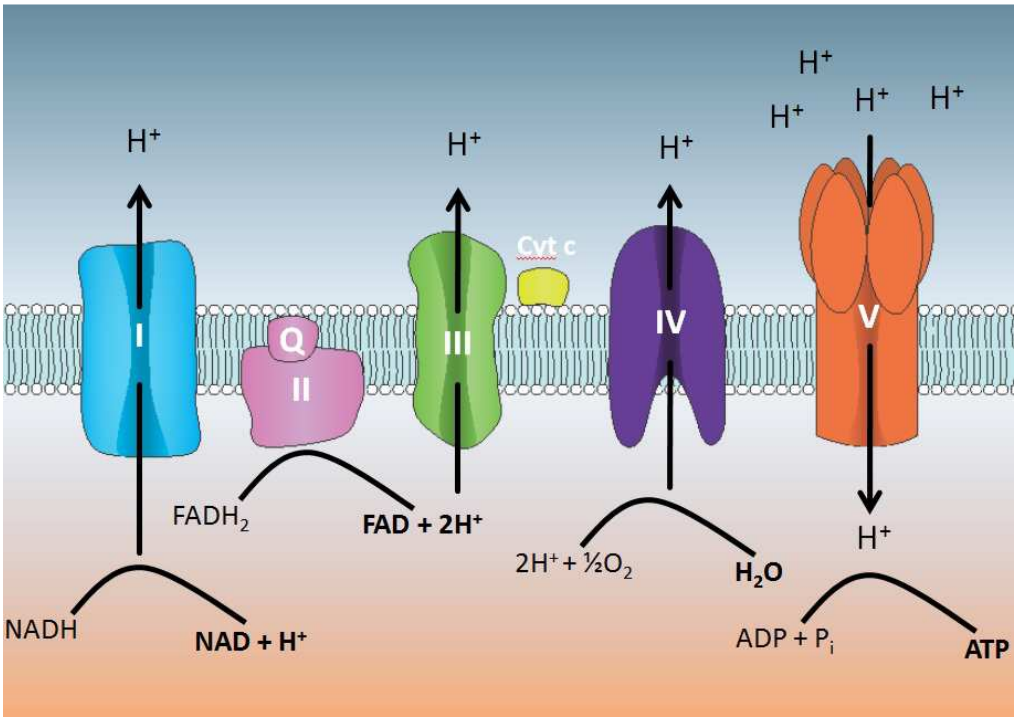

Figure 1-3 Illustration of the mitochondrial ET-pathway.

1.4.6.2 Reactive oxygen species

Electrons can leak prematurely during their transport through the ET-pathway and generate reactive oxygen species (ROS). The two main ROS are superoxide radicals (O^{-}_2), which are formed if a single electron is leaked, and hydrogen peroxide (H_2O_2), formed if two electrons leak like a pair. The amount of leak is affected by several factors but mainly it is dependent on the rate constant for the leak reaction in a certain mitochondrial site and concentration of the reduced electron donor for that site. During a state of clamped substrate concentrations, the level of available oxygen does not play a major role in the rate of electron leak. At least not until the oxygen level is nearing the K_m of complex IV [51, 52]. There are, at least, a total of 11 sites, related to substrate catabolism, in the mitochondria that produce ROS. Four sites are in the 2-oxoacid dehydrogenase complexes, there are two sites in complex I and one site in complex III. In addition, there are four sites linked to the Q-dependent dehydrogenase [53]. Due to their reactivity, ROS is likely to interfere with molecules and membranes, causing damage. Initially, it was believed that ROS was

just a negative by-product but that is no longer the general belief. In addition to apoptosis [54], ROS is also involved in processes regulating cell cycle [55], growth factor signalling [56] and transcription factors [57], just to mention a few. We will discuss how ROS leads to apoptosis in a section 1.4.6.3, for any further reading we suggest the review from Droge, 2002 [58].

1.4.6.3 Ion channels and apoptosis

For anyone who subscribes to the symbiosis hypothesis, it is easy to believe that the mitochondria would have the ability to control the transport of more than metabolic substrates. And in fact, there is a range of ion channels described in both the inner and outer membrane of the mitochondria. This current work will only focus on a subset of channels anchored in the inner mitochondrial membrane, for further reading we suggest the review of O'Rourke [59]. The aforementioned MCU facilitates Ca^{2+} uptake dependent on the mitochondrial membrane potential and the Ca^{2+}concentration in the cytosol versus the matrix. High levels of cytosolic Ca^{2+}will activate the MCU and Ca^{2+}can enter the mitochondrion. The intramitochondrial Ca^{2+}concentrations will affect the rate of OXPHOS and the Krebs cycle. One study showed a two-fold increase in oxygen consumption of skeletal muscle mitochondria when using 840nM Ca^{2+} in media compared to Ca^{2+}-free media. The effect seems to be fairly uniform over the different complexes, however, complex II is not mentioned in the study [60]. Through this mechanism, the Ca^{2+}acts as a second messenger, signalling the increased need for energy with increased muscular workload. At the same time, increased mitochondrial Ca^{2+}concentration also increases ROS production [61].

Increased Ca^{2+}concentrations in the matrix, as well as increased ROS production, can both lead to the activation of the mitochondrial permeability transition pore (mPTP). The structure of the mPTP is yet unclear but it is known that it is a pore situated in the inner mitochondrial membrane and that openings will allow molecules of up to 1500 Da to freely permeate the membrane [62, 63]. There have been suggestions that the mPTP has both physiological and pathological applications. In a non-pathological capacity, mPTP opening, with shorter duration

and smaller pore size, can allow mitochondria to be reset and thereby promote mitochondrial and cell survival [64]. There have also been studies suggesting that mPTP is involved in hypoxic preconditioning [65]. However, the mPTP can also act on a larger scale and lead to cell death rather than cell protection. As an example, in the case of ischaemia/reperfusion (I/R) Ca^{2+} is built up in the cytosol which in turn triggers Ca^{2+} transport into the mitochondrial matrix. This leads to increased ROS production and together with the Ca^{2+}, triggers the opening of the mPTP. As the cytosolic Ca^{2+} concentration remains high, so does the concentration of matrix Ca^{2+}, leaving the mPTP open. The opening of the mPTP leads to lost membrane potential and electron transfer ceases. In addition, prolonged loss of membrane potential leads to release of pro-apoptotic proteins, such as cytochrome c, into the cytosol [66, 67]. This activates caspases, which will start to break down protein and eventually kill the cell.

1.4.7 Ischaemia/reperfusion injury

Explained so far in this work is the function of the healthy heart. But as previously mentioned, there are adverse effects of prenatal hypoxia leading to a less healthy heart, such as the response to I/R. Ischaemia is simply a lack of blood supply to the heart, causing an unbalance between oxygen delivery and demand. An ischaemic period can be caused during a range of different complications, such as circulatory arrest, myocardial ischaemia and cardiac surgery which leads to damage and cell death in the affected tissue. The treatment of choice is the restoration of blood flow, which does prevent further damage. Conversely, however, this restoration of blood flow also lead to tissue damage itself [68, 69]. The majority of this damage is due to mitochondrial influences, discussed in more detail in a subsequent chapter, but there are also effects on Ca^{2+} handling.

1.4.7.1 Calcium handling effects associated with (I/R)

Originally, it was believed that altered properties of Ca^{2+} handling were the controlling factor of I/R damage, as the affected cell would store large quantities of Ca^{2+} in the mitochondrial matrix leading to swollen and dysfunctional mitochondria and cell death [70, 71]. It has later been shown that this accumulation of Ca^{2+} is

mediated by reversal of the NCX, due to elevated intracellular Na^+ levels. It is hypothesised that, during the ischaemic period, intracellular Na^+ is increased as a result of a build-up of H^+ due to anaerobic metabolism, which is transported out of the cell in exchange for Na^+ by Na^+/H^+ exchanger to salvage intracellular pH. Although the NCX is inhibited by lowered pH, its relationship with Na^+ allows the NCX to stay active and in fact, leads to an uptake of Ca^{2+} through the NCX rather than the normal extrusion of Ca^{2+} (reversed NCX). This process leads to increased mitochondrial Ca^{2+} (Ca^{2+}_m) uptake through the mitochondrial Ca^{2+} uniporter (MCU). The increased $[Ca^{2+}]_m$ will lead to depolarization of the mitochondrial membrane and opening of the mitochondrial permeability transition pore (mPTP). This leads to mitochondrial swelling and cell death [72, 73].

In support of the Ca^{2+} driven I/R injury, experiments which pharmacologically, or genetically, block NCX have shown a lessened effect of I/R injury in mice [74]. Interestingly though, in transgenic mice where NCX is overexpressed, males suffer greater damage from I/R compared to wild type. However, females with NCX overexpression do not suffer more than their female wild type counterpart [75] unless the transgenic females were oophorectomized, removing any effects from oestrogen [76]. To further support the mechanism, pharmacological blockage of Na^+/H^+ exchanger, using amiloride, delays the increase in cellular $[Ca^{2+}]$ and thereby also delays the increased in $[Ca^{2+}]_m$ [72]. Cross et al saw that the Na^+ increase after I/R was less in the females, and they, therefore, think that oestrogen is affecting this channel and thereby counteracting (or possibly just delaying) Ca^{2+} influx [76].

1.4.7.2 Is mitochondrial ET-pathway itself driving I/R damage?

As previously mentioned, the damage from a period of I/R is most likely due to excessive ROS production, which has been found in several previous studies [77-79]. There are however two confounding hypotheses of how this works. The first, which we have spoken about in the previous section, is via Ca^{2+} accumulation in the cell through the NCX, which is eventually taken up into mitochondria through the MCU; this process leads to depolarization of the mitochondria, which leads to mPTP opening, swelling and apoptosis. The second hypothesis involves complex II

substrate (succinate) build-up around the electron-accepting site of complex II, due to lack of oxygen, and in extension, a lack of a final electron acceptor. Once the cell is reperfused, electrons rush into the ET-pathway, through complex II, creating an increased redox pressure downstream in the ET-pathway that cannot be matched by the activity of complex IV. This, in turn, puts pressure on the electron-donating site in complex I, forcing complex I to go into reverse and leak the electrons out into the matrix. This generates a massive spike of ROS that in turn leads to mitochondrial, and cell, damage by membrane oxidation and altered redox signalling. The succinate build up theory has been proven in rat brain, mouse kidney, liver and heart when subjected to in vivo ischaemia [80].

1.5 Adverse effects of prenatal hypoxia

As previously mentioned, chronic prenatal hypoxia is a common complication during pregnancy and both epidemiological and animal studies have shown that it leads to adverse outcomes that are sustained until adulthood. This phenomenon, where the intrauterine environment affects the adult phenotype, is termed developmental programming. In this study, we will focus on the effects of the cardiovascular system and mainly the heart.

1.5.1 Foetal response to hypoxia

Adults and foetuses respond differently to low oxygen and use different compensatory mechanisms to mitigate injury. The adult body will respond by changing ventilation and heart rate to increase oxygen uptake, as even though levels of oxygen may be low, the amount of air in the atmosphere is great. Therefore, a healthy adult can withstand fairly large changes in environmental oxygen availability and still supply organs with oxygen to a satisfactory level [81]. Inside the womb, on the other hand, the amount of oxygen is comparatively finite and limited by the placenta. The first line of the foetal defence is that of a great margin of safety at basal conditions. The foetus is, due to different species of haemoglobin, able to bind more oxygen to the haemoglobin and release more oxygen at lower oxygen tension leading to an increased capacity to deliver oxygen [82]. The second line of defence in the foetus is to shunt blood to organs more likely

to be damaged by the lack of oxygen and the ability to hinder processes consuming oxygen [83, 84]. The shunting of the blood is believed to be facilitated by nitric oxide (NO) regulating the constriction and dilation of vessels such as the ductus venosus and arteriosus [85, 86]. In addition to regulation of NO, there has been a suggested involvement of ROS in the regulation of vasoconstriction, the theory being that NO is quenched by ROS which in turn leads to peripheral vasoconstriction [87-89]. But, if hypoxia continues and becomes chronic, the redistribution of blood flow can lead to some adverse effects [90, 91].

1.5.2 Foetal outcomes of prenatal hypoxia

There are several documented pathological effects of hypoxia on the foetus. One of the effects that, to some extent, sparked the interest in developmental programming and led to continued research of prenatal hypoxia was that of intrauterine growth restriction (IUGR). This is was what caught the attention of David Barker [8]. His work showed nutritional insults during pregnancy can lead to IUGR, but more recent research has demonstrated IUGR from hypoxic pregnancies [92, 93], even when separated from the nutritional component [94-97]. Furthermore, studies have shown decreased foetal cardiac output (mainly in the right ventricle) in sheep being subjected to chronic hypoxia at high altitude (3820m) in the absence of IUGR [98, 99]. The authors suggest that a decrease in ßl-adrenoceptors could be responsible for the decreased cardiac output [99] but, as other studies have shown increased ßl-adrenoceptor abundance, this seems less likely [100]. Furthermore, studies by Browne et al. showed decreased contractility due to changes in E-C coupling rather than ßl-adrenoceptors and suggest that the difference may lie in 'activator calcium', i.e. changes to the LTCC [101].

Studies in rats suggest an increased heart to body weight ratio [93, 102] but there is a lack of human studies regarding this. It appears that the relative increase in heart weight is mainly due to hyperplasia (increased amount of cells) of cardiomyocytes [103, 104]. Mitochondrial biogenesis plays an important role in the development of cardiac hypertrophy (increased cell size) [105, 106]. As such, the data presented by Xiao et al., which reported increases in the mitochondrial protein cytochrome c, suggests

an increased mitochondrial abundance and thereby supports the results of hypertrophy in the foetal heart subjected to hypoxia [93]. Furthermore, a cDNA array to assess gene expression profile in foetal rats subjected to hypoxia (10.5%) showed 48 genes that differed from the normoxic control. For example, there was an up-regulation of metabolic and oxidative stress-related genes, such as glutathione S-transferase Yb subunit and cytochrome oxidase, subunit I. In addition, there were downregulations in proliferation, cell signalling, protective and communication-related genes [107].

1.5.3 Adult adverse effect

There is a lack of epidemiological links between prenatal hypoxia and adverse effects on the adult human offspring. However, when considering the aforementioned IUGR and its link to adverse effects [8] there is a worrying pattern arising. Both maternal smoking and high altitude living have been linked to reduced birth weight in humans [97, 108]. These data, coupled with animal studies that show adverse effects in the adult offspring, support the idea that prenatal hypoxia can have a major and long term impact on human health.

1.5.3.1 Effects on the whole heart, organ level

The effect of prenatal hypoxia will vary depending on the extent and timing of the insult. The exact relationship between the level of hypoxia and effect is yet to be explored. Nonetheless, several complications regarding the cardiovascular system have been recorded. Rueda-Clausen et al. subjected pregnant rats to 12% oxygen for the last seven days of the pregnancy. The treatment led to IUGR in both males and females; body weight caught up at one week of age in both sexes. However, after 16 weeks the males from hypoxic pregnancies again showed a lower body weight than males from normoxic offspring. The females stayed unchanged after catching up at week one. At 12 months of age, the males from hypoxic pregnancies had a larger heart, and LV, to body weight ratio, compared to the males from normoxic pregnancies. Using working heart perfusion they found that left ventricular end-diastolic pressure (LVEDP) was almost twice as high in both males and females from hypoxic pregnancies compared to offspring from normoxic

pregnancies at 12 months of age [19]. Niu et al. subjected male rates to 13% oxygen for 12 days (GD 6-20) and they too reported increased LVEDP in adult (4 months of age) offspring, they also reported increased cardiac sympathetic dominance but no changes in protein abundance for β1-adrenergic or muscarinic receptors. Interestingly, both of these effects were reversed by maternal antioxidant treatment [31].

In addition, an altered response to adrenergic and cholinergic stimulation has been seen in several studies. Using the same treatment and model as Niu et al., Giussani et al. showed not only an increase response to the β1-adrenergic receptor agonist, isoprenaline, but also a decreased response with the muscarinic agonist, carbachol. Again, these effects were reversed with maternal antioxidant treatment [20]. Another worrying effect reported by Niu et al. is increased susceptibility to I/R injury. This is a commonly reported complication and has been seen in several studies using adult rats previously exposed 10.5% oxygen for the last six days of gestation [17, 22, 109], 11.5% oxygen for the same period [28] and 13% oxygen during GD 6-20 [31]. This increased susceptibility to I/R injury has been suggested to link to decreased levels of PKCe. Adult offspring, from hypoxic pregnancies, showed decreased levels of PKCe in the heart. In addition treatment with PKCe translocation inhibitors, to offspring from normoxic pregnancies, could mimic the increased susceptibility to I/R injury seen in offspring from hypoxic pregnancies [17, 22, 29, 109].

PKCe interacts with both contractile proteins and mitochondria and thereby plays an important role in cardioprotection [110]. In the mitochondrion, PKCe interacts with a range of proteins including cytochrome c oxidase complex IV; [111]. This is further supported by the findings of Thompson et al. who saw decreased complex IV activity in adult male guinea pigs previously subjected to 10.5% oxygen for the last 14 days of gestation. In addition to this decrease in complex IV activity, they also reported reduced cardiac output, reduced maximal oxygen consumption rates and reduced respiratory reserve capacity. However, these effects were only seen in adult male offspring, not in the female offspring [30] which further supports the link to PKCe as Xue and Zhang showed decreased PKCe levels in males but not in

females [22]. In a follow-up study, Thompson et al. went on to show decreased protein levels of all five respiratory complexes in adult male cardiac tissue from hypoxic pregnancies while the females showed decreases only in complex I, III, and IV. The same experiment was done in isolated cardiomyocytes which showed decreased protein content only for complex IV in males but none of the other male complexes and nothing in females. They also measured complex I and IV activity rates in both tissue and isolated cardiomyocytes. In both preparations complexes I and IV had decreased activity rate in male hypoxic offspring compared to male normoxic offspring but no differences in females offspring [112].

1.5.4 The unknowns

As already discussed, the effects of prenatal hypoxia in the adult heart have been explored to some extent. These previous studies, however, have mainly focused on whole heart function and prevention. Little is known about altered cellular processes and how these, in turn, affect the whole heart.

Reduced cardiac output and increased susceptibility to I/R injury have been shown in a few separate studies [28, 31, 113] but little research has been dedicated to exploring the underlying cellular alterations. One such alteration could be Ca^{2+} handling maladaptation. Niu et al. showed increased SERCA2a protein abundance in males from hypoxic pregnancies compared to males from normoxic pregnancies, which could not be reversed by maternal antioxidant treatment [31]. However, to our best knowledge, the Ca^{2+} handling properties in cardiac myocytes from adult offspring subjected to prenatal hypoxia has not been explored. Finding answers on a cellular level could better help us understand how to diagnose and possibly treat these adverse outcomes.

At the mitochondrial level, as previously discussed, there have been studies showing alterations to PKCe in prenatal hypoxia, but few studies have focused on the effects this has on cardiac function in offspring from hypoxic pregnancies. There are suggestions that PKCe could affect mitochondrial processes but to our knowledge, there are limited mitochondrial studies and in those, much has been

left unexplored. The study of Thompson et al., looking at mitochondrial oxygen consumption and protein abundance, although an important first step, left a lot of questions unanswered as the many respiratory states of the mitochondria were not thoroughly explored [30, 112]. In addition, to our best knowledge, no previous studies have explored possible changes to mitochondrial ROS production, abundance or morphology in relation to prenatal hypoxia. As there is compelling evidence for a link between mitochondria and I/R injury, exploring mitochondrial alterations in adult offspring from prenatal hypoxia could prove crucial to finally elucidate the source of the adverse outcomes.

A final consideration is a sexual dimorphism. One decade ago, Xue and Zhang pointed to a sexual dichotomy in regards to the effects of prenatal hypoxia [22]. Despite this, many studies regarding the effect of prenatal hypoxia on the adult heart are still one-sided and look mainly at males. It could possibly be argued that as males seem to suffer a greater effect [22, 30, 112], there lies more interest in the exploration of males. However, in such an argument one is likely to overlook that the answers could possibly lie in the intrinsic differences between males and females. Lately, it has become very apparent that the differences between the sexes affect the response to physiological challenges. It is crucial to assess males and females separately and to take the sex into account whilst doing basic research and possibly even when prescribing medicine [114].

1.5.5 Possible interventions

Currently, there are no obvious tools available to show that an adult was previously subjected to prenatal hypoxia during development. Birth weight may be an indication but as animal studies have shown adverse outcome with no IUGR, this is not a reliable measurement [22, 31, 98, 99]. As such, there lays great importance to characterise the phenotype and pinpoint a consistent marker for prenatal hypoxia. At the current time, there are however studies suggesting that intervention may be possible on the maternal level. Giussani's group have demonstrated that maternal antioxidant treatment can reverse the majority of adverse effects seen [31, 88, 115]. However, as treatment of non-hypoxic mothers generated an increase in SERCA2a

in the adult offspring and ROS acts as cell signalling molecules, this might be a dangerous path to walk and more studies are needed to determine whether or not this is a suitable treatment.

1.6 Aims

Prenatal hypoxia leads to developmental programming that in turn leads to adverse adult cardiac phenotypes. A common complication is increased susceptibility to I/R injury and it seems that males are more affected than females. A range of animal models and approaches have been used to generate the literature currently available. Previous literature has mainly been focused on whole heart function and, to some extent prevention, but very little research has been made on the cellular and intracellular level. In addition, although there have been results pointing toward different responses in male and female offspring, much of the current literature has overlooked this variable and not taken sex into account. Therefore, the current study aimed to:

1) Establish a murine model of chronic hypoxia (14% oxygen; GD 6-18) taking into account litter size, maternal body weight, food and water intake, offspring birth weight, sex ratio as well as to characterise the whole heart function and morphology (Chapter 2)
2) Explore the metabolic phenotype of adult offspring from prenatal hypoxia, mainly focusing on the capacity for mitochondrial oxygen consumption and ROS production, but also mitochondrial morphology and abundance (Chapter 3)
3) Asses cardiomyocyte Ca^{2+} amplitudes, SR Ca^{2+} content, Ca^{2+} clearance mechanisms and response to adrenergic agonists (Chapter 4)

2 Model validation

2.1 Introduction

There are several ways to simulate prenatal hypoxia but many of these methods come with varying degrees of clinical relevance and mimic different complications for human pregnancies. The ligation of uteroplacental vessels, bilateral uterine vessel ligation and placental restriction have all been used as models for pre-eclampsia; however, these methods do not just affect oxygen delivery, but also glucose and insulin. As such, these models make it hard to separate and interpret the impact of hypoxia from the other insults [116]. Hypoxic pregnancies where ambient oxygen levels are altered (as used in this study) are also a common way to induce prenatal hypoxia. This latter model is good for mimicking pregnancy complications at high altitude. High altitude has been shown to alter the maternal blood pressure curve associated with uncomplicated pregnancies. In the uncomplicated pregnancy maternal blood pressure declines, due to peripheral vasodilation, until week 18-20 of pregnancy where blood pressure starts to increase. At high altitude (3100 metres; approx. 14% O_2) however, blood pressure decline is lost and instead blood pressure was increased throughout the entire pregnancy, which resulted in a higher mean arterial blood pressure during week 14 through 33 compared to pregnancies at lower altitude (1260 metres; approx. 17.5% O_2). Pre-eclampsia at sea level generates a similar pattern in blood pressure, although more pronounced, thus validating studies of high altitude pregnancies for mimicking complications at sea level [87, 117, 118]. Experimentally, the oxygen levels used in previous studies vary from 9% – 14% oxygen, generating a variety of responses in the offspring. Lower levels have been suggested to cause nutrient restriction, leading to an additional insult [119, 120], which could be accounted for by pair feeding in a control group. Giussani et al. designed a prenatal hypoxia protocol, with 13% O_2, which was based on oxygen levels that are known to lead to complication of pregnancies in the Bolivian highlands (≈3600 metres) located at an altitude that has been well correlated with IUGR [97, 121]. This study also showed that

this level of hypoxia did not affect maternal food intake and, therefore, did not cause a nutritional insult [20].

Prenatal hypoxia has been studied in a range of animals, including sheep, rats, mice and guinea pigs. As previously mentioned (in section 1.3.2.), each model has its benefits and drawbacks. Mice, chosen for this study, have several advantages, e.g. mice have a short generation time which is useful for longitudinal studies and investigating multiple generations. Additionally, mice are relatively easy to modify genetically which allows the study of particular genes of interest (e.g. knockout and knockin models)[122, 123]. For this study, the obvious differences between mice and men, e.g. short gestation time and differences in physiology were considered acceptable in comparison to the advantages. The mouse model of prenatal hypoxia was novel to the University of Manchester and was developed and explored throughout the duration of this study.

In the first section of this study, our aims were to explore the effects of prenatal hypoxia on maternal parameters (food intake, water intake and body weight), offspring body weight (including whether or not there are signs of IUGR) and whole heart physiology.

2.2 Methods

2.2.1 Animal husbandry and incubations

Animal studies were performed in accordance with the United Kingdom Animals (Scientific Procedures) Act 1986 and were approved by the University of Manchester Ethics Committee.

Pregnant, previously un-littered, C57BL/J6 mice weighing 18-30 grams, were acquired from Manchester University incubator building and housed in the University of Manchester animal facilities under 12:12 light cycles with ad libitum food and water availability in normal oxygen condition (21% O_2). Mice were randomly assigned to two groups; one group was kept under normoxic (N) conditions in the normal animal facility (21% O2; N) as a control, and the other group were transferred to an oxygen-controlled environment, Coy O_2 InVivo Glove Box (Coy Laboratory Products, Grass Lake, MI) at gestation day (GD) 6, where they were subjected to a hypoxic (H) environment (14% O2; H) until GD 18, at which point they were returned to normal conditions to litter. In addition to controlling O_2 concentration, the Coy O_2 InVivo Glove Box also maintains humidity (matched to control level), CO_2 and has a separate air-lock chamber which can be purged for transferring materials; this system makes the chamber ideal for long-term studies. Maternal food intake (FI) and water intake (WI) were monitored daily (weekends exempt) and are reported as a relative change from GD3 to assure that the hypoxic insult was not accompanied by a nutrient insult. In addition, maternal body weight (BW) was measured at the same time as food and water for the normoxic group. However, this was not possible for the hypoxic group, as the setup did not allow for safe weighing of the dams in the hypoxic chamber, as such these days were not monitored. The mice littered at GD 20-22 day in the animal facility, in normoxic conditions. If the litter was larger than six pups it was culled down to six to assure standardized maternal care and feeding. When possible, the cull was made to leave three of each sex. Sexing was done by visual determination of the presence or absence of dark pigmentation on the perineum [124, 125]. The offspring were weaned off the mother at 4-6 weeks of age. Offspring were then kept in the same

conditions up until an age of between four and ten months old (experiment dependent, specified in each subsection) upon which they were sacrificed by cervical dislocation.

2.2.2 Model validation and characterisation of the cardiac phenotype

Before assessing the impact of prenatal hypoxia on cellular and intracellular function (chapter 3 and 4), the whole heart function and structure were assessed both at rest and after an in vitro period of I/R. Increased susceptibility to I/R injury is a common characteristic of adults from hypoxic pregnancies. As previously mentioned, a link between I/R damage and mitochondrial ROS production has been established and this led us to take an interest in the programming of mitochondrial function following a prenatal hypoxic insult. As such, it is important to explore the response to I/R in our model as well as to characterise any alterations to the normal cardiac function.

2.2.2.1 Echocardiography

Mice (from normoxic and hypoxic pregnancies) of 25±2 weeks of age had fur from the neckline to mid-chest level removed with hair removal cream (Veet, Slough, UK) one day prior to echocardiography. On the day of data collection, mice were anaesthetized using isoflurane and kept anesthetised on a heated mat by the use of a nose cone with a continuous flow of 1.0% isoflurane mixed with 0.5 L/minute 100% O_2. Preheated (37°C) ultrasound gel was applied to the chest and transthoracic two dimensional and M-mode echocardiography was performed by Dr Min Zi (Elizabeth J. Cartwright's group, University of Manchester, UK) [126, 127]. Parameters recorded were: body weight (BW), heart rate (BPM), left ventricular diameter (dD and sD; diastolic and systolic, respectively), intraventricular septum diameter (dIVS and sIVS), posterior wall thickness (dPW, sPW) and ejection fraction (EF).

2.2.2.2 Ischaemia-reperfusion

Adult male and female offspring (39 ± 2 weeks of age) from hypoxic and normoxic pregnancies were sacrificed by cervical dislocation, and the heart was rapidly

excised and washed in ice-cold phosphate-buffered saline (PBS). The aorta was cannulated with a 24 gauge reusable feeding needle (Fine science tools, Heidelberg, Germany) and sutured using cotton thread. The feeding needle was attached to a 1ml syringe filled with ice-cold Krebs solution (NaCl 120mM, $NaHCO_3$ 25mM, KCl 5.9mM, $MgSO_4$ 1.2mM, $CaCl_2$ 1.75mM and glucose 10mM) that had previously been aerated with 95% O_2 and 5% CO_2 for a minimum of 30 minutes. The positioning of the cannula was deemed correct if the coronary arteries were cleared of blood when the solution was carefully pushed through using the 1ml syringe. The heart was then rapidly transferred to a langendorff perfusion system with gravity fed Krebs (figure 2-1); constant pressure at 100 cm H_2O; constantly aerated with 95% O_2 and 5% CO_2). Krebs was heated so the effluent reached 37°C. The left atrium was removed with a single cut and a deflated silicone balloon (kindly produced and donated by Dr Junhui and Prof. Murphy, Bethesda, MD) was inserted into the lumen of the left ventricle and then inflated to reach a diastolic pressure of 5-10mmHg. The balloon was tied onto thin tubing, filled with PBS, and connected to a pressure transducer (ADInstrument MLT0380D, Colorado Springs, CO) to a computer running LabChart (LabChart 7 Pro, ADInstruments, Colorado Springs, CO). The heart was left to stabilize for 15 minutes and then lowered into a jacketed beaker filled by the effluent of the heart. The beaker was covered with parafilm and perfusion was stopped for 20 minutes (ischaemia). The heart was then reperfused for 30 minutes by allowing Krebs to once again flow and values were taken at -10, -5, 5, 10, 15, 20 and 30 minutes where minute zero is the start of the ischaemia.

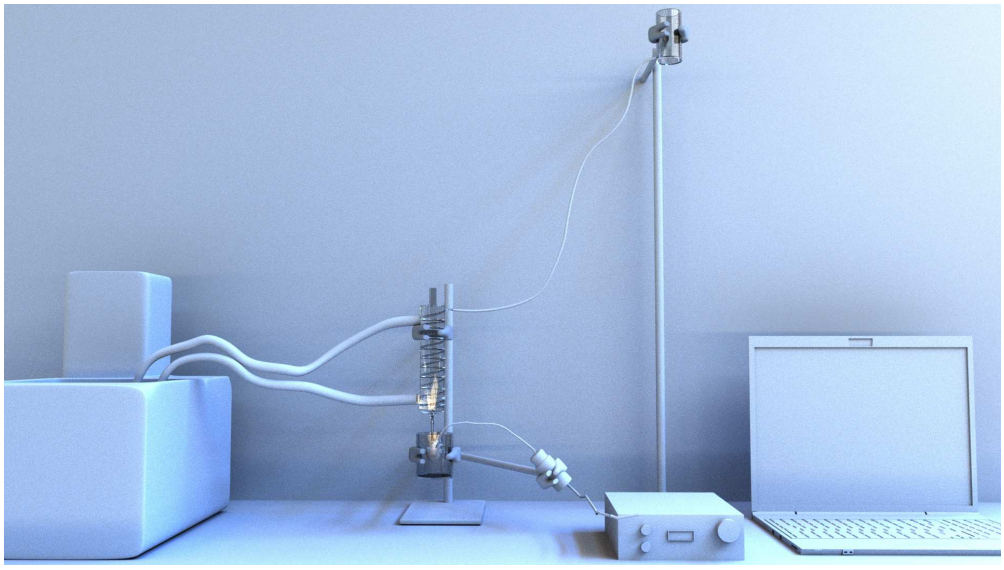

Figure 2-1 Gravity fed langendorff. A representative picture of the gravity-fed langendorff set up for the I/R challenge.

2.2.3 Statistical analysis

Maternal body weight (BW), food intake (FI) and water intake(WI) are expressed as scatter plots (including all measured points). BW was statistically tested using mixed-effects analysis comparing treatments at day 6 and 19 and showed no differences between dams from normoxic environment compared to hypoxic environment at day 6 or 19. The FI and WI data from the dams in a normoxic environment were statistically compared with data from dams in a hypoxic environment by fitting linear regression curves to compare slopes. Offspring BW is presented as scatter plots expressing means ± SEM. These data were statistically compared by mixed-effect analysis using maternal oxygen level as random effect and Tukey's correction for multiple comparisons test. Maternal data were compared normoxic versus hypoxic treatment and for offspring; BW was compared within sexes between treatments. Fitted slopes were compared statistically using Graphpad Prism®, version 8 (Graphpad Software, San Diego, CA). Ischaemia-reperfusion data are presented as scatter plots expressing mean ± SEM. The data were only statistically tested for females, due to low n-values in the male group, using Wilcoxon test in SigmaPlot, version 12.5 (Systat, San Jose, CA).

2.3 Results

2.3.1 Biometrics

Maternal body weight (figure 2-2 A) is presented as an accumulative increase. . The data showed no significant difference between normoxic (N) and hypoxic (H) dams at day 6 (p=0.41) or day 19 (p=0.63, n=16 N and 11 H). Maternal food intake (figure 2-2 B) is presented as accumulative food intake, also fitted with a linear regression curve. No significant difference was recorded as the slopes of the two regressions were tested against each other (p=0.44, n=16 N and 11 H). In addition, maternal water intake is presented as an accumulative water intake (figure 2-2 C) and linear regression curves were again fitted and compared but showed no significant difference (p=0.28, n=16 N and 11 H). To assess if the hypoxic offspring exhibit IUGR, offspring body weight was monitored weekly at weeks 0-5 as well as 8 and 12 of age (figure 2-2 D and E, males and females, respectively). A mixed-effect analysis showed no significant differences in birth weight (week 0, p=0.97 in males and p=0.95 in females, n=20-24) between the groups. At week 3, the males from normoxic pregnancies were significantly heavier than the females from hypoxic pregnancies. At week 5 and onwards, both groups of males were heavier than either group of the females. There was still no significant difference between mice subjected to prenatal hypoxia compared to mice from normoxic pregnancies within the sexes (p=0.60 for males and p=0.82 for females, n=5-7) at week 12.

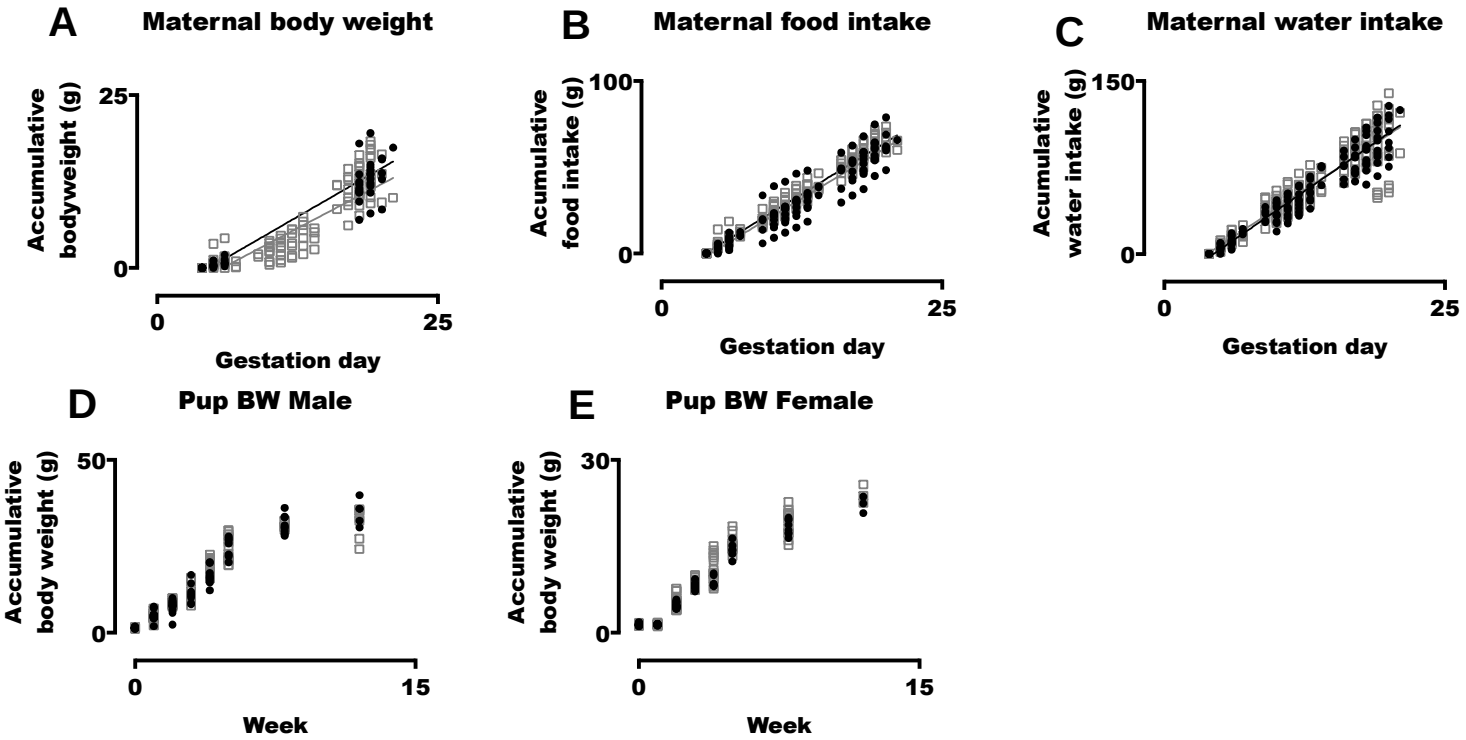

Figure 2-2 Maternal BW, FI, WI and pup BW. Maternal health was assessed by measuring body weight (A) food (B) and water intake (C) throughout gestation. Hypoxic dams are symbolized in filled circles and normoxic in grey boxes. Data are presented in scatter plots containing all data points, n=16N, 11H dams. Maternal FI and WI data and fitted with linear regressions to allow comparison between groups. Maternal BW was tested using mixed-effects analysis comparing hypoxic and normoxic treatment at day 6 and 19. There were no differences between treatments in BW, FI or WI. Offspring from hypoxic and normoxic pregnancies were observed for body weight. No differences in body weight in males from hypoxic pregnancies (black circle) compared to normoxic pregnancies (grey square; D) nor in females from hypoxic pregnancies (black circle) compared to normoxic pregnancies (grey square; E) at any of the time points measured. Data are presented as mean ± SEM, n=20-24 pups at week 0 and n=5-7 pups at week 12 and tested for mixed-model effects with Tukey's correction for multiple comparisons.

2.3.1.1 Litter sizes and sex ratios

Litter size and sex ratios were noted before culling to further assess the effect of hypoxia during pregnancy. Total litter size was 6.1 ± 0.5 from normoxic pregnancies and 6.6 ± 0.6 for hypoxic pregnancies. There were no differences in the litter sizes or in the ratio between males and females when comparing litters from hypoxic pregnancies with litters from normoxic pregnancies (figure 2-3).

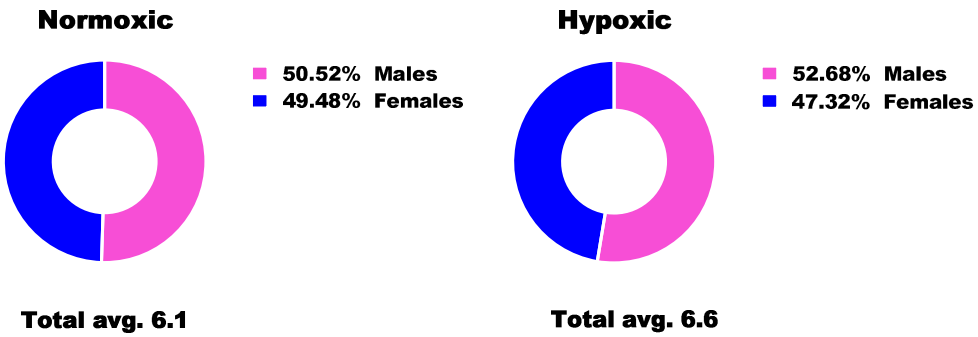

Figure 2-3 Litter sizes and sex ratio. There were no differences in litter size or sex ratio between litters from hypoxic and normoxic pregnancies as tested with both two-way ANOVA (based on percentages) and a Fishers exact test (on the sum of all animals). Presented as a total mean for both groups and a percentage of males and females in each group with males in pink and females in blue; n=16 normoxic litters and n=17 hypoxic litters.

2.3.2 Echocardiography

Echocardiography allowed for the assessment of whole heart function at rest. There were no significant differences seen in the parameters measured (in mm unless stated otherwise): left ventricular diastolic diameter (dD), left ventricular systolic diameter (sD), diastolic intraventricular septum (dIVS), systolic intraventricular septum (sIVS), diastolic posterior wall thickness (dPW), Systolic posterior wall thickness (sPW) and ejection fraction (EF, in %). Recorded values for these parameters are presented in table 2.1.

	MALE				FEMALE			
	Normoxic		Hypoxic		Normoxic		Hypoxic	
	Average	SEM	Average	SEM	Average	SEM	Average	SEM
Body weight (g)	36.45	1.06	40.36	1.85	29.68	4.46	32.82	1.78
HR (bpm)	494.00	7.94	539.40	14.92	540.00	31.94	529.40	16.78
dD	4.20	0.15	4.51	0.12	3.98	0.07	4.06	0.06
sD	2.54	0.14	2.68	0.17	2.65	0.09	2.42	0.13
dIVS	0.86	0.02	1.02	0.02	0.85	0.02	0.93	0.04
sIVS	1.42	0.04	1.63	0.05	1.29	0.06	1.44	0.06
dPW	0.82	0.01	0.78	0.03	0.72	0.06	0.81	0.06
sPW	1.26	0.04	1.25	0.08	1.13	0.01	1.26	0.06
EF (%)	77.77	2.34	78.69	2.77	70.00	3.64	78.59	2.97

Table 2.1 Echocardiography parameters.
There were no significant differences in the whole heart parameters measured. Data are presented as mean ± SEM, n=3 offspring from normoxic pregnancies of each sex and n=6 offspring from hypoxic pregnancies of each sex.

2.3.3 Ischaemia-reperfusion

Subjecting hearts from hypoxic and normoxic pregnancies to in vitro ischaemia/reperfusion (I/R) on a langendorff perfusion system allowed us to assess susceptibility to I/R injury. Males (figure 2-4 A) and females (figure 2-4 B) were subjected to a 20-minute long ischaemic period, in vitro, on a langendorff setup. This was followed by 30-minute long reperfusion. Left ventricular developed pressure (LVDP) was measured before the ischaemic period and during reperfusion. There were no differences in recovery of left ventricular developed pressure between offspring from hypoxic pregnancies compared to offspring from normoxic pregnancies (not tested statistically due to low power).

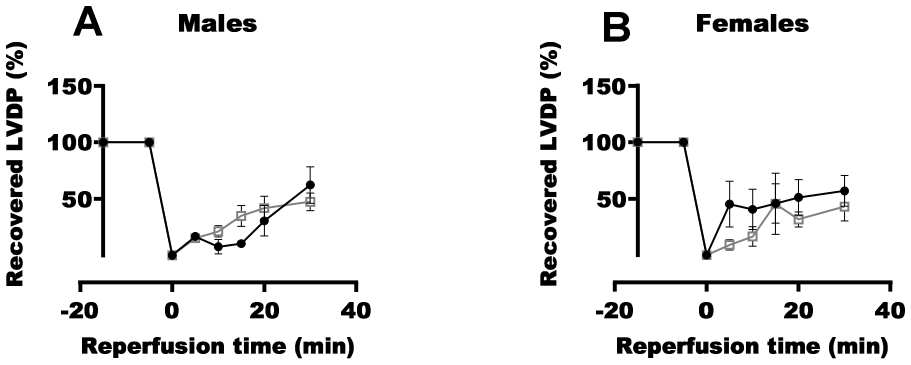

Figure 2-4 I/R recovery. Recovery from ischaemia-reperfusion was not statistically tested for males (A) and showed no differences between females (B) in offspring from normoxic pregnancy (black filled circles) compared to offspring from hypoxic pregnancies (open grey square). Data are presented as mean ± SEM, n=2-6 for males and 3-4 for females.

2.4 Discussion

This study showed no changes in maternal body weight, food intake or water intake. Additionally, there were no changes in basal heart function and no ventricular hypertrophy. The offspring showed no signs of nutrient restriction or IUGR and there were no differences in response to I/R in offspring from hypoxic pregnancies compared to offspring from normoxic pregnancies. The model did not show any of the conventional traits of prenatal hypoxia, but, as discussed in chapter 3, is not exempt from a cellular phenotype.

2.4.1 Maternal data

The link between altitude and weight loss is well established regarding its occurrence, although the mechanisms are somewhat debated. A combination of reduced food intake and increased metabolic rate at high altitude (>2700 metres) has been shown to lead to weight loss [128, 129], with energy regulating hormones such as ghrelin and leptin being suggested as key regulators of this phenomenon [129, 130]. Food intake and body weight reduction due to hypoxia have previously been seen during a hypoxic period in both pregnant rats [18, 131-134] and mice [135, 136], that showed reduced food intake. In three of the aforementioned cases [131, 132, 136], the reduced food intake was accompanied by a reduction in maternal body weight gain. Maternal body weight was not reported in the other studies [18, 133, 135]. While maternal nutrition itself can affect a developing foetus [18, 137-139], lack of difference in maternal food intake, water intake and body weight in the current study, suggests that any phenotype alterations are solely due to the hypoxic insult [31].

2.4.2 Intrauterine growth restriction

David Barker's theory stated that IUGR was the cause of altered adult phenotypes [26]. There are many reports of IUGR coupled with hypoxic pregnancies in both rats [18, 19, 131-133, 140, 141] and mice [135, 142, 143]. However, in support of the data presented here, several studies have shown adverse adult phenotypes in the absence of IUGR following hypoxic pregnancies [20, 22, 31, 144, 145]. Moreover, the occurrence of IUGR is

difficult to predict. One study with 14% O_2 during GD 18-21 showed a 20% decrease in birth weight [141] while another study showed no changes in birth weight, using 14% O_2 during GD 17-21 [146], despite the insult in the latter study lasing one day longer, both studies were done using rats so the reasons for these discrepancies are unclear. It is worth noting that neither study reported maternal food intake. While interesting, the reasons for these discrepancies cannot be discerned in this current study.

2.4.3 Litter size and sex ratios

Hypoxic pregnancies have been shown to reduce litter sizes in a few studies with rats [132, 134, 147] and one study in mice [143]. In these studies, however, O_2 levels varied between 9.5-12%, and to our knowledge, alterations in litter size have not been shown in studies with higher levels of O_2 concentration.

As previously mentioned, there are differences in the response to prenatal hypoxia when comparing male and female offspring. Therefore, this study also investigated the number of males and females born from hypoxic pregnancies compared to normoxic pregnancies. No differences were seen in this current study which may or may not explain the lack of this metric in previous literature. Another explanation for the lack of reported sex ratios could stem back to the issue raised in Lee's review from 2018 [148] where it was pointed out that during 1909-2009, only 15% of biomedical research included both males and females.

2.4.4 Whole heart function

2.4.4.1 Resting

Resting whole heart function in the adult offspring was not affected by prenatal hypoxia in the current study. While a subset of previous studies has seen changes to resting heart function such as ventricular wall hypertrophy and impaired relaxation in adult offspring from hypoxic pregnancies compared to normoxic pregnancies [31], several studies show that the main adverse outcome of prenatal hypoxia is intolerance to stressors. Most commonly reported is an increased susceptibility to

I/R injury and decreased LV recovery post-ischaemia in adult offspring from hypoxic pregnancies [29, 31, 109, 113]. In addition to this, experimental studies have also shown altered handling of cholinergic and adrenergic tones in adult rats from hypoxic pregnancies [31], as well as in foetal and juvenile chicks incubated in hypoxic conditions [33, 149].

2.4.4.2 Response to I/R challenge

Due to the proposed increased susceptibility to stressors (discussed in the previous section) excised adult hearts from hypoxic pregnancies were subjected to an in vitro I/R challenge. In the current study, no differences were seen between offspring from hypoxic pregnancies compared to offspring from normoxic pregnancies. This could be explained by circumstances discussed in study limitations (section 2.4.5), but could possibly also be explained by the milder nature of the insult as previous studies showing increased susceptibility to I/R, have used 13% O_2 or lower.

2.4.5 Study limitations

As stated in the discussion, there are doubts regarding the I/R data. The langendorff whole heart I/R preparation was new to our group and there was little to no knowledge regarding the technique in our vicinity. Experiments were performed on a trial and error basis with help, via email communication, from Junhui Sun, a staff scientist in Elizabeth Murphy's group at the National Heart, Lung, and Blood Institute in Bethesda, Maryland. While other studies report left ventricular end-diastolic pressure (LVDP) >80mmHg at baseline [20, 109, 150], this study generated at best 65.74mmHg in one normoxic male with the second normoxic male at 16.55mmHg. Hypoxic males spanned from 66.18mmHg to 2.12 mmHg. Similar span was seen in females, both normoxic (5.92mmHg to 46.8mmHg) and hypoxic (1.39mmHg to 20.04mmHg). As such, it can be concluded that these data are not particularly reliable and therefore this study would have benefited from more time to perfect the technique. In addition, to the aforementioned issues, the number of repeats was very low.

3 Metabolic study

3.1 Introduction

The effects of prenatal hypoxia on cardiac structure and function have previously been studied in the adult offspring with a variety of outcomes, seemingly dependent on oxygen level, duration of insult and animal model. The most frequent complication and the complication with the most supporting literature is that of increased susceptibility to ischaemia/reperfusion (IR) injury [17, 22, 28, 29, 31, 109, 144]. Myocardial infarction and associated I/R injuries are still a great concern in the world. Although there are reports of a decline in the instance of ischaemic heart diseases, acute myocardial infarction still affects more than 1 in 100 people and, due to an ageing population, the years of subsequent disability related to ischaemic heart diseases are still growing [151]

The link between mitochondria and I/R injury is well-established with increased mitochondrial ROS production leading to cellular damage and apoptosis [70-75, 152]. Comparatively recently, a more causative effect has been suggested, whereby mitochondria act as the catalyst for the increase in ROS production. The hypothesis states that during the ischaemic period, complex II substrate, succinate, builds up in the mitochondrial matrix due to a lack of oxygen, the final electron acceptor. Once reperfused, redox potential in the ET-pathway (e.g. the Q-pool) is increased to a level where complex I begin to run in reverse. This creates a greatly increased electron slippage out of complex I and, subsequently a spike in ROS production, leading to damage [80]. The baseline production of ROS is a balance between mitochondrial respiration and redox potential in the ET-pathway. Therefore, one explanation for the increased susceptibility to I/R injury in offspring from hypoxic pregnancies is that they're prone to greater ROS production due to differences in electron transport chain function programmed by prenatal hypoxia. Moreover, although often overlooked, there are sex-dependent differences in the ability to tolerate I/R in adult offspring from hypoxic pregnancies [22]. For example, recent studies have shown pregnant guinea pigs subjected to 10.5% oxygen produce

offspring with IUGR, but only males show signs of altered basal heart function, while females cardiac function is similar to controls. In line with this data, male guinea pigs from hypoxic pregnancies had decreased mitochondrial respiratory capacity, decreased complex IV activity and decreased protein expression of all five respiratory complexes of the mitochondria. The same study showed prenatal hypoxia had no effects on female mitochondrial oxygen consumption or complex IV activity. However, protein expression of complex I, III and IV was lower in females from hypoxic pregnancies, compared to normoxic pregnancies [30, 112]. Unfortunately, these studies did not investigate how prenatal hypoxia may impact other aspects of mitochondrial physiology, including mitochondrial ROS production, the response to I/R, mitochondrial morphology or activity of antioxidant systems. Therefore, additional studies are necessary to fully answer the question of whether prenatal hypoxia alters mitochondrial function and ROS production, in the absence of any nutritional stress.

In this current study, we hypothesised that altered mitochondrial function in males from hypoxic pregnancies would lead to increased ROS production. We hypothesised that prenatal hypoxia would have less of an effect on the female mitochondrial phenotype, and in this way, they would be somewhat protected from the negative effects of prenatal hypoxia.

3.2 Methods

3.2.1 High-resolution oxygen consumption and ROS production

Mitochondrial oxygen consumption was assessed by high-resolution respirometry using an Oroboros Oxygraph-2k (Oroboros Instruments, Innsbruck, Austria) which measures the oxygen content in a semi-closed chamber. In addition to this, Oroboros instruments have developed a fluorescent probe to excite and measure fluorophores at different wavelengths (O2k-Fluo LED2-Module, Oroboros Instruments, Innsbruck, Austria); this module was used in the current study to measure ROS production. A small piece (~50mg) of fresh left ventricular tissue from adult mice from hypoxic and normoxic pregnancies, sacrificed by cervical dislocation, was homogenized (IKA Ultra-turrax T25) in mitochondrial respiration media (MiR05; containing: EGTA 0.5mM, $MgCl_2$ 3mM, K-mes 60mM, KH_2PO_4 10mM, HEPES 20mM, sucrose 110mM and 1% BSA). Subsequently, 0.16 ±0.04 mg of homogenised tissue was injected into each chamber of the Oxygraph-2K. The two chambers of the Oxygraph were prepared with 10µM Amplex® UltraRed and 1U/ml horseradish peroxidase (HRP). Amplex® UltraRed oxidizes in the presence of H_2O_2 and forms resorufin in the presence of H_2O_2, using HRP as a catalyst (figure 3-1). Amplex® UltraRed was excited at 563nm and emission was read at 587nm.

This method allowed for sensitive measurements of H_2O_2 production. In addition, 5U/ml superoxide dismutase (SOD) was added to convert superoxide into H_2O_2, allowing the majority of extracellular ROS to be quantified as fluorescence through the Amplex® UltraRed system.

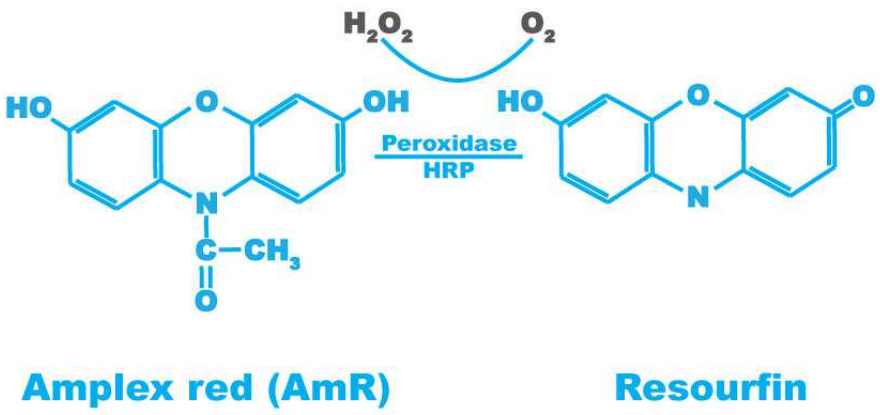

Figure 3-1 AmR oxidates to form the fluorophore resorufin

3.2.1.1 Substrate-inhibitor titration (SUIT) protocol

Leak respiratory state, through complex I, was achieved by the addition of 5mM pyruvate (P), 2mM malate (M) and 10mM glutamate (G) to each chamber which assured full substrate saturation at complex I. Full saturation minimizes the risk of any limiting factors occurring within the Kreb's cycle. In this state, a lack of ADP means protons cannot enter the matrix through complex V, therefore protons can only re-enter the matrix via proton leak pathways. As soon as oxygen consumption was stable, ADP was injected to saturated concentrations (5mM) to activate oxidative phosphorylation through complex I pathways ($OXPHOS_{CI}$). To saturate complex II pathways, 10mM of succinate was added to the chambers ($OXPHOS_{CI+CII}$) followed by titration of Carbonyl cyanide-*4*-(trifluoromethoxy)phenylhydrazone (FCCP) to a final concentration of 0.1-0.3µM, to uncouple the ET-pathway. This latter state allows the free movement of protons from the inter-membrane space across the inner membrane to the mitochondrial matrix and thereby assesses the maximum uncoupled ET-pathway capacity ($ET\text{-}max_{CI+CII}$), which removes any respiratory limitation from complex V. During $ET\text{-}max_{CI+CII}$, 0.5µM rotenone (complex I blocker) was added to assess the succinate driven oxygen consumption separately ($ET\text{-}max_{CII}$). To block the ET-pathway and assess residual non-mitochondrial oxygen consumption (ROX), 2.5 µM of complex III

inhibitor, antimycin A, was added. At this point, there will be no electrons transported to complex IV. N,N,N',N'-tetramethyl-p-phenylenediamine (TMPD) can act as an electron donor straight to complex IV and therefore allow measurement of maximum capacity of the complex. TMPD is easily auto oxidised, therefore 2mM of ascorbate was added with the TMPD to keep it in its reduced state. Due to the reactive nature of TMPD, a separate background measurement after the addition of TMPD was needed; this was done by adding 50mM of sodium azide, a complex IV inhibitor (see top trace figure 3-2 for sample trace). The oxygen consumption rate after sodium azide addition was subtracted from the oxygen consumption before addition to establish maximal capacity of complex IV.

3.2.1.2 Effect of CIV inhibition on ROS production

A separate protocol was used to assess the impact of changes in complex IV on ROS production. The homogenate sample was incubated with substrates for $OXPHOS_{CI+CII}$ and measurement of ROS production (HRP, AmR, SOD, P, M, G, ADP); the sample was then left to respire until a steady state was reached. Thereafter, sodium azide was titrated in 0.25mM steps from 0 to 1.75 mM to inhibit complex IV (see the bottom trace of figure 3-2 for sample trace). The resulting value from measured ROS production is presented in relation to simultaneously measured oxygen consumption to allow for assessment of alterations to electron slippage. In a theoretical ET-pathway where there was no slippage, all electrons would be accounted for in O_2 consumption in a relationship of four electrons per one O_2.

3.2.1.3 Calculations and normalisation

All homogenates used in the Oxygraph O2k were frozen to allow for assessment of CS activity (see 3.2.2.2 for detailed methods) at a later date. All O_2 consumption data were normalized to CS activity (O_2/CS). The respiratory acceptor control ratio (RCR) is a measurement of OXPHOS coupling efficiency. RCR was calculated by dividing oxygen consumption after the addition of succinate (with complex I and complex II substrates as well as ADP; $OXPHOS_{CI+CII}$) with oxygen consumption during leak (complex I substrates only). The phosphorylation system control ratio (P/E), a measurement of how well the phosphorylation system matches the ET- pathway

capacity, was calculated by dividing oxygen consumption after the addition of succinate (with complex I and complex II substrates as well as ADP; $OXPHOS_{CI+CII}$) with oxygen consumption after the addition of FCCP (ET-max_{CI+CII}). The leak control ratio was calculated by dividing oxygen consumption in leak state (complex I substrates only) with the oxygen consumption after addition of FCCP (ET-max_{CI+CII}). A completely uncoupled system shows L/E=1 and completely coupled at L/E=0. For assessment of the effect of sodium azide on ROS production, the value of ROS given was divided by the amount of O_2 consumed (ROS/O_2).

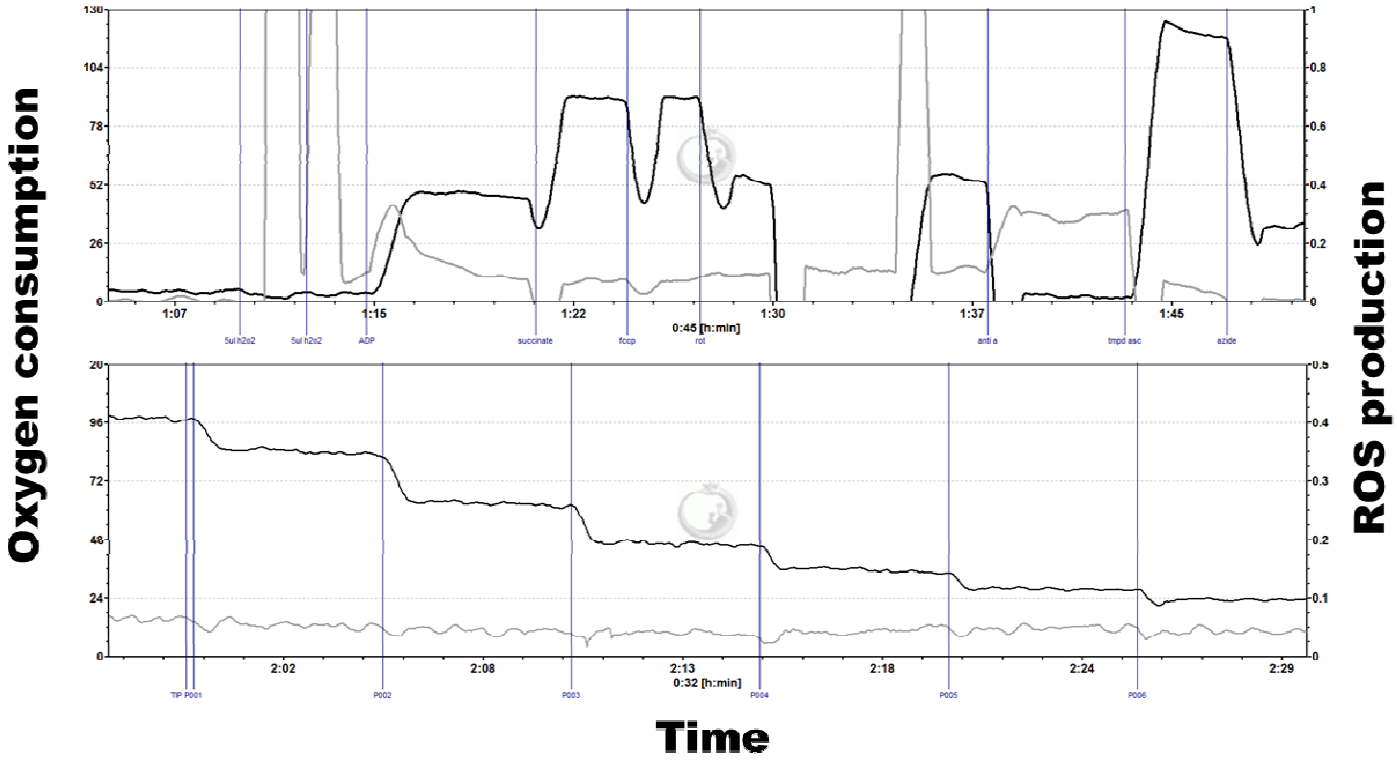

Figure 3-2 Sample trace from intact mitochondria. Oxygen consumption and ROS production measured in an Oroboros Oxygraph O2k with attached O2k-Fluo LED2-Module. Left Y-axis signifies oxygen consumption (black line) and right Y-axis, ROS production (grey line). In the top trace; a SUIT protocol, each titration step can be seen in blue below the X-axis. Injections are, in order, 2x 5 µl H_2O_2, ADP, succinate, FCCP, rotenone, antimycin A, TMPD+ascorbate and sodium azide, Not shown is the addition of 2 µl Amplex Ultrared, 5 µl horseradish peroxidase, 5 µl SOD, 5 µl malate, 5 µl pyruvate and 10 µl glutamate. In the bottom trace; CIV inhibition with azide, each vertical blue line represents one titration of 0.25mM azide not seen in the figure is titration of 2 µl Amplex Ultrared, 5 µl horseradish peroxidase, 5 µl SOD and substrates for $OXPHOS_{CI+CII}$

3.2.2 Spectrophotometry

Spectrophotometric assays were undertaken to assess protein content and the enzymatic activity of different complexes in the ET- pathway. Citrate synthase was also measured and considered as an indicator of mitochondrial density; this parameter was then used to normalize oxygen consumption to mitochondrial content.

3.2.2.1 Protein content

Protein content was assessed using Quick start Bradford dye reagent (Bio-Rad laboratories, Watford, UK); 5µl of the sample was left to react with 250µl Bradford quickstart reagent for 5 minutes in a 96 well plate. Quickstart BSA standard set (Bio-Rad laboratories, Watford, UK) were put in separate wells on the same plate and were used to create a standard curve to which samples were compared. Absorption was thereafter read at 550nm using a BioTek Synergy HTX multimode reader (BioTek, Swindon, UK) at 25°C.

3.2.2.2 Enzyme activity assays

Enzyme activity assays were inspired by Spinazzi et al. [153] and adapted to run in a 96 well plate. Approximately 20-50mg of tissue was homogenized in solution containing 20mM TRIZMA-base, 40mM KCl, 2mM EGTA and 250mM Sucrose (pH 7.4) using a FastPrep-24^{TM} 5G instrument (MP Biomedicals, Santa Ana, CA). The tissue was homogenized in two cycles of 30 seconds with a 180-second pause in-between. Samples were then spun at 600g for 10 minutes at 4°C and the supernatant was stored in -80°C until the day of the assay. Maximal enzymatic activity rate (V_{max}) was assessed with a BioTek Synergy HTX multimode reader (BioTek, Swindon, UK) at 37°C. The buffer components for each individual; assay are given below.

3.2.2.3 Citrate synthase

Citrate synthase activity was assessed in the presence or absence of oxaloacetate. Free acetyl-CoA would react with 5,5'-dithiobis(2-nitrobenzoic acid) and result in 5-

thio-2-nitrobenzoic acid that was read at 412nm over 10 minutes in a buffer with 100mM TRIS-base, 0.1% Triton-X-100, 0.5mM oxaloacetate, 0.3mM acetyl-CoA, 0.15 mM 5,5-dithiobis(2-nitrobenzoic acid) at pH 8.0.

3.2.2.4 Mitochondrial complex assays

Potassium phosphate buffer (KP) was used as the assay buffer for measuring the enzymatic activity of complex I, II and IV of the ET- pathway. The pH of the phosphate buffer was 7.5 and was achieved by titrating K_2HPO_4 with an equal concentration of KH_2PO_4.

Mitochondrial complex I activity was assessed by reading the reduction of 1,2-Diamino-2-methylpropane (DCPIP) at 600nm over 5 minutes. Assays were run in 50mM phosphate buffer with the addition of 3mg/ml BSA, 80µM DCPIP, 100µM NADH, 60µM Coenzyme Q_1 and 300µM KCN. To assure specificity, one replicate well included rotenone to block complex I (10µM). Complex II was also assessed by reading the reduction of DCPIP at 600nm over 5 minutes but in 25mM phosphate buffer with the addition of 80µM DCPIP, 20 mM succinate, 50µM decylubiquinone and 300µM KCN. For specificity, complex II activity was blocked in one replicated well using 10mM malonate. Mitochondrial complex IV activity was assessed in 50 mM KP buffer with 60µM reduced cytochrome c (cyt-c). Cyt-c was oxidized through complex IV and the change in redox status could be measured as absorption at 550nm over time without further chemical addition. To assure specificity complex IV was blocked in one replicate using 300µM KCN. The quality of the reduced cyt-c was assessed by measuring absorption of 20 µM reduced cyt-c at 550 nm and 565 nm, quality was deemed acceptable if this measurement generated a ratio of 6 or higher. KP buffer for complex I and complex II had pH 7.5 while the KP buffer for CIV had pH 7.0.

3.2.2.5 Calculations

For protein content, a standard curve was plotted with linear regression and accompanying formula. Formula was then applied to sample values to acquire the concentration in mg/ml. Values, for enzyme activities, were acquired as V_{max}

(maximum activity over time) and divided by protein content to correct for protein content in each sample.

3.2.3 Electron microscopy: Tissue preparation

Approximately two-millimetre pieces of the free wall of the left ventricle were dissected and immediately transferred to a solution of 2% formaldehyde, 2% glutaraldehyde and 0.1M HEPES for fixation. Tissue was removed from the initial fixation solution and prepared by Samantha Forbes at the Electron microscopy core facility at University of Manchester using what is known as the Elisman protocol [154]. Briefly, the tissue was stained with a series of different heavy metals to allow for increased resolution and contrast whilst imaging [155]. Following this, the tissue was dehydrated (stepwise), infiltrated with Taab 812 Hard Resin (stepwise), embedded in silicon wells and finally polymerized at 60°C for 24 hours.

3.2.4 Electron microscopy: Image acquisition

Images were taken at two different magnifications (x890 and x4800) using a transmission electron microscope (TEM; FEI Tecnai12 BioTwin at University of Manchester, EM facility). The lower resolution was used to analyse the mitochondrial abundance and the higher for cristae density within the mitochondria. Image analysis was done by our very talented student, Hajani Premanandhan.

3.2.4.1 Mitochondrial abundance

For mitochondrial abundance measurements, five images per mouse were acquired with n=2 (10 images) for males and females from normoxic pregnancies and n=4 (20 images) for males and females from hypoxic pregnancies. Using the freehand tool in the software Image J (version 1.52k, National Institute of Health, MD) mitochondria were traced and total area was expressed relative to the total area of the cell, which was also traced by the use of the freehand tool (see example in figure 3-3). Abundance is presented as a percentage, calculated as shown in equation 3-1

$$\text{Mitochondrial abundance as percentage } = \frac{total\ mitochondrial\ area\ (\mu m2)}{total\ cell\ area\ in\ image\ (\mu m2)} * 100$$

Equation 3-1 Mitochondrial abundance as percentage.

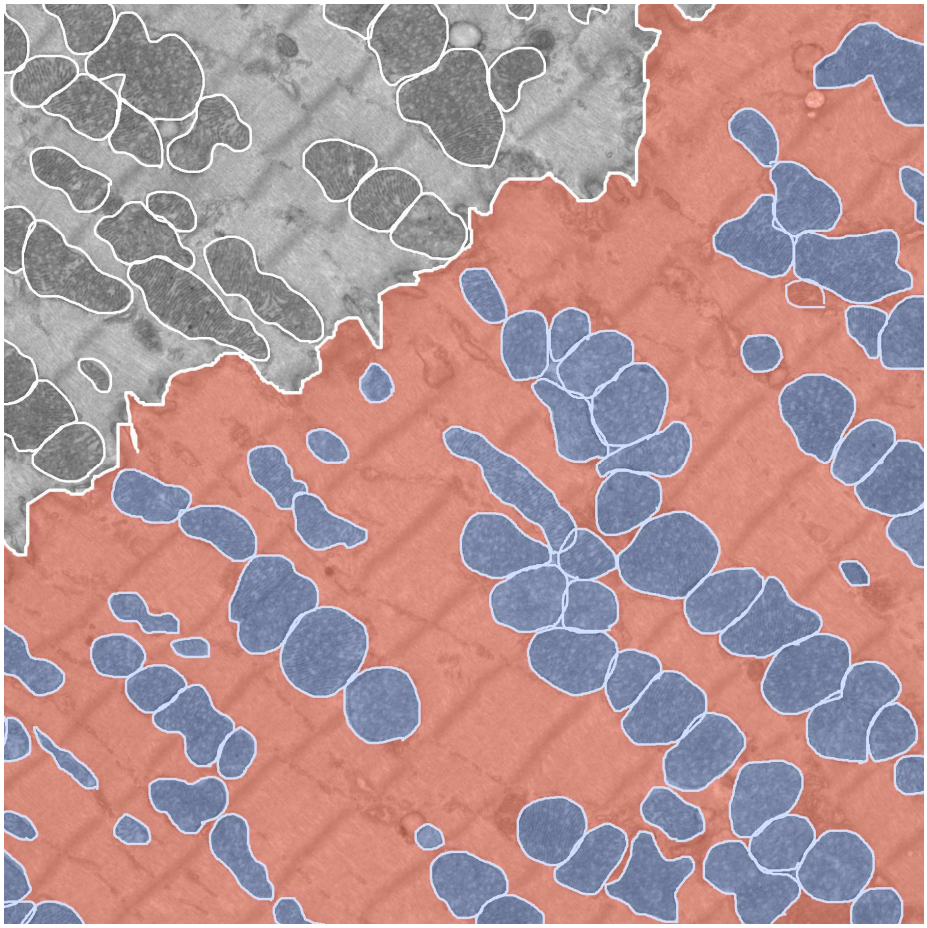

Figure 3-3 Mitochondrial abundancy analysis. Example image showing a subsection of an EM-image at 890x. Mitochondria- and cell-borders are marked with a white line. For calculations, total mitochondrial area (in blue) was divided with total cell area (red) including total mitochondrial area, and considered abundance for one cell.

3.2.4.2 Mitochondrial cristae density

High-resolution images of between 50 and 150 mitochondria per animal were examined for cristae density. To measure this parameter, the number of cristae was calculated across a 5 µm section of the mitochondrion (Feret's diameter [156]). The profile for this section was plotted in Image J (Analyze > Plot Profile) and peaks, ranging in intensity from at least 150 to 50 were counted to represent cristae density (figure 3-4 for reference).

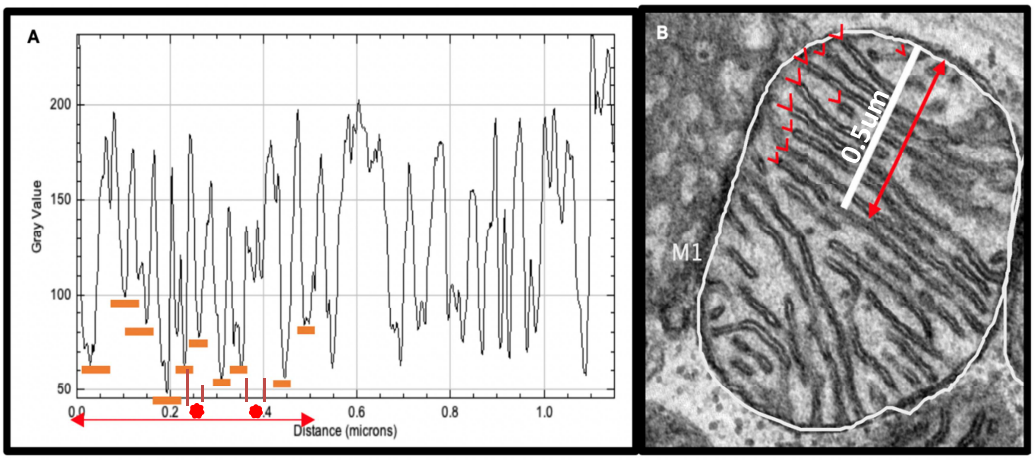

Figure 3-4 Determining crista density from EM. A TEM image of a mitochondrion (B) at x4800 is analyzed using a plot profile (A). Peaks are counted as cristae if the grey value spans 100 units or more, shown here as orange lines in the plot profile and as red crosses in image. The white line is 0.5um for scale.

3.2.5 Quantification of protein expression

Western blots were performed for quantification of expression for proteins related to the ET-pathway. Left ventricular wall tissue was dissected and rapidly snap-frozen in liquid nitrogen and stored in -80°C until use.

3.2.5.1 Protein extraction

Western blots were performed, with assistance from Callum Quinn, for quantification of expression for proteins related to the ET- pathway. Left ventricular wall tissue was dissected and rapidly snap-frozen in liquid nitrogen and stored in -80°C until use.

3.2.5.2 Protein extraction

Samples were homogenized, using a FastPrep-24™ 5G instrument (MP, Biomedicals, Santa Ana, CA; same cycles as described in chapter 3.2.2.1) in Radio-Immuno Precipitation Assay buffer (RIPA; Phosphate buffered saline, Igepal CA360 1%, sodium deoxycholate 0.5% and sodium dodecyl sulfate 0.1%) with added phosphatase and protein inhibitors (Phenylmethanesulphonylfluoride 0.1mg/ml, sodium orthovanadate 100mM, aprotinin 1mg/ml and leupeptin 1mg/ml). Samples were then again stored in -80°C and were discarded after two freeze-thaw cycles.

3.2.5.3 Protein content

Protein content was determined using the Bio-Rad DC protein colourimetric assay kit (BioRad, Hercules, CA) following instructions given in the accompanying instruction manual. Briefly, a combination of an alkaline copper tartrate solution and folin reagent is added to the sample in a 96-well plate. The mix then develops a colour which, measured using BioTek Synergy HTX multimode reader (BioTek, Swindon, UK), is relative to the concentration of protein in the sample. Bio-Rad protein standards (BioRad, Hercules, CA) were measured simultaneously in separate wells and used to create a concentration curve to which the samples were compared.

3.2.5.4 Sample preparation

For each sample, 10µg of protein was prepared with 1x NuPAGE® Lithium Dodecyl Sulphate (LDS; anionic detergent adding a negative charge to the proteins) Sample Buffer from 4x stock and 1x NuPAGE® Sample Reducing Agent from 10x stock (both Thermo Fisher, UK). The final volume was adjusted to 20µl with RIPA and denatured on a hot block at 70°C. The LDS sample buffer contained the dyes Coomassie G250 and Phenol red to allow for visual confirmation of the protein position during the running of the gel. To further help to unfold the proteins, the reducing agent contained 500mM of dithiothreitol leading to a reduction of covalent disulphide bonds and unfolding of the protein.

3.2.5.5 Gel electrophoresis

NuPAGE™ Novex™ 4-12% Bis-Tris pre-cast polyacrylamide protein gels were used for separation of the proteins. The gels were inserted into XCell SureLock® Mini-Cell (Thermo Fisher, UK) as described in the XCell SureLock® Instruction Manual with 1x MOPS running buffer (made from 20x NUPAGE MOPS SDS Running Buffer; Thermo Fisher, UK) in the upper and lower buffer chamber. The upper buffer chamber was then prepared with 0.25% of NuPAGE® Antioxidant before each of the 20µl of prepared sample solution was loaded into separated wells in the gel. One well was loaded with 7µl Precision Plus Protein™ All Blue Prestained Protein Standards (Bio-Rad, USA) as a 'ladder' to identify the different molecular weights on the gel. As an internal control, one sample was loaded onto each gel to allow for comparison between gels. Gels were run at room temperature at 200V for 45 minutes.

3.2.5.6 Protein transfer

As the electrophoresis was running, XCell II™ Blot Module (Thermo Fisher, UK) transfer kits were prepared by cutting Amersham Protran supported 0.45 nitrocellulose membrane (GE Healthcare, UK) and filter paper to size. One membrane and two filters per gel were then soaked in 1x transfer buffer made from 20x NUPAGE® Transfer Buffer (Thermo Fisher, UK) with the addition of 20% methanol. Methanol is added as it helps increase the affinity of proteins to the membrane by removing SDS.

Once electrophoresis was complete, the gel was removed from the casing. The gel was made to fit the membrane by cutting off the wells at the top and removing the ridge at the bottom. The gel was placed with the membrane, sandwiched between foam pads and filter paper (all soaked in transfer buffer) with care taken to avoid air bubbles. Each transfer kit was prepared with two filter paper-gel-membrane-filter paper sandwiches and extra foam pads on each side of the two sandwiches were used to allow sufficient contact between gel and membrane to ensure good protein transfer.

Transfer kits were then inserted into the tank module and secured in place by the gel tension wedge. The transfer was run at 30V for 70 minutes with Milli-Q ddH_2O in the outer chamber as a coolant and 1x transfer buffer with 20% methanol and 0.1% antioxidant in the inner chamber. This preparation is in accordance with the XCell II™ Blot Module Instruction Manual.

Once transferred, membranes were placed in LI-COR Revert™ total protein stain (LI-COR, Lincoln, NE) for 5 minutes and imaged on a LI-COR Odessey® CLx at 700 nm wavelength. The total protein stain allows for visual confirmation of satisfying transfer and was after used to normalise for levels of loading (described in more detail below). Membranes were then washed with LI-COR Revert™ Wash Solution to remove the total protein stain.

3.2.5.7 Blocking and detection of protein

To reduce background noise and non-specific binding, membranes were blocked with 5% milk in tris buffered saline plus tween (TBS-T) in room temperature and subsequently washed in TBS-T for 3 x 5 minutes. Primary antibody cocktail (Abcam ab110413; Abcam, Cambridge, UK) was diluted 1:1000 in TBS-T and 5% milk and incubated at 4°C on roller overnight. The cocktail contains antibodies for subunits on each of the five respiratory complexes (CI subunit NDUFB8, CII-30kDa, CIII-Core protein 2, CIV subunit I and CV alpha subunit).

Following primary antibody incubation, membranes were washed in TBS-T for 3 x 5 minutes. Secondary antibody (IRDye® 800CW Goat anti-Mouse IgG_{2a}-Specific, LI-COR) was diluted 1:20,000 in TBS-T with 5% milk and membrane was incubated for 1 hour, on a rocker, in room temperature covered by aluminium foil to minimize light exposure. Protein content was visualised at 800 nm using LI-COR Odessey® CLx.

3.2.5.8 Analysis of Western blots

For acquisition and analysis of protein abundance as well as total protein, the software Image Studio™ was used (LI-COR). For total protein, the 'Analysis > Draw rectangle' function was used. The rectangle was placed in such a way that it

encompassed a large area in one well but avoiding any possible artefacts on the membrane. This allows for accurate quantification of a range of proteins and avoids misrepresentation by technical artefacts. Background was chosen as a field, 2 pixels wide, on each side of the measured box and was subtracted from the total fluorescent value.

Protein bands were analysed by the built in function 'Analysis > Add rectangle' where the size of the rectangle is chosen by the software. This allows for unbiased quantification of the protein abundance. Background was set as 2 pixels around the entire rectangle and was, again, automatically subtracted from the total fluorescent value.

The antibody used in this study generated five separate bands, one for each protein corresponding to the five complexes of the ET- pathway (figure 3-5). The value for each separate protein in each sample was divided by the total value for the total protein as well as the internal control.

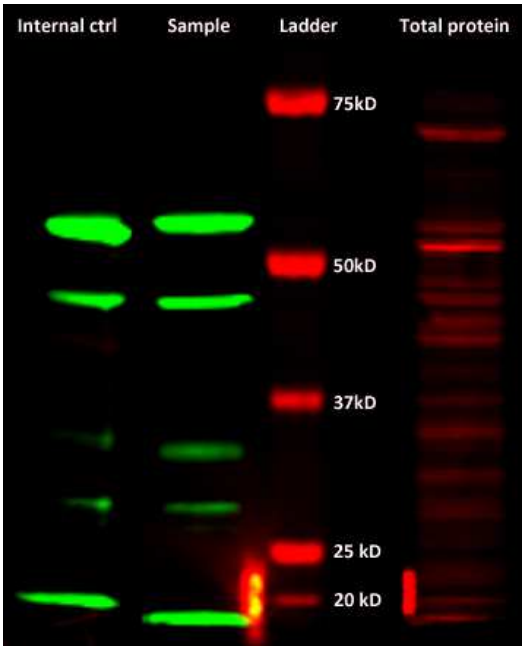

Figure 3-5 Western blot representative image. Each gel was loaded with an internal control (random LV mouse sample that was reused for all blots), samples and ladder. To

allow for normalization to loading, a total protein stain was used. The bands shown in sample and internal control lanes are, top to bottom; complex V, complex III, complex IV, complex II, and complex I.

3.2.6 Antioxidant activity assays

Left ventricular tissue was homogenized using a FastPrep-24^{TM} 5G homogeniser at 6m/sec during 2 x 30 second cycles with 1 minute in between, in dibasic potassium phosphate buffer with 0.2 M KH_2PO_4 and 0.2 M K_2HPO_4 in pH 7.8 at 4°C. Samples were subsequently centrifuged at 600G for 10 minutes at 4°C. The supernatant was divided into aliquots, snap frozen in liquid nitrogen and then kept in -80°C until time of experiment with no freeze thaw cycles to avoid deterioration. Protein content was determined by the use of Quickstart Bradford dye reagent (Bio-Rad Laboratories, USA) to allow for normalisation (as described in 3.2.2.1). The following antioxidant experiments were performed by Hajani Premanandhan.

3.2.6.1 Superoxide dismutase activity

A modified version of the protocol described by Sun et al, as well as Weydert and Cullen, was used for measurement of SOD activity [157, 158]. Briefly, xanthine-xanthine oxidase is used to produce $O_2^{\bullet-}$ in the presence of nitroblue tetrazolium (NBT). The reduction of NBT by $O_2^{\bullet-}$, forms diformazan which optical density can be measured and quantified at a wavelength of 560nm. In the presence of SOD, the reduction of NBT becomes competitive. Thereby, by monitoring the reduction rate of NBT in the presence and absence of a SOD containing sample, the SOD content of the sample can be quantified by quantifying non-reduced NBT. Bathocuproine disulfonic acid disodium salt (BCDA) and diethylenetriaminepentaacetic acid (DETAPAC) were both added to avoid unwanted free radical production.

Homogenates from samples (n= 3 from each experimental group) were diluted with 50mM potassium phosphate buffer to concentrations 1:1, 1:25. 1:50 and 1:75 and 10µl was added to 96-well plate (in triplicates). The final assay mix contained 0.13 mg/mL BSA in 1 mM DETAPAC, 1 U of catalase, 56 µM of NBT, 0.01 M of xanthine, 5 mM phosphate buffer and 50µM BCDA that was added to a xanthine oxidase

solution (13 U/mL xanthine oxidase and 1.34 mM of DETAPAC) in sequential order to avoid premature reactions. 250 µL of this final assay mix was then added to the samples in the 96-well plate and immediately read at 560 nm in a spectrophotometer (BioTek Synergy HTX multimode reader) in 25°C.

3.2.6.2 Catalase activity

Catalase activity was assessed by measuring the clearance of H_2O_2 in LV samples, prepared as described above. We utilized the reaction of AmplexUltrared, in the presence of horseradish peroxide, measuring the optical absorbance of resorufin (detailed in section 3.2.1). A known quantity of H_2O_2 was added with or without sample and discrepancies between the two was attributed to endogenous H_2O_2 clearance (mainly mediated by catalase).

Briefly, samples (n= 3 from each experimental group) was diluted with 50mM potassium phosphate buffer to generate dilutions of 1:1, 1:20, 1:50 and 1:75. A volume of 50 µL of sample was added to a 96-well plate (in triplicates) followed by 100 µl of working assay mix (10 mM AmplexUltrared, 1 U/l horseradish peroxide and 50 mM sodium citrate, pH6). Reaction was triggered by the addition of 50 µl of 160 µM H_2O_2 and read at 565 nm in a spectrophotometer (BioTek Synergy HTX multimode reader). Mean absorbance after 5 minutes was compared to that of a standard curve (addition of known concentrations of catalase instead of samples) and activity was expressed as µmol H_2O_2 clearance per mg.

3.2.7 Statistical analysis

All data are expressed as means ± SEM and were graphed using Graphpad Prism®, version 8 (Graphpad Software, San Diego, CA). Throughout, offspring from normoxic pregnancies are denoted by N and from hypoxic pregnancies by H. Males are shown in filled pink circles and females in open blue boxes. All data, save complex IV inhibition, cristae density and antioxidant activity, were statistically tested using a 2-way ANOVA, with sex and intrauterine oxygen levels as two between-subject factors using SigmaPlot version 12.5 (Systat, San Jose, CA) and Tukey's correction for multiple comparisons test to determine significant

differences between groups. Prior to the ANOVA, oxygen consumption was transformed using the natural logarithm and all data was tested for equal variance and normal distribution (Shapiro-Wilk). For complex IV inhibition, a linear regression curve was fitted to the data to assess if the slope was significantly non-zero using Graphpad Prism®, version 8 (Graphpad Software, San Diego, CA). Mitochondrial cristae density was tested by a linear mixed model with treatment (hypoxic/normoxic), sex and animal as co-factors using IBM SPSS Statistics version 25 (IBM, Chicago, IL). Antioxidant activity and protein abundance for complex III-V were assessed by a Kruskal-Wallis test using Graphpad Prism® as they did not pass normality test, equal variance test or both.

3.3 Results

3.3.1 Spectrophotometry

There were no significant differences in citrate synthase (CS) activity (figure 3-6 A) between gender or treatment. Prenatal hypoxia had no effect on complex I and complex II activity (figure 3-6 B and C, respectively) in males but these parameters were significantly reduced in females. Complex IV activity (figure 3-6 D) was, again, unchanged in males but increased in females.

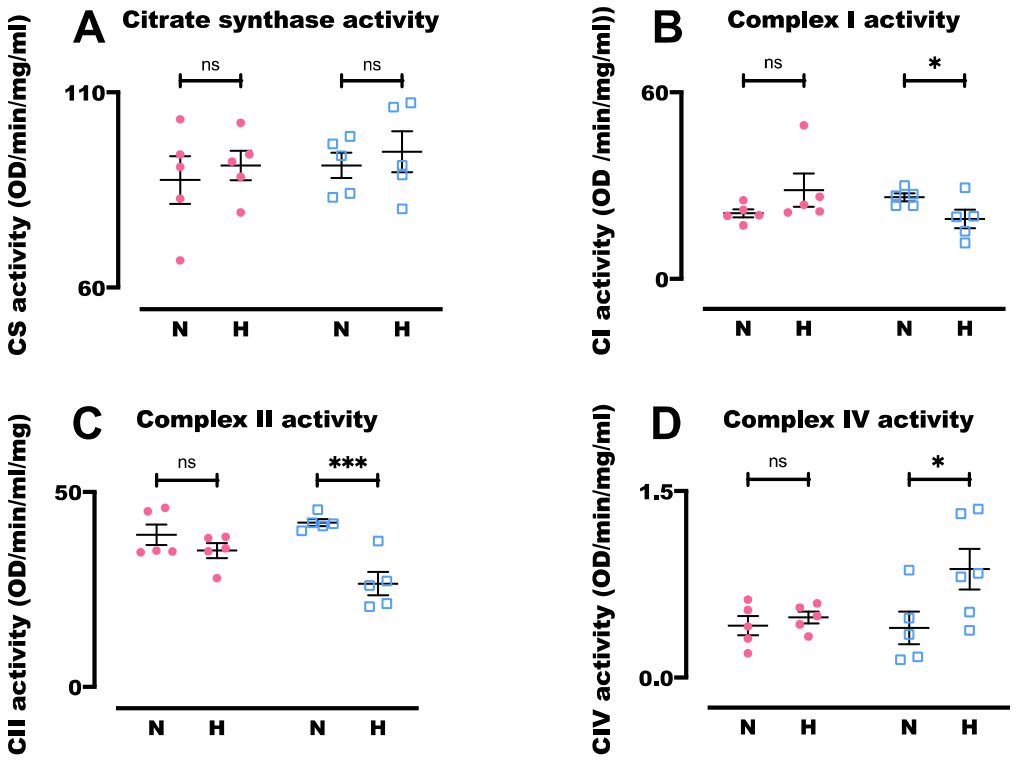

Figure 3-6 Enzyme activity assays. Prenatal hypoxia did not lead to any changes in citrate synthase activity (A). However, both complex I (B) and complex II (C) activity were lower in adult female offspring following prenatal hypoxia. To the contrary, complex IV activity (D) was higher in adult female offspring following prenatal hypoxia. No differences in complex activities were recorded in the males subjected to prenatal hypoxia compared to the normoxic males. Males are shown in filled pink circles and females in blue open boxes. Data are presented as mean ± SEM, n=5-6 animals in each group. Significance was given by two-way ANOVA with a Tukey's posthoc. For all panels *$p < 0.05$, ***$p<0.001$.

3.3.2 High-resolution respirometry

3.3.2.1 Effects of prenatal hypoxia on mitochondrial oxygen consumption

For males, previous exposure to prenatal hypoxia had no significant effect on any of the mitochondrial respiratory parameters tested, except for the phosphorylation system control (P/E) ratio, which was increased in males from hypoxic pregnancies (figure 3-7). In contrast, females from hypoxic pregnancies exhibited increased oxygen consumption in the OXPHOS state (figure 3-7 B and C) and after uncoupling (figure 3-7 D and E), regardless of substrate combination. Furthermore, oxygen consumption rate through complex IV was greater in females previously exposed to prenatal hypoxia, compared with normoxic controls (figure 3-7 F). While Leak oxygen consumption rate in females was unchanged by prenatal hypoxia (figure 3-7 A), the increased OXPHOS meant the respiratory control ratio (RCR), and therefore mitochondrial efficiency, was significantly greater in females from hypoxic pregnancies (figure 3-7 G). Lastly, while the P/E ratio was similar between females, the leak control (L/E) ratio was lower in females previously exposed to prenatal hypoxia, compared with controls (figure 3-7 I).

3.3.2.2 Gender differences in mitochondrial oxygen consumption

In adult offspring from normoxic pregnancies (control), there were gender-dependent differences in oxygen consumption. Females respired less during leak state as well as in $OXPHOS_{CI}$, and in the uncoupled state, $ET\text{-}max_{CI+CII}$, compared to males (figure 3-7 A, B and D). This difference was inversed, meaning males respired less, if the offspring had been subjected to prenatal hypoxia in several states namely, OXPHOS state, regarding of substrate combination, as well as during the uncoupled state ($ET\text{-}max_{CI+CII}$) and when complex IV was assessed separately with TMPD (figure 3-7 B, C, D and F).

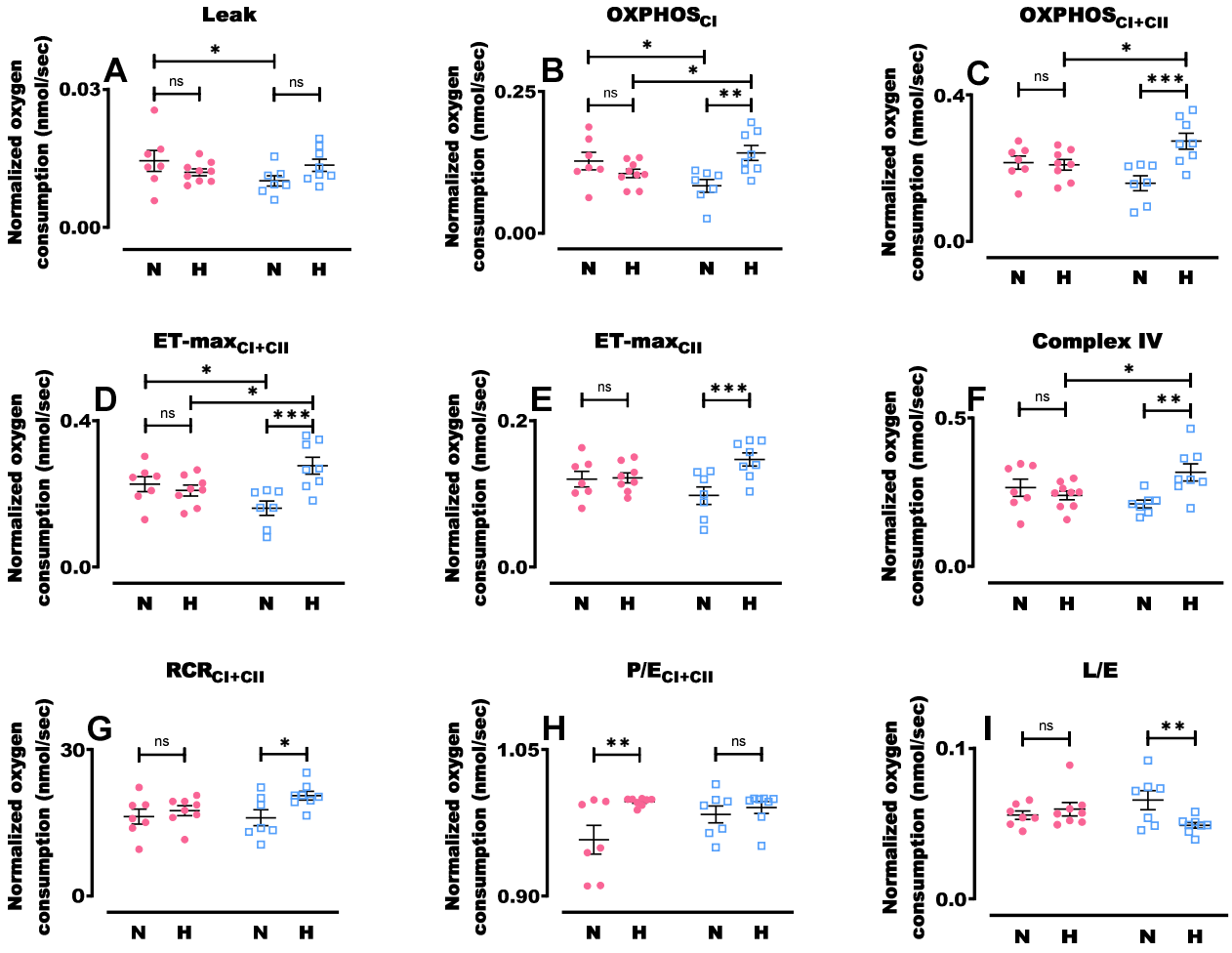

Figure 3-7 Effect of prenatal hypoxia on intact mitochondrial oxygen consumption and coupling control ratios. Few differences were seen in males. Females from hypoxic pregnancies had higher respiratory rates with more efficient production of ATP. A) Leak oxygen consumption with Complex (C) I substrates, B) OXPHOS with CI substrates, C) OXPHOS with CI+II substrates, D) uncoupled state with CI+II substrates, E) uncoupled state with the addition of CI blocker rotenone, F) oxygen consumption through CIV, G) respiratory acceptor control ratio, H) phosphorylation system control ratio and I) leak control ratio. Males shown in pink filled circles and females in blue open boxes. Data presented as mean ± SEM, n=7-9 in each group. Significance is given by two-way ANOVA with a Tukey's post-hoc. *$p < 0.05$, **$p<0.01$, ***$p<0.001$.

3.3.3 Reactive oxygen species production

3.3.3.1 Effect of prenatal hypoxia on mitochondrial ROS production

ROS was measured simultaneously with oxygen consumption. In males from hypoxic pregnancies, there were increases in ROS production during Leak, $OXPHOS_{CI}$ and $OXPHOS_{CI+CII}$ (figure 3-8 A, B and C, respectively), compared to males from normoxic pregnancies. There were, however, no differences in ROS production during the two uncoupled states ($ET\text{-}max_{CI+CII}$ and $ET\text{-}max_{CII}$, figure 3-8 D and E) between males from normoxic and hypoxic pregnancies. Females from hypoxic pregnancies showed no difference in ROS production during Leak state or $ET\text{-}max_{CI+CII}$ (figure 3-8A and D respectively). However, during $OXPHOS_{CI}$ and $OXPHOS_{CI+CII}$ as well as during $ET\text{-}max_{CII}$ (figure 3-8 B, C and E, respectively), there was decreased ROS production by females from hypoxic pregnancies compared to females from normoxic pregnancies.

3.3.3.2 Gender differences in mitochondrial ROS production

Throughout all states that were measured, females from normoxic pregnancies produced more ROS than males from normoxic pregnancies (figure 3-8 A-E). This difference, however, was abolished in offspring from hypoxic pregnancies.

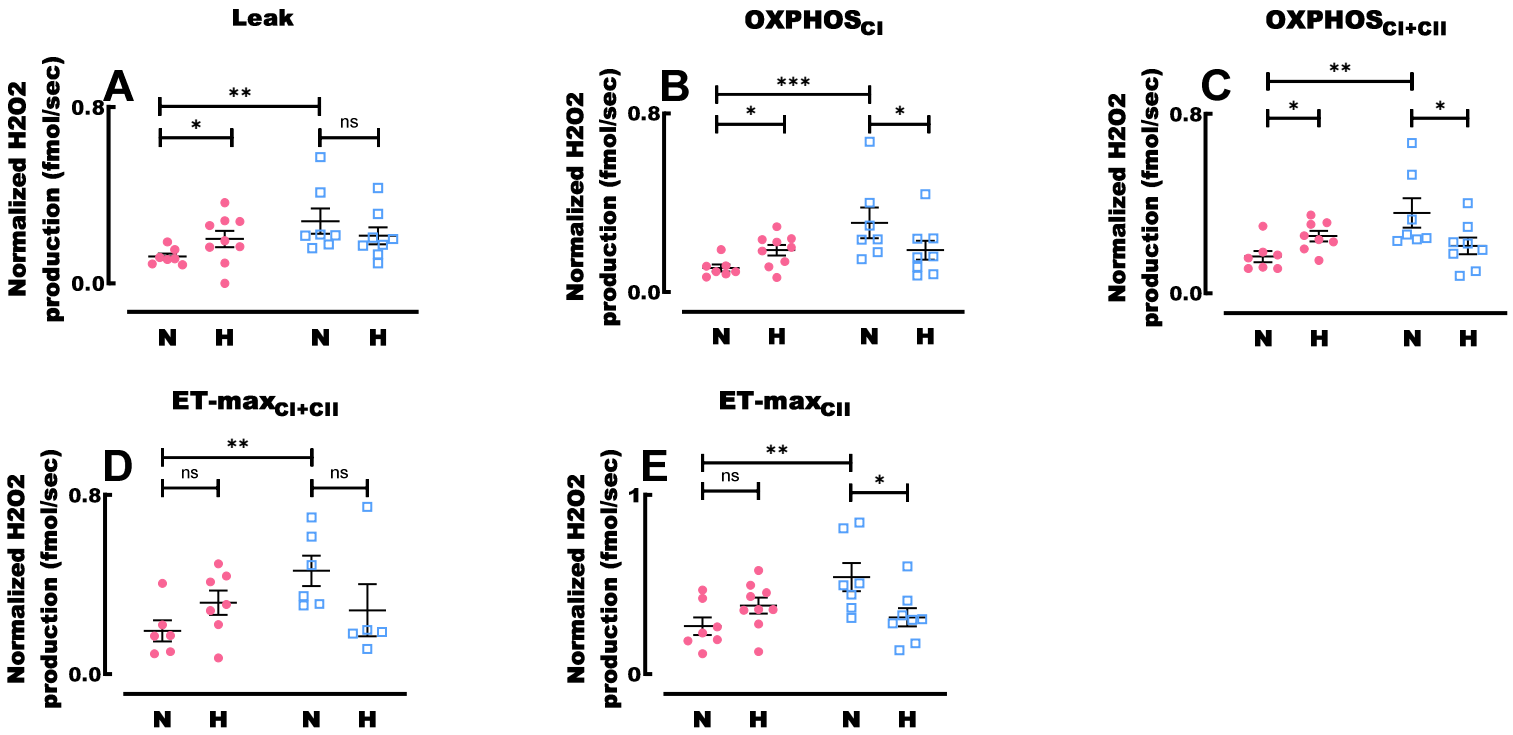

Figure 3-8 Effect of prenatal hypoxia on ROS production in intact mitochondria. Males from hypoxic pregnancies showed a higher ROS production, while respiration was coupled, compared to males from normoxic pregnancies. Females from hypoxic pregnancies produced less ROS during OXPHOS states, regarding substrates, and during the ET-max$_{CII}$ state. A) Leak state, B) OXPHOS with complex I substrates, C) OXPHOS with complex I and II substrates, D) uncoupled state with complex I and II substrates, E) uncoupled state with complex I blocked by rotenone. Males are shown in pink filled circles and females in blue open boxes. Data are presented as mean ± SEM, n=6-9 in each group. Significance was given by two-way ANOVA with a Tukey's post-hoc. For all panels *$p < 0.05$, **$p<0.01$, ***$p<0.001$.

3.3.4 The role of complex IV in ROS production

The altered oxygen consumption and ROS production in females from hypoxic pregnancies could be explained by numerous factors, one being the increased oxygen consumption of complex IV (figure 3-7 F). To explore this possibility, sodium azide was titrated (0-1.75mM in 0.25mM increments) into one chamber of the Oroboros Oxygraph O2k containing a homogenate from a normoxic female with substrates for the $OXPHOS_{CI+CII}$ state. This led to dose-dependent inhibition of complex IV, seen as inhibition in oxygen consumption (figure 3-9 A). Linear regression was fitted with a slope of -0.4167, which was significantly non-zero ($p=0.0005$; $R^2=0.8879$). The experiment was repeated with the addition of substrates allowing for simultaneous measurement of ROS production. The measured ROS production was divided with the corresponding O_2 consumption (figure 3-9 B). Linear regression gave a slope of 0.0005372, which was significantly non-zero ($p<0.0001$; R2=0.9332). In aggregate, these results suggest that ROS production is inversely related to complex IV activity.

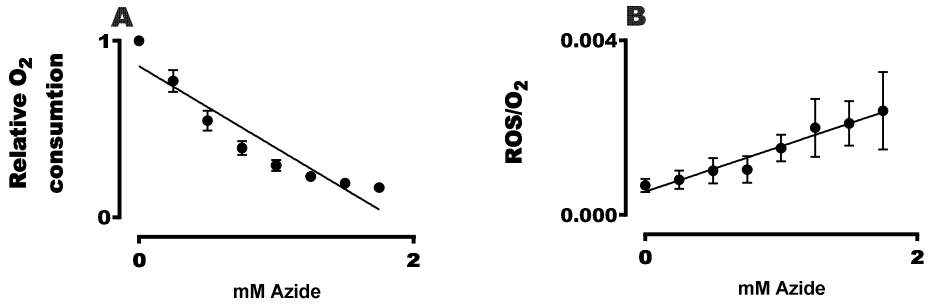

Figure 3-9 CIV inhibition. Complex IV inhibition using azide led to significantly reduced oxygen consumption (A) and increased ROS production in relation to oxygen consumption (B). Data are presented as mean ± SEM, n=4 adult females from normoxic pregnancies in both panels. A linear regression curve was fitted to the data and was significantly different from zero.

3.3.5 Protein abundance

Western blots were performed to assess the level of proteins related to each complex in the ET-pathway (figure 3-7). Compared to females from normoxic pregnancies, females from hypoxic pregnancies showed no significant differences in protein content with regards to complex I, complex II, complex III, complex IV or complex V (figure 3-10 A-E, respectively). Males from hypoxic pregnancies had lower protein content with regards to complex I and complex II (figure 3-10 A and B) but no differences in regards to complex III, complex IV or complex V (figure 3-10 C-E, respectively) compared to males from normoxic pregnancies.

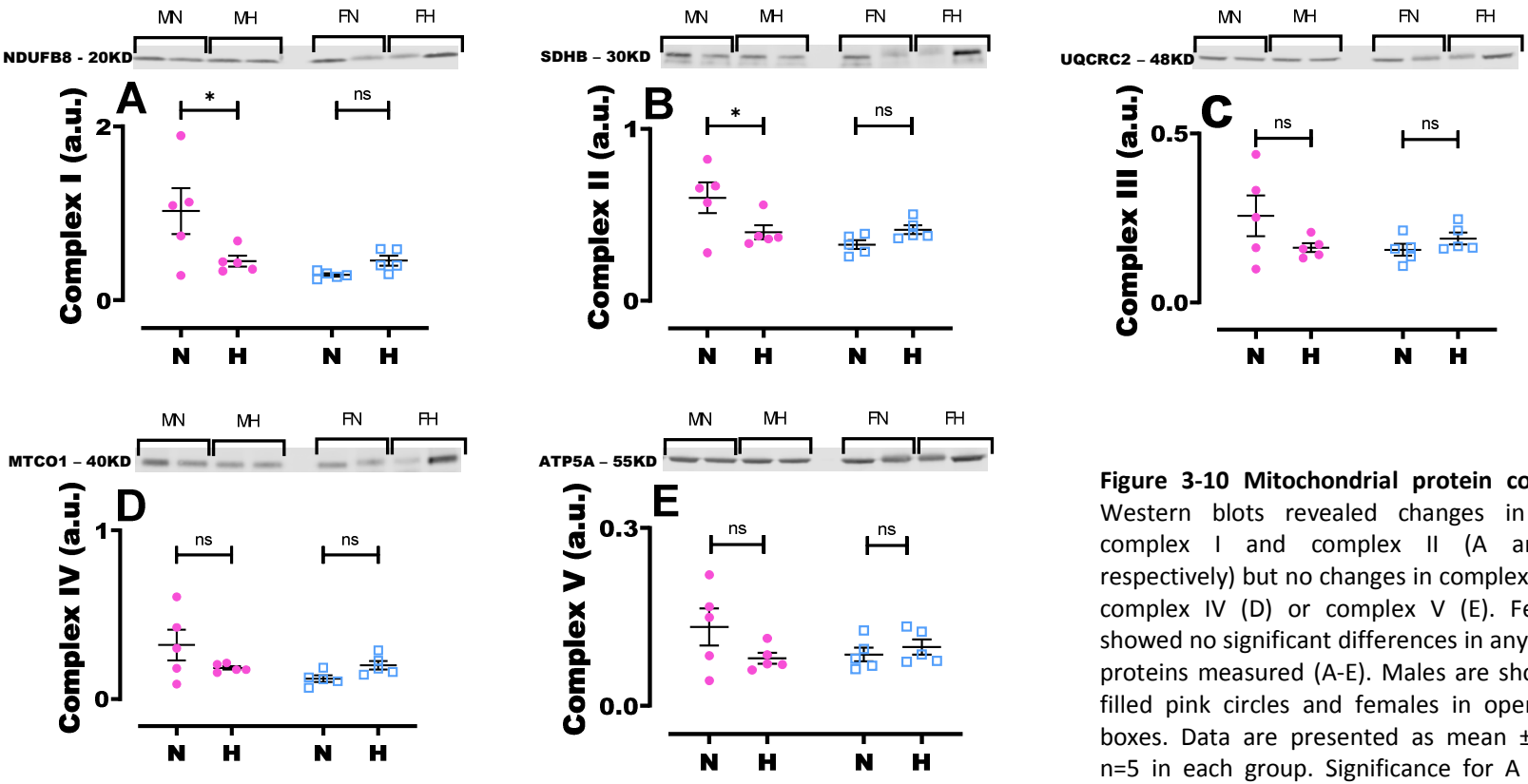

Figure 3-10 Mitochondrial protein content. Western blots revealed changes in male complex I and complex II (A and B, respectively) but no changes in complex III (C), complex IV (D) or complex V (E). Females showed no significant differences in any of the proteins measured (A-E). Males are shown in filled pink circles and females in open blue boxes. Data are presented as mean ± SEM, n=5 in each group. Significance for A and B was given by two-way ANOVA with a Tukey's post-hoc, C-E with Kruskal-Wallis test. For all panels *$p < 0.05$.

3.3.6 Electron microscopy

Electron microscopy, used to determine mitochondrial structural properties, revealed prenatal hypoxia had no effect on mean mitochondrial density per cell (figure 3-11 A). Cristae density (figure 3-11 B) of the mitochondria was significantly lowered in both males and females from hypoxic pregnancies. There was also a difference comparing between the sexes, i.e. normoxic males had higher cristae density than hypoxic females and vice versa (figure 3-11 B).

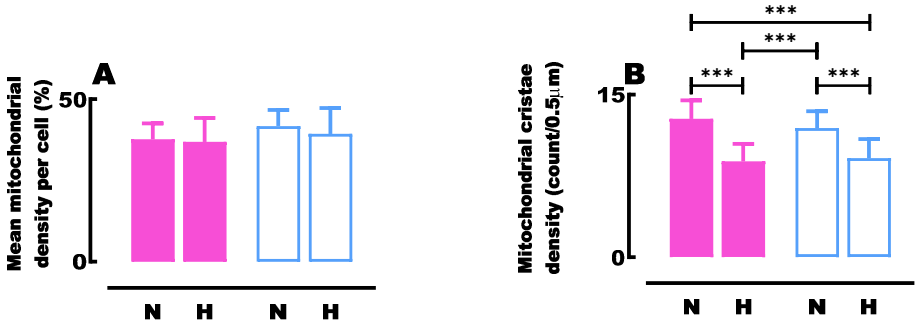

Figure 3-11 Mitochondrial and cristae density. Electron microscopy revealed no differences in mean mitochondrial density (A). Cristae density (B) however, was lower in both hypoxic males compared to normoxic males (pink bars) and hypoxic females compared to normoxic females (blue bars). Data are presented as mean ± SEM n=2 normoxic and n=5 hypoxic animals. For mitochondrial density n=5 images per animal and for mitochondrial cristae n=50-150 mitochondria per animal. Significance was given by two-way ANOVA with a Tukey's post-hoc for abundance and linear mixed model for cristae density. For all panels *p < 0.05, **p<0.01, ***p<0.001.

3.3.7 Antioxidant activity

Two components of the antioxidant system were assessed during this study. Firstly capacity for H_2O_2 clearance (mainly due to catalase) was unchanged in both males and females from hypoxic pregnancies compared to their counterparts from normoxic pregnancies (figure 3-12 A). The second antioxidant component measured, SOD activity, was also unchanged when comparing offspring from hypoxic pregnancies with offspring from normoxic pregnancies (figure 3-12 B).

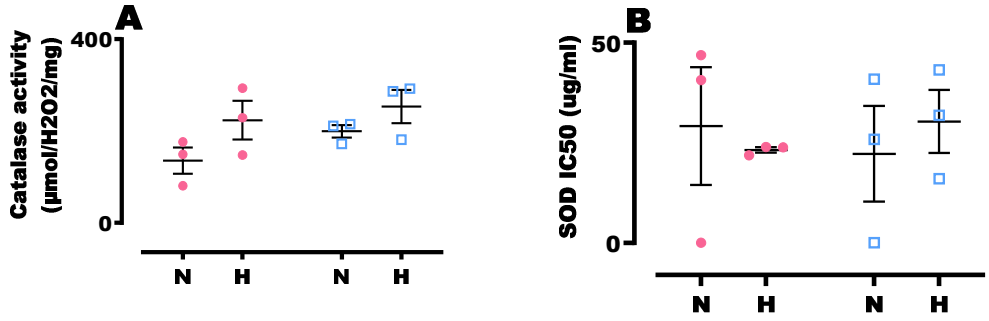

Figure 3-12 Antioxidant capacity. Both H_2O_2 clearance and SOD activity were unchanged in adult offspring subjected to prenatal hypoxia. Males are shown in pink filled circles and females in blue open boxes. Data are presented as mean ± SEM, n=3 in each group and statistically tested by a Kruskal-Wallis test.

3.4 Discussion

This study has shown that prenatal hypoxia affects mitochondrial function of adult offspring in a sex-dependent matter. Gender dichotomy, following prenatal insults, has been reported previously. Bae et al observed increased susceptibility to I/R injury following prenatal cocaine exposure in male rats [159] while Lawrence et al reported more pronounced adverse effects in female rats exposed to prenatal nicotine, following an ischaemic period [160]. Furthermore, in agreement with the work presented here, there have also been previous reports of sex-dependent differences following prenatal hypoxia. Xue and Zhang showed increased susceptibility to I/R in adult male rats from hypoxic pregnancies when compared to female rats [22]. In addition, Thompson et al saw reduced basal functionality in male adult guinea pigs from hypoxic pregnancies, but not in females [30]. Although neither echocardiography nor I/R experiments showed any significant changes in our study (as mentioned in chapter 2), a range of metabolic processes were altered which may have implications for energy and ROS balance when the heart is under stress.

3.4.1.1 Mitochondrial density

With our combined results of citrate synthase activity and mitochondrial density from EM studies, we concluded that there were no alterations to mitochondrial abundance following prenatal hypoxia in males or in females. Larsen et al concluded that the top three biomarkers for mitochondrial abundance in skeletal muscle were, in order, cardiolipin, citrate synthase and complex I activity [161]. Our study supports this finding in regards to citrate synthase (as strengthened by the measurement of mitochondrial density through EM) but not in the case of complex I. At this point, it should be noted that Larsen et al expressed a bigger difference, in regard to accuracy, between complex I activity and citrate synthase than that between cardiolipin and citrate synthase and that this current study, therefore, in no way, invalidates the results of Larsen et al.

3.4.1.2 Mitochondrial cristae density

Our study showed reduced mitochondrial cristae density in adult offspring from hypoxic pregnancies in both males and females. Nielsen et al. suggested that increases in cristae density can facilitate increased oxygen uptake and studies have shown that endurance training may increase cristae density in skeletal muscle [162]. The findings in this study, however, are quite contrary to the findings of Nielsen et al.; we see hypoxic pregnancies have decreased cristae density which is associated with no change in adult male mitochondrial respiration, and an increase in respiratory capacity in adult female offspring. With the data available to us, it is difficult to conclude the reason for this discrepancy. It is, however, worth noting that Nielsen et al. used only male subjects and that respiratory capacity was examined by whole body maximal oxygen uptake. It is also worth considering that the breaking of the cell membrane, during homogenization, could lead to mitochondria which are structurally similar to that of isolated mitochondrial preparations; i.e. swollen mitochondrial morphology, diluted matrix content and disorganized cristae [163]. This morphological disturbance could over shadow any in vivo alterations caused by decreased crista density.

3.4.1.3 Mitochondrial enzyme activities

Male offspring showed no significant changes in the activity of complex I, II or IV. In contrast, previous studies have shown reduced amounts of proteins for complex IV subunit I and IV, reduced mRNA expression of COX4.1 and COX5b as well as reduced complex IV activity in male adult guinea pigs, but no differences in females [30, 145]. The discrepancies in these studies could be explained by different hypoxic conditions as Al-Hasan and Thompson subjected their sows and dams to 10.5% O_2 for a shorter period of gestation, compared to our study which used 14% O_2 for the majority of the gestation. The lowered activity and expression of complex IV in the male guinea pig model were hypothesised to be due to altered PKCε expression which has been reported to be repressed in adult males from hypoxic pregnancies [29]: Furthermore, PKCε may also interact with complex IV subunit IV expression and complex IV activity [111, 164]. In addition, PKCε is believed to be cardioprotective and

interact with the mPTP [165, 166]. The reduction in PKCε, shown by others, could not only be responsible for reduced complex IV but also increase the chance of the mPTP opening, leading to cell death. We believe that the lack of alteration to complex activity in the males in our study is due to the comparatively mild level of hypoxia. It is worth noting however, the variation in male protein abundancy of complex IV subunit I across the males. Although not statistically significant, male offspring from normoxic pregnancies had a wide spread of data in complex IV subunit I abundance, while in males from hypoxic pregnancies the spread of data was narrow. This suggests that prenatal hypoxia may have had a mild affect complex IV activity in males.

Interestingly, while previous work on prenatal hypoxia at 10% oxygen found clear effects on male mitochondrial enzymatic activity, there were no significant effects on females. In contrast, the present study found no effects in males, but female offspring from hypoxic pregnancies had lowered activity of complexes I and II, as well as higher activity in complex IV, compared to females from normoxic pregnancies. As far as Complex IV goes, to our knowledge, this is novel information which is further strengthened by the significantly increased level of oxygen consumption in the intact mitochondria (figure 3-7 F) as well as a trend towards increased protein abundance of complex IV subunit I (figure 3-10 D). We believe that this is a reflection of the aforementioned lack of alteration to PKCε and could partly explain the protection to I/R injury seen in females (further discussed in section 5.4). This theory is currently only speculative and needs further studying. Although no changes are seen in protein abundance regarding complexes I and II, we saw reduced enzymatic activity in females from hypoxic pregnancies compared to females of normoxic pregnancies. It is reasonable to think that, as electron transport, through complexes I and II are greatly involved in the production of the aforementioned ROS spike following I/R [80], this could be a protective response to lessen damage following reperfusion. As blockage of complex I reduce ROS production during reperfusion, reduced complex I activity might play a similar role (further discussed in section 5.4).

3.4.1.4 Male intact mitochondrial oxygen consumption and ROS production

In line with the enzymatic activity data above, intact mitochondrial oxygen consumption was unchanged between males from normoxic pregnancies compared to males from hypoxic pregnancies, regardless of respiratory state. However, the calculated phosphorylation system control ratio (P/E) is increased in males from hypoxic pregnancies compared to males from normoxic pregnancies. This tells us that males from hypoxic pregnancies are less limited by their phosphorylation system and/or the pressure from the proton motive force [167, 168]. There were however significantly higher levels of ROS production in males from hypoxic pregnancies during Leak state, $OXPHOS_{CI}$ and $OXPHOS_{CI+CII}$, compared to their normoxic counterparts. Despite this, the difference in ROS production was not seen during the uncoupled state with or without rotenone; this result could be explained by the loss of the tight link between membrane potential and ROS production due to the uncoupled membrane [169]. When uncoupled, the forces asserted on the ET-pathway by the proton gradient, is relieved, which, in theory could lead to less electron slippage. However, examining the separate data points it is worth considering that this might just be the result of a statistical false negative.

The reason for the increased male ROS production, in the coupled states, therefore cannot be discerned from this current study. Preliminary SOD data show that two out of three samples have lower activity in males from hypoxic pregnancies compared to males from normoxic pregnancies. As the ROS measurements in the current study are under saturated SOD levels, it is unlikely that changes in endogenous SOD production was the cause to the increased ROS production seen in males subjected to prenatal hypoxia but it cannot be conclusively excluded and should be further investigated.

3.4.1.5 Female intact mitochondrial oxygen consumption and ROS production

Females showed increased oxygen consumption, accompanied by decreased ROS production, in all states apart from leak and the uncoupled state. As ROS production is a balance between respiratory rate and redox potential in the ET-pathway [170-172], an increase in oxygen consumption combined with reduced ROS

production points towards involvement of altered redox potential in the ET-pathway or alterations to antioxidant capacity. Although underpowered in this current study, we saw no effect of prenatal hypoxia on female antioxidant activity. The altered redox potential hypothesis is supported by the lack of significant differences in leak and uncoupled state. While leak state causes high redox and membrane potential, uncoupling the ET-pathway creates the opposite situation with no membrane potential and low redox potential [173, 174]. In both cases the ET-pathway is kept in, what can only be described as, a theoretical maximum, which would overshadow the innate changes caused by different prenatal environments. Once the forces of membrane and redox potential are lessened, by the addition of ADP, the differences become apparent. We believe that the reduced activity of complexes I and II in the females reduce pressure, asserted by the transported electrons, in the ET-pathway. Alterations to complex I alone would affect ROS production as complex I is one of the major sources for ROS [175]. In turn, increased activity and respiratory capacity of complex IV further reduced pressure by facilitating more electrons and maintaining an intermediate redox potential inside the ET-pathway. To test the latter hypothesis, we performed experiments where we partially inhibited complex IV. We saw that sodium azide was able to block respiration in a dose-dependent manner and while doing so, ROS production was increased in relation to oxygen consumption. By doing this we confirmed that complex IV can affect ROS production, which supports our hypothesis. The same response has been shown previously in whole embryonic chick cardiomyocytes where reduced complex IV did not only lead to increased ROS production but also decreased contractility [176].

Could these alterations in the ET pathway be an explanation for why females from hypoxic pregnancies have greater recovery from I/R compared to males from hypoxic pregnancies [22]? It stands to reason that lowered complex II activity could lessen the sudden influx of electrons from succinate build up, and lowered complex I activity would reduce the amount of RET; therefore, the ET-pathway would be more capable of handling the electron burst during reperfusion due to the

increased activity in complex IV. However, this is all theoretical and requires further investigation.

3.4.1.6 Sexual dimorphism

We showed a sexual dimorphism of intact mitochondrial function in adult offspring from normoxic pregnancies. We saw that females had lower oxygen consumption in Leak, OXPHOS and ET-max (figure 3-7 A, B and D, respectively) compared to that of males. In addition, we showed increased ROS production from adult females from normoxic pregnancies compared to that of adult males from normoxic pregnancies, in all states measured (figure 3-7 A-E). If subjected to prenatal hypoxia, however, females showed increased respiration in states; OXPHOS I, OXPHOS I+II, ET-max and after isolation of complex IV (figure 3-7 B, C, D and F, respectively) compared to males from hypoxic pregnancies. As such, we see the opposite difference compared to offspring from normoxic pregnancies. This could be explained by alterations in ROS production. As ROS production is increased in males and decreased in females, following prenatal hypoxia, it is likely that this increase ROS production is inhibiting respiration. In addition, oxygen consumption in males is more affected by ROS production compared to females [177]. The differences seen in offspring from normoxic pregnancies are contradictory to those reported by Khalifa et al. Their study, like ours, was on homogenates from C57BL6 male and female hearts, but at an age of six weeks compared to seven months in the current study. However, although they do not report any significant differences, by visual assessment of the graphs presented, there seemed to be trends towards increased oxygen consumption in female mitochondria in all states. They also report higher ROS production in males compared to females [178]. The reason for these discrepancies remains unknown to us.

3.4.2 Study limitations

Time constraints affect all studies, including this one. This chapter covers some of the limitations and explains some methodological choices.

3.4.2.1 Mitochondrial preparation

Complimentary to this study it would have been beneficial explore the differences in intact mitochondrial oxygen consumption and ROS production in other mitochondrial preparations. The homogenization preparation used here has advantages and disadvantages, as does any technique. Compared to isolated mitochondria, homogenates allow for assessment of mitochondrial functionality of different cell types (e.g. cardiac myocytes, fibroblasts and adipocytes) and with all mitochondrial subpopulations present (e.g. subsarcolemmal, interfibular or nuclear). In contrast, different populations of mitochondria can be separated during differential centrifugation that is associated with the classical methods of mitochondrial isolation. Tissue homogenisation also requires less tissue compared to mitochondrial isolation [179]. While older publications mention 0.5g as a small piece of tissue [180], the manual of Abcam's isolation kit still suggests 0.2-0.4g of heart tissue (Abcam Mitochondrial Isolation Kit for Tissue, ab110168). As this study aimed to assess left ventricle only, the available amount of tissue was often 5-10 times less than 0.2g. This meant that several animals would have had to be used for mitochondrial isolation. Permeabilized fibres are also commonly used preparations which wield the advantage of using a mitochondrial preparation in close proximity to intact intracellular architecture (e.g. the sarcoplasmic reticulum, myofilaments) which allows for intracellular signalling. For comparison, in homogenates and isolated mitochondria these connections are severed or absent. However, it is very difficult to accurately normalise values for protein or mitochondrial content in permeabilised fibres because the fibre bundles are extremely small (<2mg) and full of water; in contrast, it is very easy to accurately assay for protein or markers of mitochondrial content (e.g. citrate synthase) in homogenates and isolated mitochondria with very little margin for error (Doerrier et al., MiPNet17.03(4:1-12), 2015). In addition, permeabilized fibres have large diffusion distances and hyperoxic

respiration media is required. Intact cells have the upside of high relevance to an in vivo environment, similar to permeabilized fibres. They are also relatively easy to normalise but it has been suggested that different results can be generated based on normalization method [181]. Intact cells do not allow for easy access to the mitochondria while the cell membrane is still intact. They can, however, be permeabilized with detergents (e.g. saponin or digitonin), but optimisation of concentration is crucial as high concentrations of e.g. digitonin can act in an inhibitory manner [182]. For this current study, it was decided that the method of homogenised tissue with the advantages e.g; original abundancy of mitochondria, easy access for substrate and inhibitors, accurate normalisation options and the possibility to use one animal for several experiments (due to the need of small amount of tissue) outweighed any negatives.

3.4.2.2 Antioxidant assays

The modest number of animals in this study does not allow for a true representation of possible changes. An n of 3 per group generated far less than the recommended 0.8 in statistical power with only 0.093 for males and 0.12 for females regarding H_2O_2 clearance as well as, 0.058 for males and 0.064 for females regarding SOD activity. Calculations suggested that to achieve a statistical power of 0.8, an additional 14 male and 19 female animals would be needed for H_2O_2 clearance. In regards to SOD activity an additional 5 males and 282 females were suggested necessary by calculations. The data presented suggest a trend towards increased activity in SOD in males from hypoxic pregnancies compared to males from normoxic pregnancies, but we cannot conclude anything at the current time.

3.4.2.3 Western blots

Western blotting has become one of the most commonly performed techniques for protein identification and semi-quantification [183]. The method allows for qualitative assessment of protein content and size. It is highly sensitive and can detect nano to picomolar concentrations, but as with any method, it has its limitations. Western blotting is a complicated procedure and there are many steps where results can be skewed. One study showed that almost 80% of the total variance of their western

blotting results was due to the analyst performing the method [184] making comparison of quantification difficult between experiments performed by different researchers. As such, although help was given by a very talented and capable student, Callum Quinn, the addition of a second analyst could cause additional variance. The study also pointed out a range of error sources including inhomogeneous electrical fields during electrophoresis and transfer. With this in mind, we interpret the results with some caution. Going forward from here, we recommend the combination of western blot for quality control and addition of the enzyme-linked immunosorbent assay (ELISA) which would allow for accurate quantification [185].

4 Calcium handling

4.1 Introduction

In the previous chapters, we have shown that our model expressed a mitochondrial phenotype with increased ROS production in males from hypoxic pregnancies and decreased ROS production in females from hypoxic pregnancies when comparing to their normoxic counterparts. In addition, we have shown that complex IV activity was higher in females from hypoxic pregnancies, compared to females from normoxic pregnancies, and that altered complex IV activity affected ROS production. Although the study showed no differences in adult whole heart function, previous literature has shown isolated hearts from hypoxic pregnancies exhibit diastolic dysfunction, heightened contractility and enhanced sympathetic sensitivity [31, 33, 109].

Considering the nature of the heart and the cardiomyocyte, it is easy to understand that Ca^{2+} handling plays an important role in its function, and that dysfunctional Ca^{2+} handling can be linked to cardiovascular diseases e.g. heart failure [186, 187]. Ca^{2+} handling in the cell is controlled by a range of processes (described in more detail in 1.4.1.1) some of which are affected by alterations in ROS production. As an example, increased H_2O_2 levels affect E-C coupling and can increase the activity of ryanodine receptors and decrease the activity of SERCA, for review, see [188]. In fact, previous studies have shown increased SERCA2a abundance in adult offspring from hypoxic pregnancies [31] but to our knowledge, no studies have looked at the effect prenatal hypoxia on adult cardiomyocyte contractility and Ca^{2+} handling.

Isolated cardiomyocytes allow for the exploration of intracellular Ca^{2+} concentrations while allowing for pharmacological alteration of cardiomyocyte function. Therefore, this section of the study aimed to assess Ca^{2+} handling in the cardiomyocyte both during baseline and isoprenaline-induced (β-adrenoreceptor agonist) contractions. This section also aimed to investigate the amount of Ca^{2+} stored in the SR and the kinetics of Ca^{2+} clearance from the cell.

4.2 Methods

4.2.1 Cell isolation

Alterations to Ca^{2+} handling were measured in isolated LV cells from 19 C57BL/6 mice (n=5 male normoxic, n=4 male hypoxic, n=6 female normoxic and n=4 female hypoxic) at 23±6 weeks of age. The perfusion solution was prepared by mixing an isolation solution (134mM NaCl, 10mM HEPES-acid, 11.1mM glucose, 1.2mM NaH_2PO_4, 1.2mM $MgSO_4$ and 4mM KCl, pH 7.34) with taurine solution (115mM NaCl, 10mM HEPEPS-acid, 11.1mM glucose, 1.2mM NaH_2PO_4, 1.2mM $MgSO_4$, 4mM KCl and 50mM taurine, pH 7.34) in a 1:1 ratio. Mice were sacrificed by cervical dislocation and hearts were rapidly excised and washed in ice-cold perfusion solution. The aorta was cannulated using a 24-gauge reusable feeding needle (Fine science tools, Heidelberg, Germany), attached to a 1ml syringe containing perfusion solution and sutured using cotton thread. A small amount of perfusion solution was carefully pushed through the needle and the position was deemed correct if the coronary arteries cleared of blood. The heart was then rapidly mounted onto a langendorff perfusion system set to 37°C and perfusion was started immediately, using a peristaltic pump, creating a constant flow of 5ml/minute. The heart was left to wash through for 4-5 minutes to assure all blood was washed out of the arteries. Following this wash step, a three-way tap was used to switch to a separate perfusion solution containing 1.33mg/ml Type II collagenase (Worthington, USA), which was manually recirculated using a Pasteur pipette, to start digestion. Digestion was carried out for 9-13 minutes and optimal digestion was determined by assessing the firmness of the heart through careful pinching. Once digested, the ventricles were cut down and carefully washed with 0.5ml perfusion solution which was then carefully removed. Following this, the tissue was minced with scissors in stop solution (9-10ml perfusion solution containing 12.5µM $CaCl_2$ and 0-1ml fetal bovine serum) and filtered through a matrix filter (CellMicroSieves™, 200µm pore, Fisher Scientific, UK). This step was repeated two times, on the remaining tissue, with decreasing amounts of fetal bovine serum (1ml, 0.5ml and 0ml); the volume was corrected with perfusion solution. In the latter repeats, the tissue was also

subjected to trituration with a Pasture pipette to further separate the cells. In total, this led to three subsets of cell suspensions with varying levels of fetal bovine serum. Viability of cells from each subset was assessed visually with a light microscope and cells presenting with well-defined membranes and visual sarcomeres were kept and used experimentation.

4.2.2 Cell preparation and loading

The cells, chosen for experiments were kept in a 'half-in-half' solution made up by mixing taurine solution and normal Tyrode's (NT; 134mM NaCl, 10mM HEPES-acid, 11.1mM glucose, 1.2mM MgCl. 4mM KCl_2 and 1mM $CaCl_2$, pH 7.34) in a 1:1 relationship. This 'half-in-half' solution gave the cells a chance to recover from the isolation in a medium with lower Ca^{2+} levels. Cells were then loaded with 100nM of the cell-permeable Ca^{2+} indicator fura-2-acetoxymethyl ester (Fura2-AM; Invitrogen) for 10 minutes at room temperature. The ester group allows the compound to cross the cell membrane. Once inside the cell, the ester is cleaved off by esterase and Fura2-AM is left as a charged fluorophore with diminished cell permeability. During the 10 minutes, cells would sediment and once loading was complete, the majority of the supernatant was removed and the cells were re-suspended in a fresh solution of NT and taurine solution (1:1 relationship) to allow for de-esterification of the indicator and to stop further loading.

4.2.3 Field stimulation and measurement of calcium

Loaded cells were left to settle on a microscope slide in a custom-made field stimulating bath (figure 4-1). Briefly, the bath had two 1mm thick silver electrodes running along the bottom of the bath thus covering the bottom surface with an electrical field controlled by a Grass instruments SD9 stimulator. The stimulator would trigger a 0.4ms pulse with each received digital trigger signal from an Axon Digidata 1440A (Molecular Devices, CA). Cells were imaged on a Nikon Eclipse Ti fluorescence microscope (Scientifica, UK). Ca^{2+} was measured by excitation of the ratiometric dye fura-2 AM. The dye was excited at wavelengths 340nm and 380nm, using a xenon arc lamp (Cairn Research, UK). Emission was measured at 510nm

amplified by a photon multiplier tube and digitised by the DigiData 1440A. All signals were recorded using Clampfit (Clampfit 10.4, Axon Instruments) which also generated a raw ratio from the 340nm signal and the 380nm signal (see example in figure 4-2). During baseline measurement, cells were washed with a constant flow of NT and stimulated at 0.5Hz (see sample trace figure 4-3) and a minimum of 10 stable contractions were recorded. To measure the Ca^{2+} stored in the SR, stimulation was turned off and the flow of NT was switched to an NT solution containing caffeine and 2,3-Butanedione 2-monoxime (BDM; 10mM and 10mM, respectively); caffeine increases the opening probability of the ryanodine receptors allowing all the Ca^{2+} in the SR to be released (see sample trace figure 4-6). The caffeine solution was on for 3 seconds (pre-determined as the time needed to release all Ca^{2+} from the SR) after which the flow was switched from caffeine solution back to NT. Once the trace with caffeine had peaked and returned to base level, stimulation was started again and the cell was left to stimulate until the trace stabilised. Following this, the flow was changed to an NT solution containing 100nm isoprenaline (ISO) to stimulate the beta-adrenergic pathway. ISO gradually increased the amplitude of the fluorescence trace (see sample trace figure 4-4), thus cells were left in ISO until a peak was reached and the traces were once again stable. Once cells had reached satisfactory stability (see sample trace figure 4-5), 10 contractions were measured after which stimulation was again turned off and the cells were subjected to another 3 seconds of caffeine solution (see sample trace figure 4-7). The cells were again left to stabilize after which the protocol was terminated. The viewpoint was then moved so that the cell was just outside the field of view and 4 sweeps of background fluorescence were recorded.

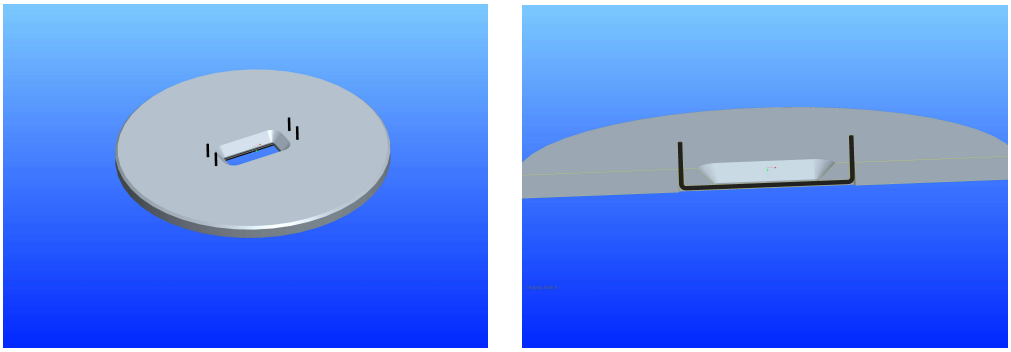

Figure 4-1 Custom made stimulator bath. Schematic Images showing the custom made stimulator bath. The image on the left shows the bath as a whole while the image on the right is a cross-section to clarify the position of the electrodes. The model was created by David Chorlton in collaboration with the authors.

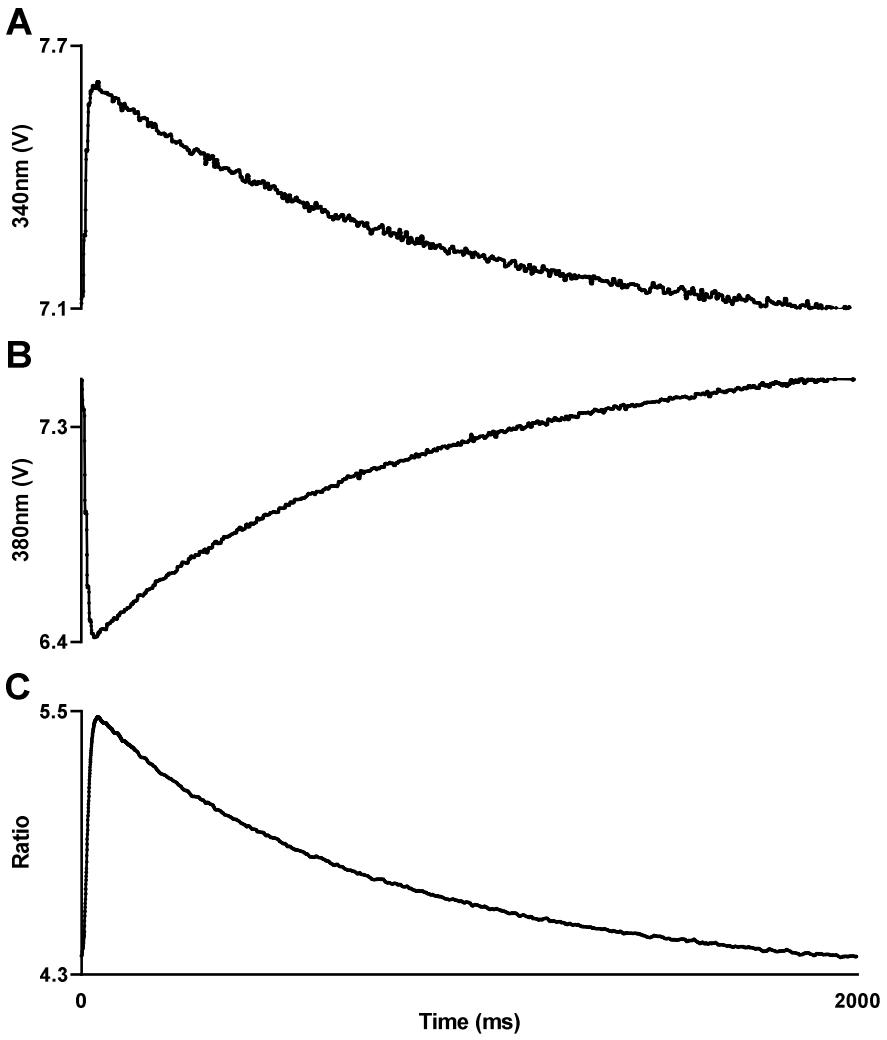

Figure 4-2 Sample trace from Clampfit. As Fura-2 is a ratiometric dye, it excites at two wavelengths which are then recorded separately. Top trace from the 340 nm excitation (A) and mid trace from the 380nm excitation (B). Clampfit then calculates a ratio of the two recordings, which correspond to intracellular Ca^{2+} concentration (C).

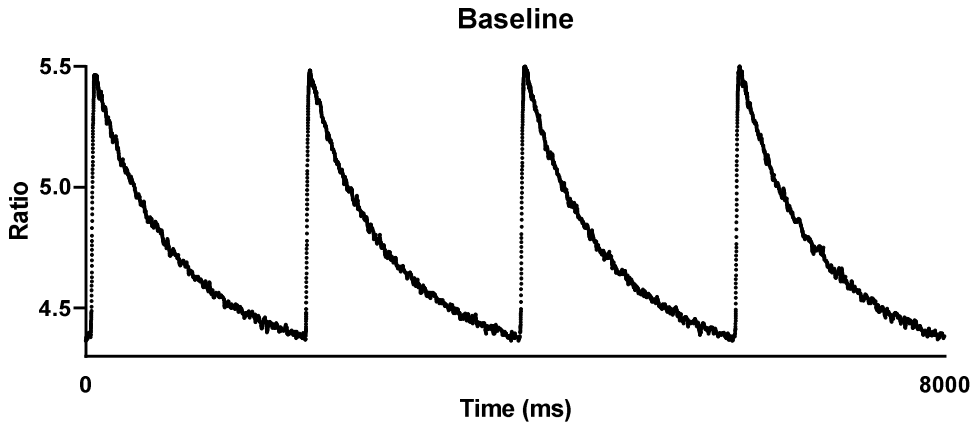

Figure 4-3 Sample trace of baseline. The sample of raw ratio trace from 8 seconds of stimulation (0.5hz) with NT solution.

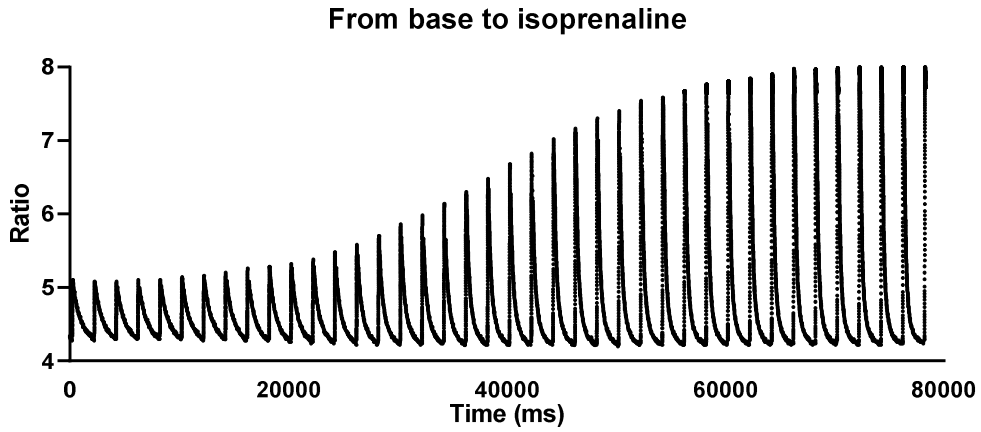

Figure 4-4 Sample trace of baseline fluorescence to fluorescence with isoprenaline. A sample trace to show the transition from the baseline to when the isoprenaline is at full effect.

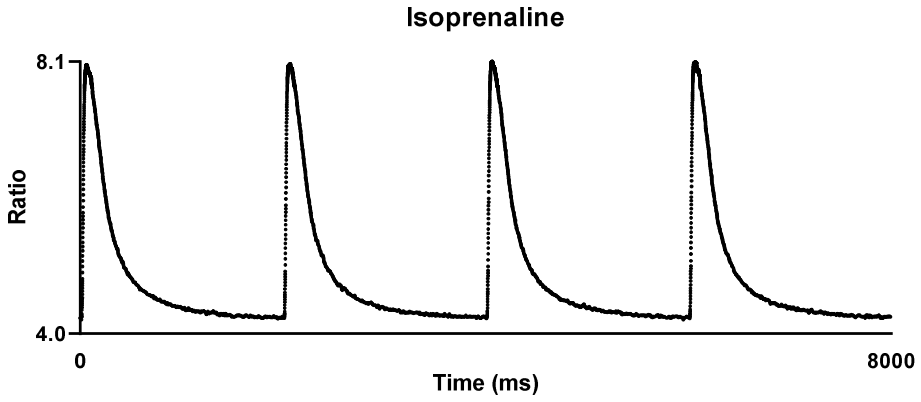

Figure 4-5 Expanded sample trace of isoprenaline. The sample of raw ratio trace from 8 seconds of stimulation (0.5hz) with isoprenaline solution.

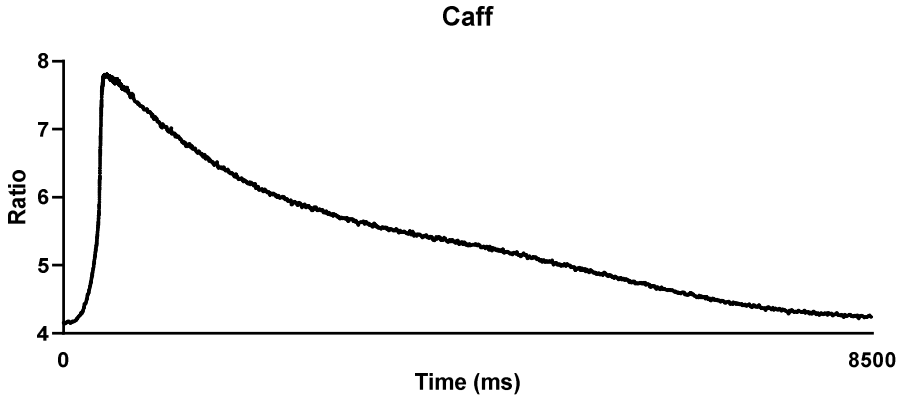

Figure 4-6 Sample trace of baseline caffeine. The sample of raw ratio trace from 8.5 seconds of no stimulation following caffeine solution.

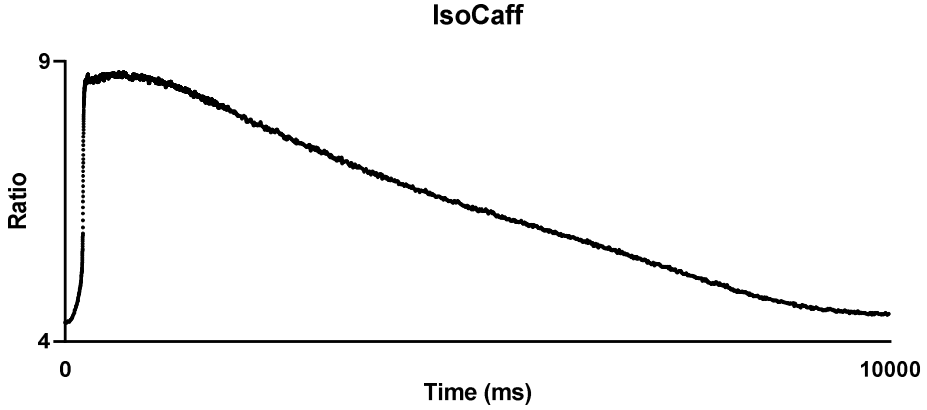

Figure 4-7 Sample trace of isoprenaline caffeine. The sample of raw ratio trace from 10 seconds of no stimulation following caffeine solution.

4.2.4 Western blots

Western blots were performed as previously described in chapter 3.2.5 with only a few alterations, including loading of 5µg tissue (compared to 10µg) as well as the modifications detailed below.

4.2.4.1 Blocking and detection of protein

For reduction of background noise and non-specific binding, membranes were blocked with SuperBlock™ (Thermo Fisher, UK) at room temperature and subsequently washed in TBS-T for 3 x 5 minutes. Membranes were then incubated on an orbital roller with a SERCA2a primary antibody (sc73022; Santa Cruz Biotechnology, Inc., TX) diluted 1:5000 in TBS-T at 4°C overnight.

Following primary antibody incubation, membranes were washed in TBS-T for 3 x 5 minutes. The secondary antibody was a horseradish peroxidase-conjugated, Pierce goat anti-mouse, which was diluted 1:20,000 in TBS-T. The membranes were incubated for 1 hour, on a rocker at room temperature. Protein reactivity was detected using chemiluminescence (Price Supersignal West Pico, Thermo Fisher, UK) imaged digitally in a Syngene Chemi genius (Syngene, UK) and analysed with the software Genesnap (Syngene, UK).

4.2.5 Calculations

Fluorescent traces (equating to Ca^{2+}) were analyzed using an excel based program detailed in Greensmith 2014 [189]. Briefly, 10 sweeps from the 340 and the 380 channels were averaged and exported from Clampfit (Clampfit 10.4, Axon Instruments). In addition to this, 4 sweeps from the no-cell measurements were also averaged and exported. In Greensmith's program, the no-cell measurement is subtracted from the raw 340 and 380 measurements to remove the background signal from non-cellular sources. Following that, the 340 signal is divided by the 380 signal (see equation 4-1) to give a single curve representing intracellular Ca^{2+} concentration.

$$Ratio = \frac{340nm}{380nm}$$

Equation 4-1 Calculation of fluorescence ratio. The ratio for the Ca^{2+} measurements is calculated by dividing the 340nm signal with the 380nm signal.

4.2.5.1 Rate of decay

The rate constant of decay, which is a measurement of Ca^{2+} clearance in the cell, was also calculated by Greensmith's program. The program fits a single exponential curve, to the Ca^{2+} transient, between the peak and the baseline.

4.2.5.2 SERCA activity

The main route of Ca^{2+} clearance in a myocyte is through SERCA, and as such, it is a major controlling factor of the previously mentioned rate of decay. To measure SERCA activity, the activity of additional Ca^{2+} clearance pathways (mentioned in section 1.4.1) are determined while the cell is treated with caffeine. As the open probability of the ryanodine receptors is heightened during incubation with caffeine, the clearance of Ca^{2+} through SERCA is nullified and the remaining Ca^{2+} clearance pathways become responsible. As such, by subtracting the rate of decay during caffeine with the rate of decay during baseline, we get insight into the activity of SERCA (see equation 4-2).

$$SERCA\ activity = Rate\ of\ decay_{Baseline} - Rate\ of\ decay_{Caff}$$

Equation 4-2 Equation for calculation of SERCA.

4.2.6 Statistics

Ca^{2+} handling data are expressed as means ± SEM and were graphed using Graphpad Prism®, version 8 (Graphpad Software, San Diego, CA). Throughout, males are shown in filled pink circles and females in open blue boxes. Data were tested for equal variance and normal distribution before statistically tested using a 2-way ANOVA, with sex and intrauterine oxygen levels as two between-subject factors using SigmaPlot version 12.5 (Systat, San Jose, CA) and Tukey's correction for multiple comparisons test to determine significant differences between groups.

4.3 Results

4.3.1.1 Calcium handling

To assess the impact of prenatal hypoxia on Ca^{2+} handling in the adult cardiomyocyte, LV cells were isolated and field stimulated while loaded with the Ca^{2+}-sensitive dye fura-2AM. There were no differences seen in either males or females from hypoxic pregnancies regarding systolic Ca^{2+} transient amplitude during stimulation in NT (figure 4-8 A) or during stimulation in ISO (figure 4-8 B), compared to offspring from normoxic pregnancies.

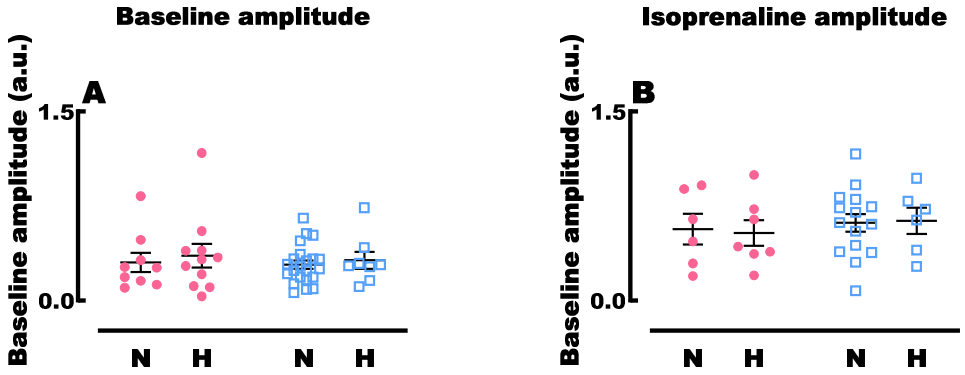

Figure 4-8 Ca^{2+} amplitudes. Ca^{2+} transient amplitudes were measured by stimulating isolated LV cardiomyocytes loaded with the fluorescent dye fura-2. There were no differences during baseline concentrations (A) or during contractions under the influence of isoprenaline (B). Males are shown in filled pink circles and females in open blue boxes. Data are presented as mean ± SEM, n=9 cells from 5 normoxic males, 11 cells from 4 hypoxic males, 22 cells from 6 normoxic females and 8 cells from 4 hypoxic females for baseline amplitude. For isoprenaline amplitude, n=6 cells from normoxic males, 6 cells from hypoxic males, 15 cells from normoxic females and 6 cells from hypoxic females with the same amount of animals as baseline amplitude. Significance was tested by two-way ANOVA with a Tukey's posthoc.

4.3.1.2 SR calcium content

The amount of Ca^{2+} stored in the SR was assessed in offspring from hypoxic pregnancies and compared to offspring from normoxic pregnancies. There were no differences in SR Ca^{2+} content, under baseline conditions or following application of ISO (figure 4-9 A and B respectively), in either males or females from hypoxic pregnancies compared to offspring from normoxic pregnancies.

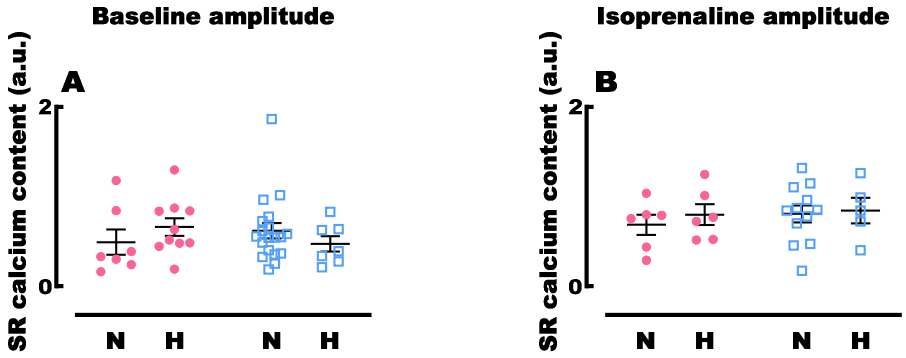

Figure 4-9 SR content. SR content was measured by the addition of caffeine to baseline and isoprenaline treated cells to assess Ca^{2+} loading of the SR. There were no differences during baseline (A) or under the influence of isoprenaline (B). Males are shown in filled pink circles and females in open blue boxes. Data are presented as mean ± SEM, n=7 cells from 5 normoxic males, 10 cells from 4 hypoxic males, 19 cells from 6 normoxic females and 7 cells from 4 hypoxic females for baseline SR content. For SR content with isoprenaline, n=6 cells from normoxic males, 6 cells from hypoxic males, 12 cells from normoxic females and 5 cells from hypoxic females with the same amount of animals as baseline amplitude. Significance was tested by two-way ANOVA with a Tukey's posthoc.

4.3.1.3 Calcium clearance

There was no difference in the time it takes for Ca^{2+} to be cleared from a cell in male offspring from hypoxic or normoxic pregnancies at baseline. However, females from hypoxic pregnancies were able to remove cytosolic Ca^{2+} faster than females from normoxic pregnancies (figure 4-10 A). Under the influence of ISO, however, the difference was no longer seen and neither males nor females from hypoxic pregnancies showed any differences in Ca^{2+} clearance time, compared to males and females from normoxic pregnancies (figure 4-10 B)

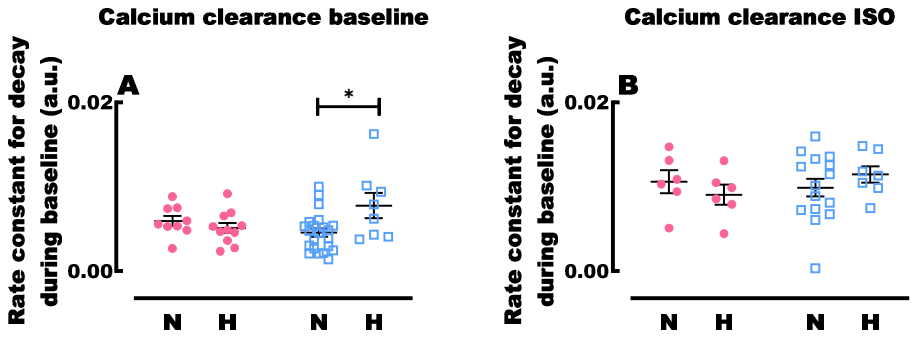

Figure 4-10 Ca^{2+} clearance. The rate with which the Ca^{2+} is removed from the cytoplasm was higher in females from hypoxic pregnancies compared to females from normoxic pregnancies during baseline but no differences in males (A). During ISO there were no differences in Ca^{2+} removal in either males or females (B). Males are shown in filled pink circles and females in open blue boxes. Data are presented as mean ± SEM, n=9 cells from 5 normoxic males, 11 cells from 4 hypoxic males, 22 cells from 6 normoxic females and 8 cells from 4 hypoxic females for Ca^{2+} clearance at baseline. For Ca^{2+} clearance with isoprenaline, n=6 cells from normoxic males, 7 cells from hypoxic males, 15 cells from normoxic females and 7 cells from hypoxic females with the same amount of animals as baseline amplitude. Significance was tested by two-way ANOVA with a Tukey's posthoc.

4.3.1.4 SERCA activity and abundance

The next series of experiments aimed to determine if Ca^{2+} removal via SERCA was altered in response to hypoxia. The data shows that although, there were no alterations to SERCA activity across groups, (figure 4-11 A), the abundance of SERCA2a protein was altered. Males from hypoxic pregnancies had higher amounts of SERCA2a protein in the LV than the males from normoxic pregnancies (figure 4-11 B).

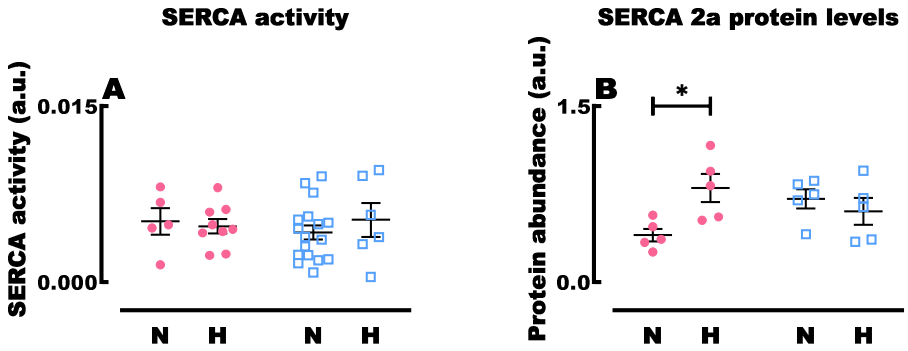

Figure 4-11 Calculated SERCA activity and protein abundance. (A)SERCA activity was calculated as the difference of Ca^{2+} removal in the presence and absence of caffeine. No differences were seen in SERCA activity in offspring from hypoxic pregnancies compared to offspring from normoxic pregnancies. (B) SERCA2a protein levels, however, were higher in males from hypoxic pregnancies compared to males from normoxic pregnancies. There were no differences in females. Males are shown in filled pink circles and females in open blue boxes. Data are presented as mean ± SEM, n=9 cells from 5 normoxic males, 11 cells from 4 hypoxic males, 22 cells from 6 normoxic females and 8 cells from 4 hypoxic females for SERCA activity at baseline. For SERCA2a protein abundance, n=5 for each group. Significance was tested by two-way ANOVA with a Tukey's posthoc.

4.4 Discussion

The results from this study showed that hypoxia during pregnancy had very little effect on Ca^{2+} handling in the heart of adult offspring. Although beat-to-beat Ca^{2+} concentrations and the amount of Ca^{2+} stored in the SR were unaltered following hypoxia, there was a sex-dependent effect on Ca^{2+} clearance and SERCA 2a activity.

4.4.1.1 Beat-to-beat calcium amplitudes

This study showed no effect of prenatal hypoxia on adult beat-to-beat Ca^{2+} transient amplitude. Neither males nor females from hypoxic pregnancies showed any differences in Ca^{2+} amplitude during baseline contractions or contractions with ISO. The lack of differences during baseline contraction was not surprising as there were no effects seen on whole heart function in this current study (Table 2.1). However, somewhat surprising was the lack of an effect during ISO, as previous studies of prenatal hypoxia have shown altered response to adrenergic signalling. Niu et al. showed an increased cardiac sympathetic dominance in rats [31]. While that study used a lower amount of oxygen (13% compared to 14% in this study) in their experiment, which could account for the differences, there are reasons to question their conclusion. The parameters presented by Niu et al. are not strictly response to adrenergic stimulation but a ratio between response to isoprenaline and carbachol (muscarinic receptor agonist). As such, an additional factor could lie in the parasympathetic response rather than the sympathetic. Previous studies have demonstrated increased β_1-adrenergic receptor expression in foetal rat hearts [102] as well as sensitivity of β-adrenergic receptors in chicken embryos [149]. This increased sensitivity in chick embryos was, however, decreased postnatally. Considering this, the age of the studied adult might be of importance. It is difficult to compare ages between species but the rats used by Niu et al were considerably younger (4 months of age) than the mice used in this current study.

4.4.1.2 Calcium clearance

As discussed in section 1.4.1, during normal contractions, a small amount of Ca^{2+} is taken into the cell through the L-type Ca^{2+} channel which in turn stimulates a greater release of Ca^{2+} from the SR through the RyR. The high concentration of Ca^{2+} in the cytosol allows for Ca^{2+} binding to the myofilaments and leads to a contraction. For relaxation, Ca^{2+} is removed from the cytosol through four different pathways. The majority of Ca^{2+} is removed by reuptake to the SR through SERCA. In addition, there is also the antiporter, NCX and ATP driven PMCA that both transport Ca^{2+} out of the cell and the MCU that transports Ca^{2+} into the mitochondria.

This study has shown that females from hypoxic pregnancies are able to extrude Ca^{2+} faster under baseline conditions (figure 4-10 A), but not while under the influence of ISO (figure 4-10 B). As there were no differences in SERCA2a activity or abundance we conclude that the difference seen in extrusion is due to one or several of the remaining three pathways [38]. Interestingly, males showed an increase in SERCA2a abundance but no difference in SERCA activity or overall Ca^{2+} extrusion. Increased SERCA in adult males from hypoxic pregnancies has previously been shown [31]. In this study, the authors speculate that the increased SERCA2a abundance could be a compensatory mechanism to combat increased diastolic Ca^{2+}. However, considering our results, it is likely that the SERCA2a abundance is a compensatory mechanism for a lowered activity. We speculate that the lack of difference in SERCA activity, in the presence of increased protein abundance, could be due to inhibitory effects of phospholamban [190] or the increased ROS production in the male offspring from hypoxic pregnancies [191]. This would make an interesting area of future study.

5 General discussion

This study aimed to develop a mouse model of prenatal hypoxia and assess the impact on birth weight and the adult cardiac phenotype. Specifically, adult whole heart function, response to I/R, alterations to mitochondrial function and morphology as well as cellular Ca^{2+} handling and response to a β-adrenoreceptor agonist were studied.

5.1 A brief summary of the results

During the hypoxic insult, there were no alterations to maternal body weight, food or water intake. At birth the offspring from hypoxic pregnancies showed no signs of IUGR and body weight stayed un-affected throughout adulthood. Adult whole heart function was assessed by echocardiography which showed no differences between offspring from hypoxic pregnancies compared to offspring from normoxic pregnancies. Prenatal hypoxia showed no effect on the response to an in vitro I/R challenge.

Mitochondrial abundance in left ventricular tissue was not affected by prenatal hypoxia as assessed with EM and by the exploration of citrate synthase activity. However, mitochondrial cristae density was reduced in both male and female offspring from hypoxic pregnancies. Complex I, II and IV activity was also assessed. There was no impact of prenatal hypoxia seen in males. Females, however, had reduced activity of complex I and II but increased complex IV activity. High resolution respirometry coupled with simultaneous fluorescent measurement of ROS production allowed for assessment of mitochondrial respiration and ROS production throughout several mitochondrial respiratory states. Mitochondria from male and female offspring responded differently to the prenatal insult. While males from hypoxic pregnancies showed lessened limitation from the phosphorylation system and/or the indicated pressure from the proton motive force, there were no other alterations in the mitochondrial oxygen consumption measurements. Females, on the other hand, showed increased respiration in most respiratory states measured. Regarding ROS production, compared to their normoxic

counterparts, males from hypoxic pregnancies produced more ROS in almost all states measured while females from hypoxic pregnancies produced less ROS is most states measured. Additional experiments lead us to the conclusion that this relief of ROS production in the females was most likely due to increased activity of complex IV.

Ca^{2+} handling in isolated cardiomyocytes was largely unaltered by prenatal hypoxia. There were no differences in Ca^{2+} amplitude in males or females during baseline or under the influence of isoprenaline. There were no changes in SR Ca^{2+} loading during baseline or with isoprenaline. However, adult females from hypoxic pregnancies showed an increased Ca^{2+} clearance during baseline but no difference in SERCA 2a protein abundance, compared to females from normoxic pregnancies. Conversely, males from hypoxic pregnancies had increased SERCA 2a protein abundance but no difference in Ca^{2+} clearance, compared to males from normoxic pregnancies. The results of this study are detailed in table 5.1.

		Sex *(males vs females)*		Treatment *(hypoxic vs normoxic)*	
	Parameter	**Normoxic**	**Hypoxic**	**Male**	**Female**
Model validation	Body weight	↑	↑	↔	↔
	Litter size	↔	↔	↔	↔
	Heart rate	↔	↔	↔	↔
	Whole heart basal function	↔	↔	↔	↔
	Ischaemia/reperfusion			↔	↔
Enzyme activity	Citrate synthase activity	↔	↔	↔	↔
	Complex I activity			↔	↓
	Complex II activity			↔	↓
	Complex IV activity			↔	↑
Oxygen consumption	Leak + CI substrates	↑	↔	↔	↔
	OXPHOS + CI substrates	↑	↓	↔	↑
	OXPHOS + CI+II substrates	↔	↓	↔	↑
	ET-max + CI + CII	↑	↓	↔	↑
	ET-max + CII	↔	↔	↔	↑
	Complex IV	↔	↓	↔	↑
	RCR	↔	↔	↔	↑
	Phosphorylation control (P/E)	↔	↔	↑	↔
	Leak control ratio (L/E)	↔	↔	↔	↔
ROS production	Leak+ CI substrates	↓	↔	↑	↔
	OXPHOS + CI substrates	↓	↔	↑	↓
	OXPHOS + CI+II substrates	↓	↔	↑	↓
	ET-max + CI + CII	↓	↔	↔	↔
	ET-max + CII	↓	↔	↔	↓
Protein expression	Complex I	↔	↔	↓	↔
	Complex II	↔	↔	↓	↔
	Complex III	↔	↔	↔	↔
	Complex IV	↔	↔	↔	p=0.08
	Complex V	↔	↔	↔	↔
EM	Mitochondrial density	↔	↔	↔	↔
	Cristae density	↑	↓	↓	↓
	Antioxidant activity	↔	↔	↔	↔
Calcium handling	Ca amplitude (baseline)	↔	↔	↔	↔
	Ca amplitude (iso)	↔	↔	↔	↔
	SR Ca content (baseline)	↔	↔	↔	↔
	SR Ca content (iso)	↔	↔	↔	↔
	Calcium clearance (baseline)	↔	↔	↔	↑
	Calcium clearance (iso)	↔	↔	↔	↔
	SERCA activity	↔	↔	↔	↔
	SERCA2a protein	↔	↔	↑	↔

Table 5.1 Summary data for newborn and adult offspring from hypoxic pregnancies.

5.2 Study relevance

Cardiovascular disease is still one of the leading causes of death in the world today [1]. Insufficient oxygen supply to a developing foetus can lead to increased susceptibility to cardiovascular disease [14, 97, 107]. To our knowledge, there are no conclusive studies regarding maternal smoking and oxygen delivery to the foetus, but there are obvious links between smoking mothers and birth size [108]. As an example, let's consider people born in America in the year 1920. By the time they reached 20 years of age, there was ~75% chance they would be smoking if they were male and ~50% if female. These numbers have gone down but for women born in 1960 there was still ~40% chance they would have become smokers at the age of 20 [192]. As times have moved on, the general population are now more aware of the dangers involving smoking, including smoking during pregnancy. Even so, in 2005, 10%-12% of women giving birth in America reported smoking during the pregnancy [193]. As the links aren't completely clear, we can only delve so deep into this but it is an unsettling thought how many of us today could be suffering from the adverse effects of prenatal hypoxia. In addition, there are studies suggesting lowered air saturation with increased pollution which further complicates the situation [194].

5.3 Animal model and the difficulty of diagnosis

In this study, we created a mouse model of chronic prenatal hypoxia using 14% oxygen during GD 6-18. We showed no signs of effect on either the dams or the offspring at basal levels. Our echo results showed no alterations to whole heart function and we saw no differences in susceptibility to I/R injury. However, as shown in chapter 3 and 4, there is reason for concern. The main goal with most medical research is to gain understanding so to allow for prevention, treatment and/or cures for the condition studied and thereby increase a population's quality of life. However, to be able to treat or cure any ailment, there must first be a concise, conclusive way of diagnosing its presence. In the case of prenatal hypoxia this is not currently possible. The occurrence of IUGR is common with prenatal

hypoxia [19, 30, 112, 195, 196] but not obligate for adverse outcomes as seen in this current study as well as others [22, 31]. In addition, IUGR cannot be considered a hallmark of prenatal hypoxia exclusively because it also commonly occurs with other prenatal insults, e.g. nutritional deficiency and substance abuse [8, 197]. Unfortunately this current study does not further the cause of finding a concise mean of diagnosis.

This current study does, however, show that mice can be used as a suitable model for future research into the effects of prenatal hypoxia on the adult cardiac phenotype. As technology advances, we continue to find new opportunities for discovery. For example, CRISPR/Cas9 technology is allowing alterations of the genetic makeup of the mouse as a model, opening up a great range of possibilities [198, 199]. It is known that maternal antioxidant treatment can have a positive effect on the offspring's adult cardiac phenotype [31]; would there be similar a phenotype in mice with overexpressed foetal catalase or SOD activity? Such an experiment may gain insight into whether H_2O_2 or O^{2-} or both were involved in the effects of prenatal hypoxia. As some studies, including this current study, have pointed toward alterations in the mitochondrial electron transport and ROS production [30, 112] it would be of great interest to alter the activity and abundance of selected mitochondrial complexes and thereafter assess the impact of prenatal hypoxia. In addition, to allow for genetic alterations, mice also offer a short generation time [200] which makes longitudinal studies over multiple generations possible. In this regard, it would be interesting to look at the trans-generational effects of prenatal hypoxia in mice.

5.4 The importance of complex activity

Considering the nature of the ET-pathway and the need for strict coupling between the four complexes, any alterations downstream may lead to imbalanced and inadequate transport of the electrons, changing the redox potential upstream which in turn leads to greater slippage. The results of intact mitochondrial function in females from hypoxic pregnancies suggest that the relationship between the electron transport complexes has a greater impact than the activity or abundance of each separate complex. Although complex I and II activity were reduced, the

combined respiration from the complete pathway was increased. We believe that zones of increased redox potential act as a bottleneck in the pathway. As complex IV activity was increased in combination with the decrease of complex I and II, the population of Q-pool experiences a shift in redox potential as the influx of electrons transported by complex I and II are reduced in combination with increased efflux by complex IV. Studies have shown that addition of coenzyme Q10 can reduce ROS production and increase respiration [201]. We propose that the function is similar in this study where there is a shifting redox potential of the Q-pool, either due to the addition of coenzyme Q10 or as in our case, due to lowered electron influx and increased efflux.

This theory also bears relevance to other studies that have shown females from hypoxic pregnancies respond better to an I/R challenge than males from hypoxic pregnancies [22]. When the reduction of the Q-pool becomes too great, due to increased electron influx from complex II, complex I go in reverse. This leads to the reduction of NAD^+ to NADH and a spike in ROS production [80, 202]. We propose that, in the case of an adult female who has previously been subjected to prenatal hypoxia, there are several alterations that help lessen this response: 1) Complex II activity is decreased, slowing down the influx of electrons during reperfusion. 2) Complex I activity is decreased, reducing the number of electrons that are accepted for reversed efflux. 3) Complex IV activity is increased, allowing more electrons to move in the intended direction oxidising complex III and IV. Our data suggest these three parameters act as a protective response in females from hypoxic pregnancies, but they appear absent in the males. In addition, males had an increased basal ROS production which may lead to increased damage during the reversed electron transport that occurs with reperfusion.

5.5 The difference between males and females

Unfortunately, this study was not able to address the reason for the differences between the response to prenatal hypoxia in males versus females. Studies have shown that oestrogen can lower myocardial necrosis from I/R [203] and that oestrogen can have an effect on mitochondrial complex activity [204]. It is possible

that either or both of these effects play a role in developmental programming. In addition, previous studies have shown sex-dependent differences in cardiac S-nitrosylation and suggested that this can be cardioprotective in females [205]. As this current study has not added to the knowledge in this regard, it will not be discussed in any further detail.

5.6 Future work

As a first step towards identifying the mechanism for sex-dependent differences, we could subject oestrogen receptor knockout mice to prenatal hypoxia; this could give us a chance to distinguish what role oestrogen plays in developmental programming.

The theory of complex IV's involvement in ROS production and in I/R damage should be further studied. To some extent, this pathway could be studied with pharmacological inhibition of certain complexes, but it would be better to use gene-modified mice. By alteration of the genome, one could mimic the changes seen in females from hypoxic pregnancies in this study. That altered mouse could then be used to explore oxygen consumption and ROS production as well as the response to in vitro I/R. As the current study was subject to technical limitations, regarding the in vitro I/R, it would also be beneficial to repeat these experiments to assure the observations in this study were correct.

Unfortunately, this study could not answer questions regarding antioxidant systems to a satisfactory level. The activity of SOD and H_2O_2 clearance should be repeated and it would beneficial to explore protein contents related to these systems as well. It would also be interesting to assess whether or not PKCε is altered in our model of prenatal hypoxia the same way that has been shown by e.g. Xue and Zhang [22].

There is a gap in the literature regarding how maternal smoking relates to prenatal hypoxia, possibly due to the issue of separating the effects of nicotine and the combustion of the cigarette itself. However, with the fast rise of the e-cigarettes, there should now be possibilities to design a study with sufficient controls. The so-

called e-liquids are available with different amounts of nicotine content, which should allow for separation of the effects with the right combination of control groups.

Throughout the course of this study, it has occurred to us that the hormone leptin could possibly play a role in the adverse effects of prenatal hypoxia as well as other cardiovascular diseases. As an example, obesity is associated with increased risk of cardiovascular diseases, and it is also associated with increased levels of leptin (and leptin resistance) [206]. Leptin has also been associated with increased ROS production and hyperleptinaemia predicts acute cardiovascular events [207]. As discussed in section 2.4.1, leptin has been shown to increase with altitude [129, 130]. So the question is what are the leptin levels in the offspring during hypoxia and are these hypoxic offspring leptin resistant? This is an interesting avenue for future research.

6 References

1. Roth, G.A. *et al.* Global, regional, and national burden of cardiovascular diseases for 10 causes, 1990 to 2015. *J Am Coll Cardiol* **70**, 1-25 (2017).

2. Agarwal, A., Williams, G.H. & Fisher, N.D.L. Genetics of human hypertension. *Trends Endocrinol Metab* **16**, 127-133 (2005).

3. Stewart, J., Manmathan, G. & Wilkinson, P. Primary prevention of cardiovascular disease: A review of contemporary guidance and literature. *JRSM Cardiovasc Dis* **6**, 1-9 (2017).

4. Ruan, Y. *et al.* Cardiovascular disease (CVD) and associated risk factors among older adults in six low-and middle-income countries: results from SAGE Wave 1. *BMC Public Health* **18**, 778-791 (2018).

5. Forsdahl, A. Are poor living conditions in childhood and adolescence an important risk factor for arteriosclerotic heart disease? *Br J Prev Soc Med* **31**, 91-95 (1977).

6. Notkola, V. *Living conditions in childhood and coronary heart disease in adulthood: a mortality and morbidity study in two areas of Finland*. (1985).

7. Buck, C. & Simpson, H. Infant diarrhoea and subsequent mortality from heart disease and cancer. *J Epidemiol Community Health* **36**, 27-30 (1982).

8. Barker, D.J., Osmond, C., Golding, J., Kuh, D. & Wadsworth, M.E. Growth in utero, blood pressure in childhood and adult life, and mortality from cardiovascular disease. *BMJ* **298**, 564-567 (1989).

9. Hsu, C. & Tain, Y. The good, the bad, and the ugly of pregnancy nutrients and developmental programming of adult disease. *Nutrients* **11**, 894 (2019).

10. Fowden, A.L., Giussani, D.A. & Forhead, A.J. Endocrine and metabolic programming during intrauterine development. *Early Hum Dev* **81**, 723-734 (2005).

11. Zhang, L. Prenatal hypoxia and cardiac programming. *J Soc Gynecol Investig* **12**, 2-13 (2016).

12. Matu, J., Gonzalez, J.T., Ispoglou, T., Duckworth, L. & Deighton, K. The effects of hypoxia on hunger perceptions, appetite-related hormone concentrations and energy intake: A systematic review and meta-analysis. *Appetite* **125**, 98-108 (2018).

13. de Grauw, T.J., Myers, R.E. & Scott, W.J. Fetal growth retardation in rats from different levels of hypoxia. *Biol Neonate* **49**, 85-89 (1986).

14. Fowden, A.L., Giussani, D.A. & Forhead, A.J. Intrauterine programming of physiological systems: Causes and consequences. *Physiology* **21**, 29-37 (2006).

15. Padmanabhan, V., Cardoso, R.C. & Puttabyatappa, M. Developmental programming, a pathway to disease. *Endocrinology* **157**, 1328-1340 (2016).

16. Netuka, I. *et al.* Effect of perinatal hypoxia on cardiac tolerance to acute ischaemia in adult male and female rats. *Clin Exp Pharmacol Physiol* **33**, 714-719 (2006).

17. Xue, Q., Dasgupta, C., Chen, M. & Zhang, L. Foetal hypoxia increases cardiac AT(2)R expression and subsequent vulnerability to adult ischaemic injury. *Cardiovasc Res* **89**, 300-308 (2011).

18. Xu, Y., Williams, S.J., O'Brien, D. & Davidge, S.T. Hypoxia or nutrient restriction during pregnancy in rats leads to progressive cardiac remodeling and impairs postischemic recovery in adult male offspring. *FASEB J* **20**, 1251-1253 (2006).

19. Rueda-Clausen, C.F., Morton, J.S. & Davidge, S.T. Effects of hypoxia-induced intrauterine growth restriction on cardiopulmonary structure and function during adulthood. *Cardiovasc Res* **81**, 713-722 (2009).

20. Giussani, D.A. *et al.* Developmental programming of cardiovascular dysfunction by prenatal hypoxia and oxidative stress. *PLoS One* **7**, e31017 (2012).

21. Giussani, D.A. & Davidge, S.T. Developmental programming of cardiovascular disease by prenatal hypoxia. *J Dev Orig Health Dis* **4**, 328-337 (2013).

22. Xue, Q. & Zhang, L. Prenatal hypoxia causes a sex-dependent increase in heart susceptibility to ischemia and reperfusion injury in adult male offspring: role of protein kinase C epsilon. *J Pharmacol Exp Ther* **330**, 624-632 (2009).

23. Rueda-Clausen, C.F., Morton, J.S., Dolinsky, V.W., Dyck, J.R. & Davidge, S.T. Synergistic effects of prenatal hypoxia and postnatal high-fat diet in the development of cardiovascular pathology in young rats. *Am J Physiol Regul Integr Comp Physiol* **303**, R418-R426 (2012).

24. Koos, B.J. Adenosine A(2)a receptors and O(2) sensing in development. *Am J Physiol Regul Integr Comp Physiol* **301**, R601-R622 (2011).

25. Penaloza, D. & Arias-Stella, J. The heart and pulmonary circulation at high altitudes: healthy highlanders and chronic mountain sickness. *Circulation* **115**, 1132-1146 (2007).

26. Barker, D.J. The fetal and infant origins of adult disease. *BMJ* **301**, 1111 (1990).

27. Li, H. *et al.* Effects of prenatal hypoxia on fetal sheep heart development and proteomics analysis. *Int J Clin Exp Pathol* **11**, 1909-1922 (2018).

28. Rueda-Clausen, C.F., Morton, J.S., Lopaschuk, G.D. & Davidge, S.T. Long-term effects of intrauterine growth restriction on cardiac metabolism and susceptibility to ischaemia/reperfusion. *Cardiovasc Res* **90**, 285-294 (2011).

29. Patterson, A.J., Chen, M., Xue, Q., Xiao, D. & Zhang, L. Chronic prenatal hypoxia induces epigenetic programming of PKCε gene repression in rat hearts. *Circ Res* **107**, 365-373 (2010).

30. Thompson, L.P., Chen, L., Polster, B.M., Pinkas, G. & Song, H. Prenatal hypoxia impairs cardiac mitochondrial and ventricular function in guinea pig offspring in a sex-related manner. *Am J Physiol Regul Integr Comp Physiol* **315**, R1232-R1241 (2018).

31. Niu, Y. *et al.* Maternal allopurinol prevents cardiac dysfunction in adult male offspring programmed by chronic hypoxia during pregnancy. *Hypertension* **72**, 971-978 (2018).

32. Church, D.M. *et al.* Lineage-specific biology revealed by a finished genome assembly of the mouse. *PLoS Biol* **7**, e1000112 (2009).

33. Lindgren, I. & Altimiras, J. Prenatal hypoxia programs changes in beta-adrenergic signaling and postnatal cardiac contractile dysfunction. *Am J Physiol Regul Integr Comp Physiol* **305**, R1093-R1101 (2013).

34. British Heart Foundation, Vol. 2019 (n.d.).

35. Antoni, H. Electrical properties of the heart, in *Applied Bioelectricity* 148-193 (Springer New York, New York, NY; 1998).

36. Kashou, A.H., Basit, H. & Chhabra, L. Physiology, Sinoatrial Node (SA Node), in *StatPearls* (Treasure Island (FL); 2019).

37. DiFrancesco, D. & Borer, J.S. The funny current: cellular basis for the control of heart rate. *Drugs* **67 Suppl 2**, 15-24 (2007).

38. Bers, D.M. Cardiac excitation-contraction coupling. *Nature* **415**, 198-205 (2002).

39. Lu, X. *et al.* Measuring local gradients of intramitochondrial [Ca(2+)] in cardiac myocytes during sarcoplasmic reticulum Ca(2+) release. *Circ Res* **112**, 424-431 (2013).

40. Choi, H.S. & Eisner, D.A. The role of sarcolemmal Ca2+-ATPase in the regulation of resting calcium concentration in rat ventricular myocytes. *J Physiol* **515 (Pt 1)**, 109-118 (1999).

41. Eisner, D.A., Caldwell, J.L., Kistamas, K. & Trafford, A.W. Calcium and excitation-contraction coupling in the heart. *Circ Res* **121**, 181-195 (2017).

42. Bonora, M. *et al.* ATP synthesis and storage. *Purinergic Signal* **8**, 343-357 (2012).

43. Turer, A. *et al.* Remodeling of substrate consumption in the murine sTAC model of heart failure. *J Mol Cell Cardiol* **134**, 144-153 (2019).

44. Liu, Q., Docherty, J.C., Rendell, J.C., Clanachan, A.S. & Lopaschuk, G.D. High levels of fatty acids delay the recovery of intracellular pH and cardiac efficiency in post-ischemic hearts by inhibiting glucose oxidation. *J Am Coll Cardiol* **39**, 718-725 (2002).

45. Davila-Roman, V.G. *et al.* Altered myocardial fatty acid and glucose metabolism in idiopathic dilated cardiomyopathy. *J Am Coll Cardiol* **40**, 271-277 (2002).

46. Chaudhry, R. & Varacallo, M. Biochemistry, Glycolysis, in *StatPearls* (Treasure Island (FL); 2019).

47. Kumari, A. *Sweet biochemistry : remembering structures, cycles, and pathways by mnemonics*. (Elsevier, Academic Press, London, United Kingdom; 2018).

48. Kamzolova, S.V., Shishkanova, N.V., Morgunov, I.G. & Finogenova, T.V. Oxygen requirements for growth and citric acid production of Yarrowia lipolytica. *FEMS Yeast Res* **3**, 217-222 (2003).

49. Akram, M. Citric acid cycle and role of its intermediates in metabolism. *Cell Biochem Biophys* **68**, 475-478 (2014).

50. Rees, D.M., Leslie, A.G. & Walker, J.E. The structure of the membrane extrinsic region of bovine ATP synthase. *Proc Natl Acad Sci U S A* **106**, 21597-21601 (2009).

51. Hoffman, D.L., Salter, J.D. & Brookes, P.S. Response of mitochondrial reactive oxygen species generation to steady-state oxygen tension: implications for hypoxic cell signaling. *Am J Physiol Heart Circ Physiol* **292**, H101-H108 (2007).

52. Hoffman, D.L. & Brookes, P.S. Oxygen sensitivity of mitochondrial reactive oxygen species generation depends on metabolic conditions. *J Biol Chem* **284**, 16236-16245 (2009).

53. Brand, M.D. Mitochondrial generation of superoxide and hydrogen peroxide as the source of mitochondrial redox signaling. *Free Radic Biol Med* **100**, 14-31 (2016).

54. Li, N. *et al.* Mitochondrial complex I inhibitor rotenone induces apoptosis through enhancing mitochondrial reactive oxygen species production. *J Biol Chem* **278**, 8516-8525 (2003).

55. Sauer, H., Wartenberg, M. & Hescheler, J. Reactive oxygen species as intracellular messengers during cell growth and differentiation. *Cell Physiol Biochem* **11**, 173-186 (2001).

56. Thannickal, V.J. & Fanburg, B.L. Activation of an H2O2-generating NADH oxidase in human lung fibroblasts by transforming growth factor beta 1. *J Biol Chem* **270**, 30334-30338 (1995).

57. Kiritoshi, S. *et al.* Reactive oxygen species from mitochondria induce cyclooxygenase-2 gene expression in human mesangial cells: potential role in diabetic nephropathy. *Diabetes* **52**, 2570-2577 (2003).

58. Droge, W. Free radicals in the physiological control of cell function. *Physiol Rev* **82**, 47-95 (2002).

59. O'Rourke, B. Mitochondrial ion channels. *Annu Rev Physiol* **69**, 19-49 (2007).

60. Glancy, B., Willis, W.T., Chess, D.J. & Balaban, R.S. Effect of calcium on the oxidative phosphorylation cascade in skeletal muscle mitochondria. *Biochemistry* **52**, 2793-2809 (2013).

61. Sohal, R.S. & Allen, R.G. Relationship between metabolic rate, free radicals, differentiation and aging: a unified theory. *Basic Life Sci* **35**, 75-104 (1985).

62. Zorov, D.B., Filburn, C.R., Klotz, L.O., Zweier, J.L. & Sollott, S.J. Reactive oxygen species (ROS)-induced ROS release: a new phenomenon accompanying induction of the mitochondrial permeability transition in cardiac myocytes. *J Exp Med* **192**, 1001-1014 (2000).

63. Bernardi, P., Broekemeier, K.M. & Pfeiffer, D.R. Recent progress on regulation of the mitochondrial permeability transition pore; a cyclosporin-sensitive pore in the inner mitochondrial membrane. *J Bioenerg Biomembr* **26**, 509-517 (1994).

64. Lu, X., Kwong, J.Q., Molkentin, J.D. & Bers, D.M. Individual cardiac mitochondria undergo rare transient permeability transition pore openings. *Circ Res* **118**, 834-841 (2016).

65. Saotome, M. *et al.* Transient opening of mitochondrial permeability transition pore by reactive oxygen species protects myocardium from ischemia-reperfusion injury. *Am J Physiol Heart Circ Physiol* **296**, H1125-H1132 (2009).

66. Saelens, X. *et al.* Toxic proteins released from mitochondria in cell death. *Oncogene* **23**, 2861-2874 (2004).

67. Garrido, C. *et al.* Mechanisms of cytochrome c release from mitochondria. *Cell Death Differ* **13**, 1423-1433 (2006).

68. Frank, A. *et al.* Myocardial ischemia reperfusion injury: from basic science to clinical bedside. *Semin Cardiothorac Vasc Anesth* **16**, 123-132 (2012).

69. Hausenloy, D.J. & Yellon, D.M. Myocardial ischemia-reperfusion injury: a neglected therapeutic target. *J Clin Invest* **123**, 92-100 (2013).

70. Kloner, R.A., Ganote, C.E., Whalen, D.A., Jr. & Jennings, R.B. Effect of a transient period of ischemia on myocardial cells. II. Fine structure during the first few minutes of reflow. *Am J Pathol* **74**, 399-422 (1974).

71. Bush, L.R., Shlafer, M., Haack, D.W. & Lucchesi, B.R. Time-dependent changes in canine cardiac mitochondrial function and ultrastructure resulting from coronary occlusion and reperfusion. *Basic Res Cardiol* **75**, 555-571 (1980).

72. Murphy, E., Perlman, M., London, R.E. & Steenbergen, C. Amiloride delays the ischemia-induced rise in cytosolic free calcium. *Circ Res* **68**, 1250-1258 (1991).

73. Patron, M. *et al.* The mitochondrial calcium uniporter (MCU): molecular identity and physiological roles. *J Biol Chem* **288**, 10750-10758 (2013).

74. Imahashi, K. *et al.* Cardiac-specific ablation of the Na+-Ca2+ exchanger confers protection against ischemia/reperfusion injury. *Circ Res* **97**, 916-921 (2005).

75. Sugishita, K., Su, Z., Li, F., Philipson, K.D. & Barry, W.H. Gender influences [Ca(2+)](i) during metabolic inhibition in myocytes overexpressing the Na(+)-Ca(2+) exchanger. *Circulation* **104**, 2101-2106 (2001).

76. Cross, H.R., Lu, L., Steenbergen, C., Philipson, K.D. & Murphy, E. Overexpression of the cardiac Na+/Ca2+ exchanger increases susceptibility to ischemia/reperfusion injury in male, but not female, transgenic mice. *Circ Res* **83**, 1215-1223 (1998).

77. Granger, D.N. & Kvietys, P.R. Reperfusion injury and reactive oxygen species: The evolution of a concept. *Redox Biol* **6**, 524-551 (2015).

78. Ichikawa, H. *et al.* Rotenone, a mitochondrial electron transport inhibitor, ameliorates ischemia-reperfusion-induced intestinal mucosal damage in rats. *Redox Rep* **9**, 313-316 (2004).

79. Marczin, N., El-Habashi, N., Hoare, G.S., Bundy, R.E. & Yacoub, M. Antioxidants in myocardial ischemia-reperfusion injury: therapeutic potential and basic mechanisms. *Arch Biochem Biophys* **420**, 222-236 (2003).

80. Chouchani, E.T. *et al.* Ischaemic accumulation of succinate controls reperfusion injury through mitochondrial ROS. *Nature* **515**, 431-435 (2014).

81. Rowell, L.B. & Blackmon, J.R. Human cardiovascular adjustments to acute hypoxaemia. *Clin Physiol* **7**, 349-376 (1987).

82. Maurer, H.S., Behrman, R.E. & Honig, G.R. Dependence of the oxygen affinity of blood on the presence of foetal or adult haemoglobin. *Nature* **227**, 388-390 (1970).

83. Godfrey, K.M. *et al.* Fetal liver blood flow distribution: role in human developmental strategy to prioritize fat deposition versus brain development. *PLoS One* **7**, e41759 (2012).

84. Boyle, D.W., Hirst, K., Zerbe, G.O., Meschia, G. & Wilkening, R.B. Fetal hind limb oxygen consumption and blood flow during acute graded hypoxia. *Pediatr Res* **28**, 94-100 (1990).

85. Itskovitz, J., LaGamma, E.F. & Rudolph, A.M. Effects of cord compression on fetal blood flow distribution and O2 delivery. *Am J Physiol* **252**, H100-H109 (1987).

86. Kane, A.D., Herrera, E.A., Hansell, J.A. & Giussani, D.A. Statin treatment depresses the fetal defence to acute hypoxia via increasing nitric oxide bioavailability. *J Physiol* **590**, 323-334 (2012).

87. Thakor, A.S. *et al.* Redox modulation of the fetal cardiovascular defence to hypoxaemia. *J Physiol* **588**, 4235-4247 (2010).

88. Thakor, A.S. *et al.* Melatonin modulates the fetal cardiovascular defense response to acute hypoxia. *J Pineal Res* **59**, 80-90 (2015).

89. Kane, A.D. *et al.* Xanthine oxidase and the fetal cardiovascular defence to hypoxia in late gestation ovine pregnancy. *J Physiol* **592**, 475-489 (2014).

90. Poudel, R., McMillen, I.C., Dunn, S.L., Zhang, S. & Morrison, J.L. Impact of chronic hypoxemia on blood flow to the brain, heart, and adrenal gland in the late-gestation IUGR sheep fetus. *Am J Physiol Regul Integr Comp Physiol* **308**, R151-R162 (2015).

91. Allison, B.J. *et al.* Fetal in vivo continuous cardiovascular function during chronic hypoxia. *J Physiol* **594**, 1247-1264 (2016).

92. Unger, C., Weiser, J.K., McCullough, R.E., Keefer, S. & Moore, L.G. Altitude, low birth weight, and infant mortality in Colorado. *Jama* **259**, 3427-3432 (1988).

93. Xiao, D., Ducsay, C.A. & Zhang, L. Chronic hypoxia and developmental regulation of cytochrome c expression in rats. *J Soc Gynecol Investig* **7**, 279-283 (2000).

94. Jensen, G.M. & Moore, L.G. The effect of high altitude and other risk factors on birthweight: independent or interactive effects? *American journal of public health* **87**, 1003-1007 (1997).

95. Moore, L.G. Fetal growth restriction and maternal oxygen transport during high altitude pregnancy. *High altitude medicine & biology* **4**, 141-156 (2003).

96. Zamudio, S. *et al.* Protection from intrauterine growth retardation in Tibetans at high altitude. *American journal of physical anthropology* **91**, 215-224 (1993).

97. Giussani, D.A., Phillips, P.S., Anstee, S. & Barker, D.J.P. Effects of altitude versus economic status on birth weight and body shape at birth. *Pediatr Res* **49**, 490-494 (2001).

98. Kamitomo, M., Alonso, J.G., Okai, T., Longo, L.D. & Gilbert, R.D. Effects of long-term, high-altitude hypoxemia on ovine fetal cardiac output and blood flow distribution. *American journal of obstetrics and gynecology* **169**, 701-707 (1993).

99. Kamitomo, M., Longo, L.D. & Gilbert, R.D. Right and left ventricular function in fetal sheep exposed to long-term high-altitude hypoxemia. *Am J Physiol* **262**, H399-H405 (1992).

100. Browne, V.A., Stiffel, V.M., Pearce, W.J., Longo, L.D. & Gilbert, R.D. Cardiac beta-adrenergic receptor function in fetal sheep exposed to long-term high-altitude hypoxemia. *Am J Physiol* **273**, R2022-R2031 (1997).

101. Browne, V.A., Stiffel, V.M., Pearce, W.J., Longo, L.D. & Gilbert, R.D. Activator calcium and myocardial contractility in fetal sheep exposed to long-term high-altitude hypoxia. *Am J Physiol* **272**, H1196-H1204 (1997).

102. Bae, S., Xiao, Y., Li, G., Casiano, C.A. & Zhang, L. Effect of maternal chronic hypoxic exposure during gestation on apoptosis in fetal rat heart. *Am J Physiol Heart Circ Physiol* **285**, 983-990 (2003).

103. Barbera, A. *et al.* Right ventricular systolic pressure load alters myocyte maturation in fetal sheep. *Am J Physiol Regul Integr Comp Physiol* **279**, R1157-R1164 (2000).

104. Oparil, S., Bishop, S.P. & Clubb, F.J., Jr. Myocardial cell hypertrophy or hyperplasia. *Hypertension* **6**, III38-III43 (1984).

105. Nishio, M.L., Ornatsky, O.I., Craig, E.E. & Hood, D.A. Mitochondrial biogenesis during pressure overload induced cardiac hypertrophy in adult rats. *Can J Physiol Pharmacol* **73**, 630-637 (1995).

106. Zak, R., Rabinowitz, M., Rajamanickam, C., Merten, S. & Kwiatkowska-Patzer, B. Mitochondrial proliferation in cardiac hypertrophy. *Basic Res Cardiol* **75**, 171-178 (1980).

107. Zhang, L. Prenatal hypoxia and cardiac programming. *J Soc Gynecol Investig* **12**, 2-13 (2005).

108. Bernstein, I.M. *et al.* Maternal smoking and its association with birth weight. *Obstet Gynecol* **106**, 986-991 (2005).

109. Li, G. *et al.* Effect of fetal hypoxia on heart susceptibility to ischemia and reperfusion injury in the adult rat. *J Soc Gynecol Investig* **10**, 265-274 (2003).

110. Scruggs, S.B., Wang, D. & Ping, P. PRKCE gene encoding protein kinase C-epsilon-Dual roles at sarcomeres and mitochondria in cardiomyocytes. *Gene* **590**, 90-96 (2016).

111. Ogbi, M. & Johnson, J.A. Protein kinase Cε interacts with cytochrome c oxidase subunit IV and enhances cytochrome c oxidase activity in neonatal cardiac myocyte preconditioning. *Biochem J* **393**, 191-199 (2006).

112. Thompson, L.P., Song, H. & Polster, B.M. Fetal programming and sexual dimorphism of mitochondrial protein expression and activity of hearts of prenatally hypoxic guinea pig offspring. *Oxid Med Cell Longev* **2019**, 1-11 (2019).

113. Xue, Q. & Zhang, L. Prenatal hypoxia causes a sex-dependent increase in heart susceptibility to ischemia and reperfusion injury in adult male offspring: Role of protein kinase Cε. *J Pharmacol Exp Ther* **330**, 624-632 (2009).

114. Miller, V.M. Why are sex and gender important to basic physiology and translational and individualized medicine? *Am J Physiol Heart Circ Physiol* **306**, H781-H788 (2014).

115. Itani, N., Skeffington, K.L., Beck, C., Niu, Y. & Giussani, D.A. Melatonin rescues cardiovascular dysfunction during hypoxic development in the chick embryo. *J Pineal Res* **60**, 16-26 (2016).

116. Botting, K.J. *et al.* IUGR decreases cardiomyocyte endowment and alters cardiac metabolism in a sex- and cause-of-IUGR-specific manner. *Am J Physiol Regul Integr Comp Physiol* **315**, R48-R67 (2018).

117. Nicolaides, K.H., Soothill, P.W., Rodeck, C.H. & Campbell, S. Ultrasound-guided sampling of umbilical cord and placental blood to assess fetal wellbeing. *Lancet* **1**, 1065-1067 (1986).

118. Palmer, S.K. *et al.* Altered blood pressure course during normal pregnancy and increased preeclampsia at high altitude (3100 meters) in Colorado. *American journal of obstetrics and gynecology* **180**, 1161-1168 (1999).

119. Higgins, J.S., Vaughan, O.R., Fernandez de Liger, E., Fowden, A.L. & Sferruzzi-Perri, A.N. Placental phenotype and resource allocation to fetal growth are modified by the timing and degree of hypoxia during mouse pregnancy. *J Physiol* **594**, 1341-1356 (2016).

120. Gleed, R.D. & Mortola, J.P. Ventilation in newborn rats after gestation at simulated high altitude. *J Appl Physiol (1985)* **70**, 1146-1151 (1991).

121. Soria, R., Julian, C.G., Vargas, E., Moore, L.G. & Giussani, D.A. Graduated effects of high-altitude hypoxia and highland ancestry on birth size. *Pediatr Res* **74**, 633-638 (2013).

122. Recchia, F.A. & Lionetti, V. Animal models of dilated cardiomyopathy for translational research. *Vet Res Commun* **31 Suppl 1**, 35-41 (2007).

123. Camacho, P., Fan, H., Liu, Z. & He, J.Q. Small mammalian animal models of heart disease. *Am J Cardiovasc Dis* **6**, 70-80 (2016).

124. Wolterink-Donselaar, I.G., Meerding, J.M. & Fernandes, C. A method for gender determination in newborn dark pigmented mice. *Lab Anim (NY)* **38**, 35-38 (2009).

125. Deeney, S., Powers, K.N. & Crombleholme, T.M. A comparison of sexing methods in fetal mice. *Lab Anim (NY)* **45**, 380-384 (2016).

126. Liu, W. *et al.* Cardiac-specific deletion of mkk4 reveals its role in pathological hypertrophic remodeling but not in physiological cardiac growth. *Circ Res* **104**, 905-914 (2009).

127. Minamisawa, S., Gu, Y., Ross, J., Jr., Chien, K.R. & Chen, J. A post-transcriptional compensatory pathway in heterozygous ventricular myosin light chain 2-deficient mice results in lack of gene dosage effect during normal cardiac growth or hypertrophy. *J Biol Chem* **274**, 10066-10070 (1999).

128. West, J.B. *et al.* Maximal exercise at extreme altitudes on Mount Everest. *J Appl Physiol Respir Environ Exerc Physiol* **55**, 688-698 (1983).

129. Vats, P., Singh, V.K., Singh, S.N. & Singh, S.B. High altitude induced anorexia: effect of changes in leptin and oxidative stress levels. *Nutr Neurosci* **10**, 243-249 (2007).

130. Shukla, V. *et al.* Ghrelin and leptin levels of sojourners and acclimatized lowlanders at high altitude. *Nutr Neurosci* **8**, 161-165 (2005).

131. Williams, S.J., Campbell, M.E., McMillen, I.C. & Davidge, S.T. Differential effects of maternal hypoxia or nutrient restriction on carotid and femoral vascular function in neonatal rats. *Am J Physiol Regul Integr Comp Physiol* **288**, R360-R367 (2005).

132. Williams, S.J., Hemmings, D.G., Mitchell, J.M., McMillen, I.C. & Davidge, S.T. Effects of maternal hypoxia or nutrient restriction during pregnancy on endothelial function in adult male rat offspring. *J Physiol* **565**, 125-135 (2005).

133. Reyes, L.M., Morton, J.S., Kirschenman, R., DeLorey, D.S. & Davidge, S.T. Vascular effects of aerobic exercise training in rat adult offspring exposed to hypoxia-induced intrauterine growth restriction. *J Physiol* **593**, 1913-1929 (2015).

134. Huang, S.T. *et al.* Developmental response to hypoxia. *FASEB J* **18**, 1348-1365 (2004).

135. Ream, M., Ray, A.M., Chandra, R. & Chikaraishi, D.M. Early fetal hypoxia leads to growth restriction and myocardial thinning. *Am J Physiol Regul Integr Comp Physiol* **295**, R583-R595 (2008).

136. Tomlinson, T.M. *et al.* Magnetic resonance imaging of hypoxic injury to the murine placenta. *Am J Physiol Regul Integr Comp Physiol* **298**, R312-R319 (2010).

137. Kwong, W.Y., Wild, A.E., Roberts, P., Willis, A.C. & Fleming, T.P. Maternal undernutrition during the preimplantation period of rat development causes blastocyst abnormalities and programming of postnatal hypertension. *Development* **127**, 4195-4202 (2000).

138. Darby, J.R.T., McMillen, I.C. & Morrison, J.L. Maternal undernutrition in late gestation increases IGF2 signalling molecules and collagen deposition in the right ventricle of the fetal sheep heart. *J Physiol* **596**, 2345-2358 (2018).

139. Cheema, K.K., Dent, M.R., Saini, H.K., Aroutiounova, N. & Tappia, P.S. Prenatal exposure to maternal undernutrition induces adult cardiac dysfunction. *Br J Nutr* **93**, 471-477 (2005).

140. Thaete, L.G., Dewey, E.R. & Neerhof, M.G. Endothelin and the regulation of uterine and placental perfusion in hypoxia-induced fetal growth restriction. *J Soc Gynecol Investig* **11**, 16-21 (2004).

141. Thaete, L.G., Neerhof, M.G. & Caplan, M.S. Endothelin receptor A antagonism prevents hypoxiainduced intrauterine growth restriction in the rat. *Am J Obstet Gynecol.* **176**, 73-76 (1997).

142. Gortner, L. *et al.* Hypoxia-induced intrauterine growth retardation: Effects on pulmonary development and surfactant protein transcription. *Biol Neonate* **88**, 129-135 (2005).

143. Rueda-Clausen, C.F. *et al.* Effect of prenatal hypoxia in transgenic mouse models of preeclampsia and fetal growth restriction. *Reprod Sci* **21**, 492-502 (2014).

144. Zhang, P. *et al.* Long-term exposure to high altitude hypoxia during pregnancy increases fetal heart susceptibility to ischemia/reperfusion injury and cardiac dysfunction. *Int J Cardiol* **274**, 7-15 (2019).

145. Al-Hasan, Y.M., Pinkas, G.A. & Thompson, L.P. Prenatal hypoxia reduces mitochondrial protein levels and cytochrome c oxidase activity in offspring guinea pig hearts:. *Reprod Sci* **21**, 883-891 (2014).

146. Bahtiyar, M.O. *et al.* Contrasting effects of chronic hypoxia and nitric oxide synthase inhibition on circulating angiogenic factors in a rat model of growth restriction. *American journal of obstetrics and gynecology* **196**, 72.e71-72.e76 (2007).

147. Van Geijn, H.P., Kaylor Jr, W.M., Nicola, K.R. & Zuspan, F.P. Induction of severe intrauterine growth retardation in the Sprague-Dawley rat. *American journal of obstetrics and gynecology* **137**, 43-47 (1980).

148. Lee, S.K. Sex as an important biological variable in biomedical research. *BMB Rep* **51**, 167-173 (2018).

149. Lindgren, I. & Altimiras, J. Chronic prenatal hypoxia sensitizes beta-adrenoceptors in the embryonic heart but causes postnatal desensitization. *Am J Physiol Regul Integr Comp Physiol* **297**, R258-R264 (2009).

150. Sun, J. *et al.* Hypercontractile female hearts exhibit increased S-nitrosylation of the L-type Ca2+ channel alpha1 subunit and reduced ischemia/reperfusion injury. *Circ Res* **98**, 403-411 (2006).

151. Benjamin, E.J. *et al.* Heart disease and stroke statistics-2019 update: A report from the american heart association. *Circulation* **139**, e56-e528 (2019).

152. Ambrosio, G. *et al.* Evidence that mitochondrial respiration is a source of potentially toxic oxygen free radicals in intact rabbit hearts subjected to ischemia and reflow. *J Biol Chem* **268**, 18532-18541 (1993).

153. Spinazzi, M., Casarin, A., Pertegato, V., Salviati, L. & Angelini, C. Assessment of mitochondrial respiratory chain enzymatic activities on tissues and cultured cells. *Nat Protoc* **7**, 1235-1246 (2012).

154. Pinali, C., Bennett, H., Davenport, J.B., Trafford, A.W. & Kitmitto, A. Three-dimensional reconstruction of cardiac sarcoplasmic reticulum reveals a continuous network linking transverse-tubules. *Circ Res* **113**, 1219-1230 (2013).

155. Deerinck, T.J. *et al.* Enhancing serial block-face scanning electron microscopy to enable high resolution 3-D nanohistology of cells and tissues. *Microsc Microanal* **16**, 1138-1139 (2010).

156. Picard, M. *et al.* Acute exercise remodels mitochondrial membrane interactions in mouse skeletal muscle. *J Appl Physiol (1985)* **115**, 1562-1571 (2013).

157. Sun, Y., Oberley, L.W. & Li, Y. A simple method for clinical assay of superoxide dismutase. *Clin Chem* **34**, 497-500 (1988).

158. Weydert, C.J. & Cullen, J.J. Measurement of superoxide dismutase, catalase and glutathione peroxidase in cultured cells and tissue. *Nat Protoc* **5**, 51-66 (2010).

159. Bae, S., Gilbert, R.D., of, C.D.T.J. & 2005 Prenatal cocaine exposure increases heart susceptibility to ischaemia–reperfusion injury in adult male but not female rats. *J Physiol*, 149-158 (2005).

160. Lawrence, J. *et al.* Prenatal nicotine exposure increases heart susceptibility to ischemia/reperfusion injury in adult offspring. *J Pharmacol Exp Ther* **324**, 331-341 (2008).

161. Larsen, S. *et al.* Biomarkers of mitochondrial content in skeletal muscle of healthy young human subjects. *J Physiol.* **590**, 3349-3360 (2012).

162. Nielsen, J. *et al.* Plasticity in mitochondrial cristae density allows metabolic capacity modulation in human skeletal muscle. *J Physiol* **595**, 2839-2847 (2017).

163. Picard, M., Taivassalo, T., Gouspillou, G. & Hepple, R.T. Mitochondria: isolation, structure and function. *J Physiol* **589**, 4413-4421 (2011).

164. Guo, D. *et al.* Protein kinase C-ε coimmunoprecipitates with cytochrome oxidase subunit IV and is associated with improved cytochrome-c oxidase activity and cardioprotection. *Am J Physiol Heart Circ Physiol* **293**, H2219-H2230 (2007).

165. Lim, S. *et al.* Regulation of mitochondrial functions by protein phosphorylation and dephosphorylation. *Cell Biosci* **6**, 25 (2016).

166. Murriel, C.L. & Mochly-Rosen, D. Opposing roles of δ and εPKC in cardiac ischemia and reperfusion: targeting the apoptotic machinery. *Archives of Biochemistry and Biophysics* **420**, 246-254 (2003).

167. Pesta, D. & Gnaiger, E. High-resolution respirometry: OXPHOS protocols for human cells and permeabilized fibers from small biopsies of human muscle, Vol. 810 25-58 (Humana Press, Totowa, NJ; 2012).

168. Gnaiger, E. Capacity of oxidative phosphorylation in human skeletal muscle New perspectives of mitochondrial physiology. *Int J Biochem Cell Biol* **41**, 1837-1845 (2009).

169. Korshunov, S.S., Skulachev, V.P. & Starkov, A.A. High protonic potential actuates a mechanism of production of reactive oxygen species in mitochondria. *FEBS Letters* **416**, 15-18 (1997).

170. Loschen, G. & Flohé, L. Respiratory chain linked H2O2 production in pigeon heart mitochondria. *FEBS Letters* **18**, 261-264 (1971).

171. Chance, B., Sies, H. & Boveris, A. Hydroperoxide metabolism in mammalian organs. *Physiol Rev* **59**, 527-605 (1979).

172. Murphy, M.P. How mitochondria produce reactive oxygen species. *Biochem J* **417**, 1-13 (2009).

173. Valdez, L.B., Zaobornyj, T. & Boveris, A. Mitochondrial metabolic states and membrane potential modulate mtNOS activity. *Biochim Biophys Acta* **1757**, 166-172 (2006).

174. Mitchell, P. Coupling of phosphorylation to electron and hydrogen transfer by a chemi-osmotic type of mechanism. *Nature* **191**, 144-148 (1961).

175. Miwa, S., St-Pierre, J., Partridge, L. & Brand, M.D. Superoxide and hydrogen peroxide production by Drosophila mitochondria. *Free Radic Biol Med* **35**, 938-948 (2003).

176. Duranteau, J., Chandel, N.S., Kulisz, A., Shao, Z. & Schumacker, P.T. Intracellular signaling by reactive oxygen species during hypoxia in cardiomyocytes. *J Biol Chem* **273**, 11619-11624 (1998).

177. Farhat, F., Amérand, A., Simon, B., Guegueniat, N. & Moisan, C. Gender-dependent differences of mitochondrial function and oxidative stress in rat skeletal muscle at rest and after exercise training. *Redox Report* **22**, 508-514 (2017).

178. Khalifa, A.R.M. *et al.* Sex-specific differences in mitochondria biogenesis, morphology, respiratory function, and ROS homeostasis in young mouse heart and brain. *Physiol Rep* **5**, e13125 (2017).

179. Pecinova, A., Drahota, Z., Nuskova, H., Pecina, P. & Houstek, J. Evaluation of basic mitochondrial functions using rat tissue homogenates. *Mitochondrion* **11**, 722-728 (2011).

180. Mela, L. & Seitz, S. Isolation of mitochondria with emphasis on heart mitochondria from small amounts of tissue. *Methods Enzymol* **55**, 39-46 (1979).

181. Brand, M.D. & Nicholls, D.G. Assessing mitochondrial dysfunction in cells. *Biochem J* **435**, 297-312 (2011).

182. Vercesi, A.E., Bernardes, C.F., Hoffmann, M.E., Gadelha, F.R. & Docampo, R. Digitonin permeabilization does not affect mitochondrial function and allows the determination of the mitochondrial membrane potential of Trypanosoma cruzi in situ. *J Biol Chem* **266**, 14431-14434 (1991).

183. Ghosh, R., Gilda, J.E. & Gomes, A.V. The necessity of and strategies for improving confidence in the accuracy of western blots. *Expert Rev Proteomics* **11**, 549-560 (2014).

184. Koller, A. & Watzig, H. Precision and variance components in quantitative gel electrophoresis. *Electrophoresis* **26**, 2470-2475 (2005).

185. Porsch-Ozcurumez, M. *et al.* Comparison of enzyme-linked immunosorbent assay, Western blotting, microagglutination, indirect immunofluorescence assay, and flow cytometry for serological diagnosis of tularemia. *Clin Diagn Lab Immunol* **11**, 1008-1015 (2004).

186. Briston, S.J. *et al.* Impaired beta-adrenergic responsiveness accentuates dysfunctional excitation-contraction coupling in an ovine model of tachypacing-induced heart failure. *J Physiol* **589**, 1367-1382 (2011).

187. Bers, D.M. Altered cardiac myocyte Ca regulation in heart failure. *Physiology (Bethesda)* **21**, 380-387 (2006).

188. Bertero, E. & Maack, C. Calcium signaling and reactive oxygen species in mitochondria. *Circ Res* **122**, 1460-1478 (2018).

189. Greensmith, D.J. Ca analysis: an Excel based program for the analysis of intracellular calcium transients including multiple, simultaneous regression analysis. *Comput Methods Programs Biomed* **113**, 241-250 (2014).

190. Frank, K. & Kranias, E.G. Phospholamban and cardiac contractility. *Ann Med* **32**, 572-578 (2000).

191. Qin, F. *et al.* Hydrogen peroxide-mediated SERCA cysteine 674 oxidation contributes to impaired cardiac myocyte relaxation in senescent mouse heart. *J Am Heart Assoc* **2**, e000184 (2013).

192. US Department of Health and Human Services Patterns of tobacco use among U.S. youth, young adults, and adults, in *The Health Consequences of Smoking-50 Years of Progress: A Report of the Surgeon General* (Centers for Disease Control and Prevention (US), Atlanta (GA); 2014).

193. Martin, J.A. *et al.* Births: final data for 2005. *National vital statistics reports : from the Centers for Disease Control and Prevention, National Center for Health Statistics, National Vital Statistics System* **56**, 1-103 (2007).

194. DeMeo, D.L. *et al.* Ambient air pollution and oxygen saturation. *American journal of respiratory and critical care medicine* **170**, 383-387 (2004).

195. Thompson, L.P., Pence, L., Pinkas, G., Song, H. & Telugu, B.P. Placental hypoxia during early pregnancy causes maternal hypertension and placental insufficiency in the hypoxic guinea pig model. *Biology of reproduction* **95**, 128, 121-110 (2016).

196. Rueda-Clausen, C.F. *et al.* Hypoxia-induced intrauterine growth restriction increases the susceptibility of rats to high-fat diet-induced metabolic syndrome. *Diabetes* **60**, 507-516 (2011).

197. Sharma, D., Shastri, S. & Sharma, P. Intrauterine growth restriction: Antenatal and postnatal aspects. *Clinical medicine insights. Pediatrics* **10**, 67-83 (2016).

198. Jin, L.F. & Li, J.S. Generation of genetically modified mice using CRISPR/Cas9 and haploid embryonic stem cell systems. *Dong wu xue yan jiu = Zoological research* **37**, 205-213 (2016).

199. Burgio, G. Redefining mouse transgenesis with CRISPR/Cas9 genome editing technology. *Genome biology* **19**, 19-27 (2018).

200. Phifer-Rixey, M. & Nachman, M.W. Insights into mammalian biology from the wild house mouse Mus musculus. *Elife* **4** (2015).

201. Noh, Y.H. *et al.* Inhibition of oxidative stress by coenzyme Q10 increases mitochondrial mass and improves bioenergetic function in optic nerve head astrocytes. *Cell death & disease* **4**, e820 (2013).

202. Scialo, F., Fernandez-Ayala, D.J. & Sanz, A. Role of mitochondrial reverse electron transport in ROS signaling: Potential roles in health and disease. *Frontiers in physiology* **8**, 428-435 (2017).

203. Zhai, P. *et al.* Effect of estrogen on global myocardial ischemia-reperfusion injury in female rats. *Am J Physiol Heart Circ Physiol* **279**, H2766-H2775 (2000).

204. Felty, Q. & Roy, D. Estrogen, mitochondria, and growth of cancer and non-cancer cells. *Journal of carcinogenesis* **4**, 2005;2004: 2001 (2005).

205. Shao, Q. *et al.* Characterization of the sex-dependent myocardial S-nitrosothiol proteome. *Am J Physiol Heart Circ Physiol* **310**, H505-H515 (2016).

206. de Git, K.C.G. *et al.* Is leptin resistance the cause or the consequence of diet-induced obesity? *Int J Obes (Lond)* **42**, 1445-1457 (2018).

207. Koh, K.K., Park, S.M. & Quon, M.J. Leptin and cardiovascular disease: response to therapeutic interventions. *Circulation* **117**, 3238-3249 (2008).